CATTLE FEEDLOT DUST – LASER DIFFRACTION ANALYSIS OF SIZE DISTRIBUTION AND ESTIMATION OF EMISSIONS FROM UNPAVED ROADS AND WIND EROSION

by

HOWELL B. GONZALES

B.S., University of the Philippines, Los Baños Laguna, Philippines 2001

A THESIS

submitted in partial fulfillment of the requirements for the degree

MASTER OF SCIENCE

Department of Biological and Agricultural Engineering
College of Engineering

KANSAS STATE UNIVERSITY
Manhattan, Kansas

2010

Approved by:

Major Professor
Ronaldo G. Maghirang

Copyright

Abstract

Large cattle feedlots emit considerable amounts of particulate matter (PM), including TSP (total suspended particulates), PM_{10} (PM with equivalent aerodynamic diameter of 10 μm or less), and $PM_{2.5}$ (PM with equivalent aerodynamic diameter of 2.5 μm or less). Particulate emissions result from pen surface disturbance by cattle hoof action, vehicle traffic on unpaved roads and alleyways, and wind erosion. Research is needed to determine concentrations of various size fractions, size distribution, and emission rates from various sources in feedlots. This research was conducted to measure particle size distribution using laser diffraction method and estimate emissions from unpaved roads and wind erosion.

Particle size distribution and concentrations of PM_{10} and $PM_{2.5}$ at a commercial cattle feedlot in Kansas (Feedlot 1) were measured over a 2-yr period. The feedlot had a capacity of 30,000 head and total pen area of 50 ha and was equipped with a sprinkler system for dust control. Collocated low-volume samplers for TSP, PM_{10}, and $PM_{2.5}$ were used to measure concentrations of TSP, PM_{10}, and $PM_{2.5}$ at the upwind and downwind edges of the feedlot. Dust samples that were collected by TSP samplers were analyzed with a laser diffraction analyzer to determine particle size distribution. Particle size distribution at the downwind edge of the feedlot was also measured with micro-orifice uniform deposit impactor (MOUDI). The laser diffraction method and MOUDI did not differ significantly in mean geometric mean diameter (13.7 vs. 13.0 μm) but differed in mean geometric standard deviation (2.9 vs. 2.3). From laser diffraction and TSP data, PM_{10} and $PM_{2.5}$ concentrations were also calculated and were not significantly different from those measured by low-volume PM_{10} and $PM_{2.5}$ samplers (122 vs. 131 $\mu g/m^3$ for PM_{10}; 26 vs. 35 $\mu g/m^3$ for $PM_{2.5}$). Both PM_{10} and $PM_{2.5}$ fractions decreased as pen surface moisture contents increased, while the $PM_{2.5}/PM_{10}$ ratio did not change much with pen surface moisture content.

Published emission models were used to estimate PM_{10} emissions from unpaved roads and wind erosion at Feedlot 1 and another nearby feedlot (Feedlot 2). Feedlot 2 had a capacity of 30,000 head, total pen surface area of 59 ha, and used water trucks for dust control. Estimated PM_{10} emissions from unpaved roads and wind erosion were less than 20% of total PM_{10}

emissions obtained from inverse dispersion modeling. Further research is needed to establish the applicability of published emission estimation models for cattle feedlots.

Table of Contents

List of Figures viii
List of Tables x
List of Acronyms xii
List of Symbols xiv
Acknowledgements xv
Dedication xvii
CHAPTER 1 - Introduction 1
1.1 Background 1
1.2 Objectives 2
1.3 References 3
CHAPTER 2 - Literature Review 5
2.1 Particulate Emissions from Cattle Feedlots 5
2.1.1 Background 5
2.1.2 Sources of Particulate Matter in Cattle Feedlots 6
2.1.3 PM Regulations in Cattle Feedlots 6
2.1.4 Measurement of PM and Size Distribution in Feedlots 7
2.1.5 Control of PM Emissions 8
2.2 Particle Size and Size Distribution 9
2.2.1 Particle Size 9
2.2.2 Geometric Mean Diameter and Geometric Standard Deviation 10
2.2.3 Cascade Impactor 11
2.2.4 Laser Diffraction Method 12
2.2.4.1 Light Scattering Theory 12
2.2.4.2 Laser Diffraction Applications 14
2.3 Emissions from Unpaved Roads and Wind Erosion 15
2.3.1 Unpaved Roads 15
2.3.1.1 Control Strategies for Unpaved Roads 16
2.3.1.2 Previous Research on Unpaved Road Dust Emissions 17

2.3.1.3 Unpaved Road Dust Emission Models 19
2.3.2 Wind Erosion 19
2.3.2.1 Mechanism of Wind Erosion 19
2.3.2.2 Control Strategies for Wind Erosion 21
2.3.2.3 Wind Erosion Models 22
2.3.2.4 Threshold Friction Velocity 24
2.4 Summary 26
2.5 References 26
CHAPTER 3 - Laser Diffraction Analysis of Cattle Feedlot Dust 35
3.1 Introduction 35
3.2 Materials and Methods 37
3.2.1 Feedlot Description 37
3.2.2 Particulate Sampling and Measurement 38
3.2.3 Particle Size Distribution 39
3.2.4 Weather Conditions and Pen Surface Moisture Content 42
3.2.5 Statistical Analysis 43
3.3 Results and Discussion 43
3.3.1 Laser Diffraction vs. Cascade Impactor 44
3.3.2 Cumulative Fraction vs. Particle Fraction Method 46
3.3.3 Laser Diffraction vs. Low-Volume Sampler 47
3.3.4 Factors Affecting Size Distribution 48
3.3.5 Warm vs. Cold Months 50
3.3.6 Effect of Pen Surface Moisture Content 51
3.4 Summary and Conclusions 55
3.5 References 56
CHAPTER 4 - Estimating Particulate Emissions from Unpaved Roads and Wind Erosion in Cattle Feedlots 60
4.1 Introduction 60
4.2 Materials and Methods 61
4.2.1 Site Description 61
4.2.2 Field Measurement of Surface Characteristics 61

4.2.3 Estimation of Emissions from Unpaved Roads 62
4.2.4 Wind Erosion Emissions Calculation 63
4.2.4.1 EPA AP-42 Open Area Wind Erosion 63
4.2.4.2 SWEEP Model for Wind Erosion 64
4.3 Results and Discussion 66
4.3.1 Surface Material Texture Analysis 66
4.3.2 Emissions from Unpaved Roads 67
4.3.3 Emissions Due to Wind Erosion 68
4.3.3.1 US EPA AP-42 Method 68
4.3.3.2 SWEEP model 70
4.3.3.3 Comparison of the EPA AP-42 and SWEEP Model for Wind Erosion 76
4.3.4 Contributions to Total Emissions 76
4.4 Summary and Conclusion 77
4.5 References 77
CHAPTER 5 - Conclusions and Recommendations 80
5.1 Conclusions 80
5.2 Recommendations for Further Study 80
Appendix A - Supporting Data for Chapter 2 82
Appendix B - Supporting Data for Chapter 3 83
Appendix C - Supporting Information for Chapter 4 89

List of Figures

Figure 2.1 Four distinct layers of the pen surface (adapted from: ACFA, 2002) 6
Figure 2.2 Microorifice Uniform Deposit Impactor (MOUDI): (a) schematic diagram; (b) photograph 11
Figure 2.3 Interactions between particle and light beam (adapted from: Merkus, 2008) 13
Figure 2.4 Soil erosion by wind (source: http://www.weru.ksu.edu/weps/wepshome.html) 20
Figure 3.1 Feedlot 1 equipped with a water sprinkler system 37
Figure 3.2 Schematic diagram of the feedlot showing relative locations of samplers and weather station (not drawn to scale). 39
Figure 3.3 Beckman Coulter LS 13 320 Operation 41
Figure 3.4 Comparison of the MOUDI and LD in geometric mean diameters (GMDs) 45
Figure 3.5 Comparison of MOUDI and LD in geometric standard deviations (GSDs) 46
Figure 3.6 Effect of wind speed on geometric mean diameter (GMD) obtained from LD method 49
Figure 3.7 Mean volume percent at different aerodynamic diameters 51
Figure 3.8 Particle size distribution comparison between events with water application and events without water application 52
Figure 3.9 Effects of pen surface moisture content on PM concentrations measured using the LD method: (a) PM_{10} and (b) $PM_{2.5}$. 53
Figure 3.10 Pen surface moisture content dependence of PM fractions measured using the LD method: (a) PM_{10} fraction and (b) $PM_{2.5}$ fraction. 53
Figure 3.11 Effect of pen surface moisture content on $PM_{2.5}/PM_{10}$ ratio measured using the LD method 54
Figure 3.12 Effect of pen surface moisture content on mean geometric mean diameter measured using the LD method 55
Figure 4.1 Monthly PM_{10} emissions (metric tons) using the US EPA AP-42 model. Error bars represent standard deviation of the PM_{10} measurements from the mean PM_{10} emissions. .. 70
Figure 4.2 Feedlot 1 net PM_{10} flux vs. wind speed using TEOM data 71
Figure 4.3 Feedlot 2 net PM_{10} flux vs. wind speed using TEOM data 72

Figure 4.4 Monthly PM_{10} emissions (metric tons) using the SWEEP model. Error bars represent standard deviation of PM_{10} measurements from the mean PM_{10} emissions. 73
Figure 4.5 Monthly mean wind speed from 2008 – 2009. Error bars represent standard deviation of wind speeds from the mean monthly wind speed. 74
Figure C.1 SWEEP "Field Tab" Interface 89
Figure C.2 Daily output information showing the scroll down option to choose between calculated friction velocities and threshold friction velocity. 90
Figure C.3 Sample output from SWEEP showing soil loss parameters 91

List of Tables

Table 2.1 Typical Nonpoint Source Categories (US EPA, 2004) 5
Table 2.2 National Ambient Air Quality Standards for Particulate Matter 7
Table 2.3 Control efficiency guide (Countess Environmental, 2006) 17
Table 3.1 Comparison of laser diffraction and cascade impactor in geometric mean diameter and geometric standard deviation 44
Table 3.2 Comparison of cumulative fraction and particle fraction methods in determining PM fractions and concentrations 47
Table 3.3 Downwind 24-h mass concentrations ($\mu g/m^3$) - laser diffraction vs. low-volume samplers 47
Table 3.4 Upwind 24-h mass concentrations ($\mu g/m^3$) - laser diffraction vs. low-volume samplers 48
Table 3.5 Effect of sampling period (day vs night) on geometric mean diameter (from LD method) 49
Table 3.6 Comparison of mean geometric mean diameter and mean geometric standard deviation between the warm and cold months 51
Table 3.7 Effects of water application on geometric mean diameter and geometric standard deviation. 52
Table 4.1 Mean percent surface material components for the two feedlots 67
Table 4.2 Annual emission rates (metric tons/year) from the two feedlots using US EPA AP-42 wind erosion on a dry exposed surface 68
Table 4.3 Comparison of wind erosion parameters determined using US EPA AP-42 between 2008 and 2009 69
Table 4.4 Estimated PM_{10} emission rates using the SWEEP model 74
Table 4.5 Summary of the meteorological conditions 75
Table 4.6 Comparison of wind erosion parameters for the SWEEP model between 2008 and 2009 75
Table 4.7 Comparison of emission factors (kg/1000hd-day) for the two-year span 77
Table A.1 Cattle on feed 1000+ capacity feedlots (USDA NASS, [2009, 2005, 2000]) 82

Table B.1 Sample data from laser diffraction analysis 83
Table B.2 Geometric mean diameter (GMD) and geometric standard deviation (GSD) values for comparing LD and MOUDI 86
Table B.3 Geometric mean diameter (GMD) and geometric standard deviation (GSD) values for Feedlot 1 (downwind) during warm months (April to October) 87
Table B.4 Geometric mean diameter (GMD) and geometric standard deviation (GSD) values for Feedlot 1 (downwind) during cold months (November to March) 88

List of Acronyms

ACFA	Alberta Cattle Feeders' Association
AERMOD	American Meteorological Society/Environmental Protection Agency Regulatory Model
AP-42	US EPA Compilation of Air Pollutant Emission Factors
ARD	Air Resources Division
CAA	Clean Air Act
CAFO	Concentrated Animal Feeding Operation
CARB	California Air Resources Board
d_a	Equivalent aerodynamic diameter (μm)
d_p	Particle diameter (μm)
EF	Emission Factor (kg/1000 hd-day)
EU	European Union
FAO	Food and Agriculture Organization
FEM	Federal Equivalent Method
FRM	Federal Reference Method
GMD	Geometric Mean Diameter
GSD	Geometric Standard Deviation
ISO	International Organization for Standardization
LD	Laser Diffraction
LV	Low-Volume
MC	Pen surface moisture content (%)
m_j	Mass fraction of particles in the jth size range (dimensionless)
MMD	Mass Median Diameter (μm)
MOUDI	Micro-Orifice Uniform Deposit Impactor
MRI	Midwest Research Institute
MsLI	Multi-stage Liquid Impinger
NAAQS	National Ambient Air Quality Standards
NASS	National Agricultural Statistics Service
NGI	New Generation Impactor
NRC	National Research Council
NRCS	National Resources Conservation Service
NSPS	New Source Performance Standards
$PF_{2.5}$	$PM_{2.5}$ fraction
PF_{10}	PM_{10} fraction
P_i	Erosion potential (g/m^2)
PM	Particulate matter
$PM_{2.5}$	Particulate matter with equivalent aerodynamic diameter of 2.5 μm or less
PM_{10}	Particulate matter with equivalent aerodynamic diameter of 10 μm or less
PSD	Particle Size Distribution
PTFE	Polytetrafluoroethylene
RAAS	Reference Ambient Air Sampler
Re	Reynolds number (dimensionless)
s	Surface silt content (%)
SJV APCD	San Joaquin Valley Air Pollution Control District

SWEEP	Single-event Wind Erosion Evaluation Program
TEOM ™	Tapered-Element Oscillating Microbalance
TSP	Total suspended particulates
u	Wind speed (m/s)
u_t	Threshold wind speed (m/s)
u^*	Friction velocity (m/s)
u^*_t	Threshold friction velocity (m/s)
USDA	United States Department of Agriculture
US EPA	United States Environmental Protection Agency
USDA ARS	United States Department of Agriculture Agricultural Research Service
USDA SCS	United States Department of Agriculture Soil Conservation Service
VMT	Vehicle miles traveled (miles/year)
VOCs	Volatile Organic Compounds
W	Mean vehicle weight (tons)
W^*_e	Wind erosive energy (m^3/s^3)
WEPS	Wind Erosion Prediction System
WRAP	Western Regional Air Partnership
z	Height (m)
z_o	Surface roughness (m)

List of Symbols

χ	Shape factor (dimensionless)
κ	von Karman constant (0.4)
ρ_a	Air density (g/cm^3)
ρ_p	Particle density (g/cm^3)

Acknowledgements

I would like to acknowledge our dear Lord Jesus Christ who gave me wisdom and knowledge to get through with my MS studies here at Kansas State University and had kept me strong through the tumultuous times especially during the loss of my mom which occurred two weeks before I got here in the United States. You are an amazing God indeed and worthy of all praises!

Secondly, I would like to thank my wife, Gilda, for the amazing support, though there were rough times, you are indeed my inspiration on continuing my education and hopefully we can continue to be a blessing to others. To my family, my Dad who is equally supportive of me from the start of my studies here, I thank you for the love and confidence you have put in me. My sister Hazel who was all the more present and active in prayers when I was starting up to the end of my MS studies; the same with my sister Haidee who gave me an opportunity to study here and vouching for me as her little brother who wanted to pursue an advanced degree; my brother Harvey and Ate Mai and my nephews Liam and Lance who equally gave inspiration and joy especially when I talk with them online in between the stressful hours of writing the manuscript.

I would like to thank my adviser, Dr. Ronaldo Maghirang, for opening an opportunity for me to pursue graduate studies here at Kansas State University. Thank you for the knowledge that you have imparted to me from the very beginning of my MS schooling. Thank you for all the advice and thank you for your patience, support and encouragement especially throughout the writing of my manuscript.

I would like to thank both of my committee members, Dr. Jeff Wilson and Dr. Joseph Harner for their inputs and openness to inquiries regarding the writing of the manuscript. Thank you Dr. Wilson for welcoming me at USDA with open arms when I was just starting to know more about the LD instrument.

The support provided by USDA NIFA Special Research Grant, “Air Quality: Reducing Air Emissions from Cattle Feedlots and Dairies (TX and KS)” through Texas AgriLife Research and Extension Center; USDA NIFA Grant No. 2007-35112-17853, "Impact of water sprinkler systems on air quality in cattle feedlots;" and K-State Research and Extension is acknowledged. Cooperation of KLA Environmental Services and feedlot managers/operators is also greatly appreciated and acknowledged.

I also would like to thank the USDA WERU team, Dr. Tatarko, Dr Wagner and Dr. Hagen who helped me a lot in running the SWEEP model. Dr. Hagen, I am thankful to you so much for your vast inputs in my wind erosion discussion.

I would like to thank the BAE Air Quality Team for welcoming me with open arms and taught me nuances of the tasks and responsibilities of being part of the group. Thank you for all the knowledge Ate Edna, you are a big sister to me and a "boss" at the same time; your inputs and advice taught me so much. And to Henry, a brother to me who helped me a lot with my program simulation input and thank you for the help academically when I was starting as a graduate student at K-State. To Li, my "senior", who amazes me all the time and a very good friend and mentor to me when I was just starting my courses. To my buddy Curtis, yo! man! I will never forget the certificate of appreciation I got from you when I won the Final Four Tournament prediction. Haha!

To the Filipino community who have embraced Gilda and I as part of the group; all of you who were hospitable and caring to us especially Tita Beth when we first transferred to Jardine. Thank you for providing the "best" dining table to us; don't worry Tita Beth, it is well taken cared of! To Ate Peewee who was a big sister and mentor to me when I was doing the LD analysis, thank you for the knowledge you shared to me. To Kuya Eric, a big brother and a friend who accommodated me when I was starting my K-State life, you are indeed a blessing to me. To the Moog family who were equally hospitable when I was just starting to know more about Manhattan, KS, I am very blessed to have you as part of my life.

To the Living Word Church family, our pastors, the music ministry, the jail ministry, you are all indeed great spiritual blessings to us! Thank you for all the prayers and support that you have given us, your prayers are more than enough! To Grandpa Rex, Grandpa Marion, Grandma Sharry, Grandma Azer and Grandma Nancy, you are all amazing brothers and sisters in Christ! Thank you for the prayers and support all of you have given us that truly opened the windows of spiritual blessings not only to us, but to others whom we were able to inspire through the message of our Lord Jesus Christ. To Lesa and Barry Patterson, without you, we won't be having such a reliable and an almost brand new means of transportation. It really helped me a lot going to school, church, and back home especially when our old car almost died which was the time when the weather started to get cold. A really perfect blessing from God your whole family is to us! Thank you all so much!

Dedication

I would like to dedicate this manuscript to my loving, caring and very supportive late mother, Purita Gonzales, who died of cancer two weeks before I got to start my graduate studies here in the United States. I know you were happy that I got accepted for studies in the United States. I am so blessed to have a mother like you, yes we the 4-H Kids are so blessed to have a mom like you. I know that you were not able to have a glimpse of this fruit of labor of mine and also attend my graduation but I was more than inspired to dedicate this treasure to you. Though you were already gone when I started my graduate studies, mommy, I miss you, the whole Gonzales family misses you, and we all love you!

CHAPTER 1 - Introduction

1.1 Background

There is increasing concern on air pollutant emissions from cattle feeding operations because of their increasing sizes and geographic concentrations (National Research Council, 2003). These operations generally involve feeding cattle in confined, open areas, with stocking densities of about 14 m^2/hd or greater. Each cattle produces about 900 kg of dry manure during its stay in the feedlot (Sweeten et al., 1998). Warm temperatures, low humidity, and high wind speed promote rapid evaporation of water from the manure making it loose and more susceptible to suspension due to cattle hoof action and wind scouring (Amosson et al., 2006).

Emitted PM is a concern because of potential adverse health and environmental effects (Cole et al., 2008). PM, especially $PM_{2.5}$ (PM with equivalent aerodynamic diameter of less than or equal to 2.5 μm), is readily inhaled and can be deposited in lung tissue, resulting in respiratory ailments (Saxton et al., 1999). Six criteria air pollutants, including PM, and 187 air toxics are regulated by the US Clean Air Act (CAA) (US EPA, 1987) because of their risks to human health and environment. National Ambient Air Quality Standards (NAAQS) were created for the criteria pollutants to help control emissions that pose great risk to human health and environment (US EPA, 1987). Agricultural sources, including cattle feedlots, have not been included in the implementation of NAAQS. Recently, however, US EPA has amended the rule for inclusion of agricultural operations (US EPA, 2004). Also, limited information is available on emission rates from animal feeding operations (US EPA, 1995).

Measuring and characterizing PM is necessary for effective implementation of air quality standards and development of abatement measures. Two important PM characteristics are concentration and size distribution. Measurements of PM concentrations in cattle feedlots have used federal reference method (FRM) samplers (Sweeten et al., 1988; Purdy et al., 2007) and federal equivalent method (FEM) samplers (Bonifacio, 2009; McGinn et al., 2010). Measurements have considered total suspended particulates (TSP), PM_{10} (PM with equivalent aerodynamic diameter of 10 μm or less), and $PM_{2.5}$ (PM with equivalent aerodynamic diameter of 2.5 μm or less). Purdy et al. (2007) used high volume reference samplers for PM_{10} and $PM_{2.5}$ in four feedlots in Southern High Plains. Bonifacio (2009) used FEM tapered element oscillating

microbalance (TEOM^{TM}) PM_{10} monitors to measure PM_{10} concentrations upwind and downwind of two large cattle feedlots in Kansas. Guo et al. (2009) used FRM high-volume, FEM TEOM^{TM}, and low-volume PM_{10} samplers in cattle feedlots in Kansas. McGinn et al. (2010) measured PM_{10} concentrations in cattle feedlots in Australia using FEM beta attenuation mass monitors.

Various techniques have been used to measure particle size distributions (PSDs) in cattle feedlots. Coulter Counters (e.g., Wanjura et al., 2004; Purdy et al., 2007) and cascade impactors (Guo et al., 2011) have been used in several studies. In related areas, laser diffraction has been used. For example, Cao (2009) evaluated particle size distribution in a layer operation through several instruments, including laser scattering particle size analyzer, laser diffraction analyzers, and Coulter Counter.

Laser diffraction has potential to enhance measurement of size distribution and concentrations of various size fractions in animal feeding operations, including cattle feedlots. This method is easier to use and presents a wider size range compared to conventional impactors. This wider size range will be helpful in evaluating concentrations and size distributions of particles more effectively.

Limited studies have been conducted to establish contributions of unpaved roads on cattle feedlot PM emissions and none had reported emissions brought about by wind erosion in cattle feedlots. Wanjura et al. (2004) reported about 80% of total emissions from cattle feedlots are brought about by unpaved roads, while Hamm (2005) reported 53% contribution of unpaved roads toward total emissions. The San Joaquin Valley Air Pollution Control District (SJV APCD) reported an emission factor of 0.72 kg/hd-yr for unpaved roads from a cattle feedlot in San Joaquin Valley, CA. (Countess Environmental, 2006). With limited data, studies on estimating such contributions are necessary to establish better understanding of their mechanisms and develop control methods.

1.2 Objectives

This study was conducted to:

(1) Determine applicability of laser diffraction in measuring size distribution of particles emitted from cattle feedlots; and

(2) Estimate contributions of unpaved roads and wind erosion to total PM emission from cattle feedlots.

Results of the first objective can be useful in deciding whether or not to use laser diffraction as alternative for measuring PSD and PM concentration in open cattle feedlots. The second objective can be useful in estimating which of the miscellaneous sources are major contributors to PM emissions aside from cattle hoof action on pen surfaces.

1.3 References

Amosson, S.H., B. Guerrero, and L.K. Almas. 2006. Economic analysis of solid-set sprinklers to control dust in feedlots. *Journal of Agricultural & Applied Economics* 38.2 (August 2006): 456.

Bonifacio, H. F. 2009. Particulate matter emissions from commercial beef cattle feedlots in Kansas. MS Thesis. Manhattan, Kan.: Kansas State University.

Cao, Z. 2009. Determination of particle size distribution of particulate matter emitted from a layer operation in Southeastern U.S. MS Thesis. Raleigh, N.C.: North Carolina State University.

Cole, N.A., R. Todd, B. Auvermann, and D. Parker. 2008. Auditing and assessing air quality in concentrated feeding operations. *The Professional Animal Scientist* 24: 1-22.

Countess Environmental. 2006. WRAP fugitive dust handbook. Prepared for Western Governor's Association, Denver, Colo. Available at http://www.wrapair.org/forums/dejf/fdh/content/FDHandbook_Rev_06.pdf. Accessed 21 March 2010.

Guo, L., R. G. Maghirang, E. B. Razote, J. Tallada, J. P. Harner, and W. Hargrove. 2009. Field comparison of PM_{10} samplers. *Applied Engineering in Agriculture* 25(5): 737-744.

Guo, L., R. G. Maghirang, E. B. Razote, S. L. Trabue, and L. McConnell. 2011. Concentration of particulate matter in large cattle feedlots in Kansas. For: *Journal of Air & Waste Management* (In review).

Hamm, L.B. 2005. Engineering analysis of fugitive particulate matter emissions from cattle feedyards. MS thesis. College Station, Tex.: Texas A&M University.

McGinn, S.M., T.K. Flesch, D. Chen, B. Crenna, O.T. Denmead, T. Naylor, and D. Rowell. 2010. Coarse particulate matter emissions from cattle feedlots in Australia. *Journal of Environmental Quality* 39(3): 791-798.

National Research Council (NRC). 2003. Air emissions from animal feeding operations: Current knowledge, future needs. Washington, D.C.: National Academies Press.

Purdy, C.W., R.N. Clark, and D.C. Straus. 2007. Analysis of aerosolized particulates of feedyards located in the Southern High Plains of Texas. *Aerosol Science and Technology* 41(5): 497–509.

Saxton, K., D. Chandler, and W. Schillinger. 1999. Wind erosion and air quality research in the Northwest U.S. Columbia Plateau: Organization and progress. In E.E. Stott, R.H. Mohtar, and G.C. Steinhardt (eds). *Sustaining the Global Farm – Selected papers from the 10th International Soil Conservation Organization Meeting*, 24-29 May, West Lafayette, Ind.

Sweeten, J.M., C.B. Parnell, R.S. Etheredge, and D. Osborne. 1988. Dust emissions in cattle feedlots. *Veterinary Clinics of North America, Food Animal Practice* 4(3): 557-578.

Sweeten, J.M., C.B. Parnell, B.W. Shaw, and B.W. Auvermann. 1998. Particle size distribution of cattle feedlot dust emission. *Transactions of the ASAE* 41(5): 1477-1481.

U.S. Environmental Protection Agency (US EPA). 1987. *National ambient air quality standards*. 40 CFR Part 70. Research Triangle Park, NC: US EPA. Available at http://www.epa.gov/air/caa. Accessed 10 July 2010.

U.S. Environmental Protection Agency (US EPA). 1995. *AP-42: Chapter 9 Food and agricultural industries.* Research Triangle Park, NC: US EPA. Available at http://www.epa.gov/ttn/chief/ap42/ch09/index.html. Accessed 10 July 2010.

U.S. Environmental Protection Agency (US EPA). 2004. *Use of a performance based approach to determine data quality needs for the PM-coarse (PMc) standard*. Research Triangle Park, NC: US EPA. Available at http://www.epa.gov/airnow/particle/pm-color.pdf. Accessed 10 July 2010.

Wanjura, J.D., C.B. Parnell, B.W. Shaw, and R.E. Lacey. 2004. A protocol for determining a fugitive dust emission factor from a ground level area source. ASAE/CSAE Paper No. 044018. St. Joseph, Mich.: ASAE.

CHAPTER 2 - Literature Review

2.1 Particulate Emissions from Cattle Feedlots

2.1.1 Background

In the U.S., there has been a steady increase in the number of beef cattle slaughtered from 2004 to 2008, with a slight decrease in 2009 (USDA, 2009). The number of cattle feedlots, however, has generally decreased, indicating greater stocking densities (USDA, 2009, 2005, 2000). A mixture of PM and gases emanate from these feedlots (Bunton et al., 2007), raising concerns on the health of nearby residents.

Beef cattle feedlots are considered non-point or open sources because emissions do not originate from a specific source like a chimney, stack or vent (ARD-42, 2010). Airborne particles that originate from cattle feedlots and other non-point sources (Table 2.1) are called fugitive dust emissions (Ferguson et al., 1999).

Table 2.1 Typical Nonpoint Source Categories (US EPA, 2004)

Fugitive Dust	Construction Mining and Quarrying Paved and Unpaved Roads Agricultural Tillage Beef Cattle Feedlots
Open Burning	Open Burning (residential municipal solid waste, yard waste, and land clearing debris) Structure Fires Prescribed Fires Wildfires Agricultural Field Burning
Fuel Combustion	Residential Wood Combustion Other Residential Fuel Combustion Industrial Fuel Combustion Commercial/Institutional Fuel Combustion
Ammonia	Animal Husbandry Agricultural Fertilizer Application Agricultural Fertilizer Manufacturing Wastewater Treatment

2.1.2 Sources of Particulate Matter in Cattle Feedlots

PM emissions in cattle feedlots come from various sources: cattle activity inside pens, vehicle movement along unpaved roads, feed mills, and wind erosion. The major contributing source for feedlot emissions is cattle hoof action on the dry and loose pen surface, which is a mixture of soil and manure. Figure 2.1 shows a schematic diagram of the pen surface in cattle feedlots (ACFA, 2002). The topmost layer of the pen surface (i.e., manure pack) consists of manure that acts as a sponge as it absorbs water from rain, snow, or urine. It has capacity to hold enough water (up to 25 mm of precipitation) during dry periods, and water readily evaporates from the surface, making it loose. The gleyed or second layer, about 5 to 10 cm thick, is impermeable because it hinders salt, nutrient, and water penetration to lower layers. This layer is formed by the transformation of organic matter, gel, and slimes aided by poor drainage and lack of oxygen. The third layer is compacted soil/manure layer, about 15 cm thick and made of soil mixed with organic matter from manure. The last layer is natural soil, commonly loam- or clay-based soil (ACFA, 2002).

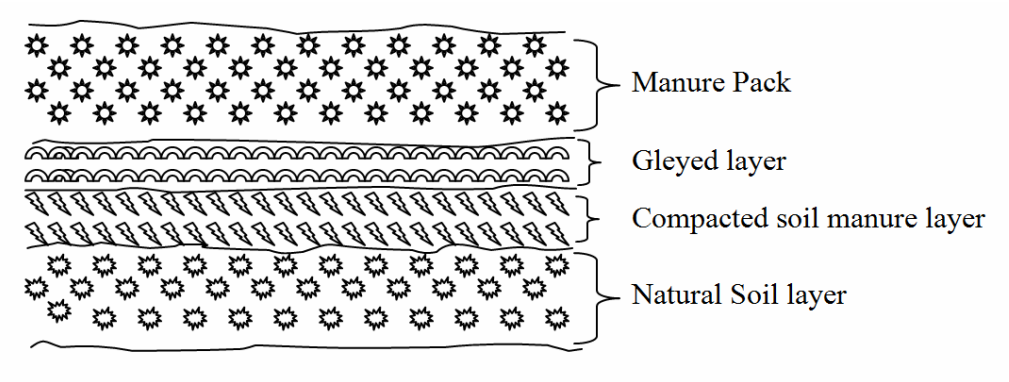

Figure 2.1 Four distinct layers of the pen surface (adapted from: ACFA, 2002)

2.1.3 PM Regulations in Cattle Feedlots

The NAAQS for PM_{10} and $PM_{2.5}$ (Table 2.2, US EPA, 2006a) have been considered applicable to open cattle feedlots. Emission factors for open cattle feedlots have also been published; for inventory purposes, a PM_{10} emission factor of 17 tons per 1000 head throughput per year (US EPA, 1997) can be used for cattle feedlots.

Table 2.2 National Ambient Air Quality Standards for Particulate Matter (Source: http://www.epa.gov/air/criteria.html)

Particle Size	Primary Standard ($\mu g/m^3$)	Averaging Times
PM_{10}	150	24 h
$PM_{2.5}$	15	Annual (arithmetic mean)
	35	24 h

2.1.4 Measurement of PM and Size Distribution in Feedlots

Limited information is available on concentrations of various size fractions and particle size distribution in cattle feedlots. Most published data have been from cattle feedlots in Texas. Sweeten et al. (1988) investigated three cattle feedlots in Texas and reported net total suspended particulate (TSP) concentration of 412 ± 271 $\mu g/m^3$ and median particle diameter of 10.2 ± 1.2 μm. They also noted that dust concentrations were high during early evening and low during early morning. In a related study, Sweeten et al. (1998) reported mean TSP concentration of 700 ± 484 $\mu g/m^3$ and mean PM_{10} concentration of 285 ± 214 $\mu g/m^3$ in three cattle feedlots in Texas. In addition, they observed mass median diameters of particles of 9.5 ± 1.5 μm for TSP samplers and 6.9 ± 0.8 μm for PM_{10} samplers.

Hamm (2005) reported a range of 113 to 6000 $\mu g/m^3$ during a summer sampling period in a feedlot in Texas. The feedlot condition was dry with an average temperature of 38 ºC during the day and 21 ºC at night, such that relatively high concentrations of PM were expected.

Purdy et al. (2007) measured PM from four large feedlots in Texas. They reported that three of the four feedlots exceeded the 24-h PM_{10} NAAQS. Mean PM_{10} particle sizes for the feedlots were measured using a laser strategic aerosol monitor. Median PM_{10} size was 8.3 μm downwind and upwind of the feedlots.

Razote et al. (2007) investigated a cattle feedlot in western Kansas using tapered element oscillating microbalances (TEOMs) and reported net PM_{10} concentrations of 115 ± 80 $\mu g/m^3$ and mean geometric mean diameter (GMD) of 11.4 ± 2.1 μm. In a related study, Guo et al. (2009) measured PM_{10} concentrations using high-volume, TEOMs, and low-volume PM_{10} samplers in two cattle feedlots in Kansas.

In two cattle feedlots in Australia, McGinn et al. (2010) reported mean 24-h PM_{10} concentrations ranging from 9 to 61 $\mu g/m^3$. Feedlot PM_{10} 24-h concentrations were close to or exceeded European Union (EU) and Australian standards twice during the 10-day sampling campaign but did not exceed the US EPA 24-h NAAQS for PM_{10}..

2.1.5 Control of PM Emissions

Feedlot operators and managers have implemented abatement strategies to control dust emissions. The most basic type of abatement is application of water. Razote et al. (2006) indicated decrease in PM_{10} emission potential of a simulated pen surface from 19.2 mg (control) to 3.4 mg (at 3.2 mm water) and 2.3 mg (at 6.4 mm water). Bonifacio et al. (2011) reported a control efficiency range of 32-80 % for PM_{10} of a water sprinkler system in a feedlot.

Pen surface moisture content should be maintained at a level that minimizes both odor and dust emissions. Davis et al. (1997) stated that the pen surface moisture content should be kept at 25 to 35 %. Too much moisture promotes fly and odor problems, while too dry of a pen can lead to significant dust problems.

Another potential abatement strategy is application of materials, including wheat straw and saw dust, on the pen surface. Other control methods include pen cleaning to reduce the amount of loose manure in the pen surface (Rahman et al., 2008). The removed manure is placed in storage or composting area and sometimes covered with soil.

Manipulation of the stocking density, the number of cattle inside the pen, is also a potential dust control measure. Increasing stocking density results in moisture accumulation, causing the pen surface to be compact and less vulnerable to PM emissions (Romanillos and Auvermann, 1999). Razote et al. (2006) mentioned that even without adding water, compacted surface layers could reduce potential emissions (with respect to vertical hoof action) by 30 %. For low and medium moisture contents (20-30 %), soil surface compaction is achieved through cattle trampling (Mullholland and Fullen, 1991; Scholefield and Hall, 1985).

Emissions can also be reduced by feeding cattle during late afternoon or early evening – periods of increased cattle activity (Sweeten et al., 1988). Wilson et al. (2002) found significant reductions in dust concentrations in cattle feedlots by altering feeding strategies. In their study, cattle in control pens were fed normal daily rations (33 %, 33 % and 34 % of total feed rations at 7:10 AM, 10:00 AM, and 12:00 PM, respectively) while cattle in another set of pens were fed

30%, 20 %, and 50 % at 7:00 AM, 10:00 AM, and 6:30 PM, respectively. Mean PM concentrations were 177 ± 2 μg/m^3 for control pens and 97 ± 16 μg/m^3 of dust for test pens.

Use of shelterbelts and windbreaks can also help in managing dust emissions from open cattle feedlots. This method utilizes trees or vegetation to capture particulates downwind and reduce wind speed toward the site, reducing potential for wind erosion (Carter, 2006).

2.2 Particle Size and Size Distribution

2.2.1 Particle Size

Particle size is one of the most important characteristics of particles. Environmental concerns associated with exposure to PM can be narrowed down into particles being inhaled, which are deposited in different areas of the respiratory system based on their size. Health-based particle-size selective sampling (TSI, 2009) classification of particles with respect to median aerodynamic diameter are as follows: 100 μm (inhalable fraction or fraction of particles that enter the respiratory system through the nose or mouth), 10 μm (thoracic fraction or portion of the inhalable fraction that passes through the larynx and penetrate into the trachea and the bronchial region of the lungs), and 4 μm (respirable fraction or portion of the inhalable fraction that enters the alveoli).

In medical research, deposition pattern and bioavailability are defined using particle size of drug materials as it is allowed to penetrate through the respiratory system during inhalation (Pilcer et al., 2008). A size range of about 1 to 5 μm is the optimum range for particles to deposit deep into the pulmonary system. Larger particles are trapped in the oro-pharynx, while submicrometer particles remain suspended in air for exhalation (Bosquillon et al., 2004).

Vincent (2007) summarized the classification of typical aerosols. Combustion sources such as fume dominate fine (diameter between 0.1 and 2.5 μm) and ultrafine particle regions (diameter < 0.1 μm), while soil dust, construction dust, and road dust are predominantly in the coarser region (diameter > 2.5 μm) (Watson et al., 2000; Lin et al., 2005).

Particle characterization usually involves defining its equivalent diameter. For a spherical particle, particle diameter is unique compared to a non-spherical particle, which does not possess a specific diameter. The concept of equivalent diameter has been used to describe sizes of non-spherical particles. This concept involves determining the size of an equivalent

sphere that embodies the same properties as the particle in question. At times a single equivalent sphere can be used to represent the behavior of a non-spherical particle in a measurement technique like sieving, sedimentation and microscopy. Some techniques require rigorous computations because the particle behaves differently in various orientations. The laser diffraction method involves measurement of the light scattering of particles, which are usually different from one angle to another. As such, the different scattering patterns are averaged during the analysis.

Another important factor that affects particle behavior is particle density. For instruments that measure volume percent, it is necessary to know particle density to compute the mass. Particle density is also important in calculating and changing from the equivalent sphere diameter (d_p) to its equivalent aerodynamic diameter (d_a). Another critical parameter is particle shape. Various descriptive terms can be applied to particle shape, but for ease of analysis, this property is captured by the incorporation of shape factor (χ) into equations for particle size analysis. For spherical particles, $\chi = 1$.

2.2.2 Geometric Mean Diameter and Geometric Standard Deviation

A size distribution is a collection of particles characterized by properties, such as aerodynamic diameter, number, mass or volume fraction. A size distribution is considered monodisperse if 90 % of particles are within 5 % of the median size and polydisperse otherwise (Merkus, 2008). In cattle feedlots, particle size distributions are polydisperse.

For a given size distribution, characteristic parameters are geometric mean diameter (GMD) and geometric standard deviation (GSD) (US EPA, 2010). The GMD (μm) gives the central tendency of a particle size distribution and is expressed as follows (Hinds, 1999):

$$\ln \text{GMD} = \frac{\sum m_j \ln d_{pj}}{\sum m_j} \tag{2.1}$$

where d_{pj} = geometric mean of the jth size range, μm

m_j = mass fraction of particles in the jth size range

The geometric standard deviation (GSD) describes how wide the size distribution is around the GMD and can be calculated as (Hinds, 1999):

$$\ln \mathrm{GSD} = \left(\frac{\sum m_j \left(\ln \frac{d_{p_j}}{\mathrm{GMD}} \right)^2}{\sum m_j} \right)^{1/2} \tag{2.2}$$

2.2.3 Cascade Impactor

Size distribution of airborne particles is typically measured using a cascade impactor. In a cascade impactor, impaction is achieved though a jet of particle-laden air, which is allowed to make contact with a flat impaction plate (Figure 2.2). Particles are separated by having large particles retained on the plate, while smaller particles are delivered with the airflow out of the impaction region, left uncollected. Particles collected on an impaction plate are of specific aerodynamic diameter (Heyder et al., 1986; Marple et al., 1991). The particle size distribution is determined based on the obtained mass fractions of specific size ranges.

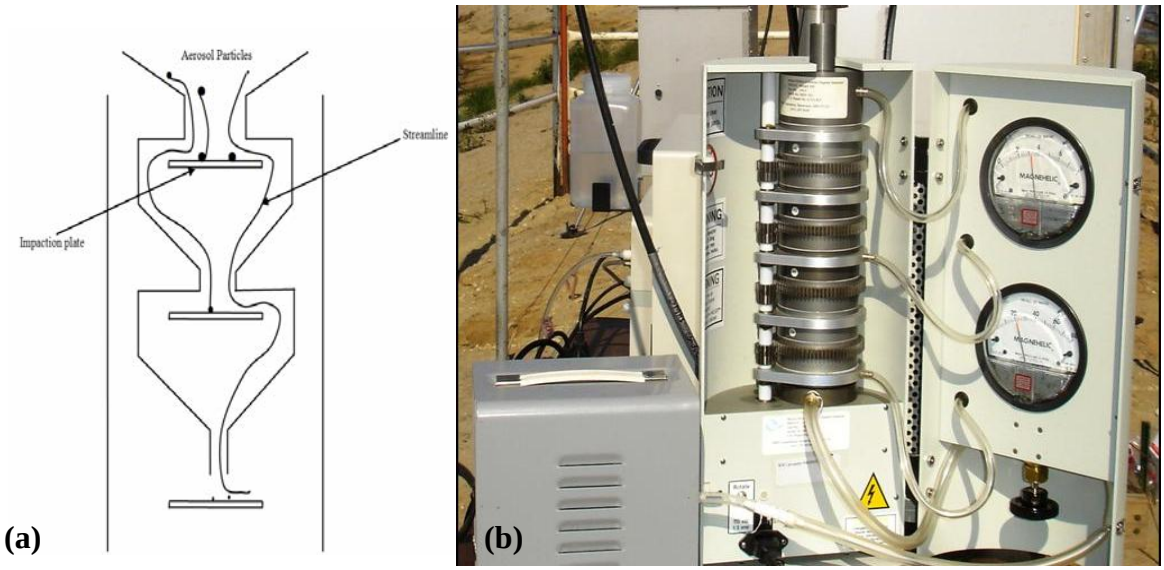

Figure 2.2 Microorifice Uniform Deposit Impactor (MOUDI): (a) schematic diagram; (b) photograph

Various types of cascade impactors are available commercially. This study used the microorifice uniform deposit impactor (MOUDI model 100-R, MSP Corp., 2006), which has

been used in various research. Kleeman et al. (1999) used the MOUDI in evaluating the particle size distribution of emissions from wood burning, meat charbroiling, and cigarette smoking. Wood smoke and meat charbroiling had dominant particles in the range of about 0.1 to 0.2 μm, while particles in cigarette smoke was in the range of 0.3 to 0.4 μm. Kleeman et al. (2000) reported that the smoke from gasoline-powered, light-duty vehicles and light-duty diesel trucks did not differ with particle sizes ranging from 0.1 to 0.2 μm. In a city with dense traffic, Martuzevicius et al. (2004) reported a significant amount of $PM_{2.5}$ was contributed by particles with d_{50} = 0.32 to 1.0 μm. Fang et al. (2005) evaluated the particle size distribution of atmospheric aerosols at a traffic site during the winter period using MOUDI and nano-MOUDI. The average mass median diameter (MMD) of particles was 0.99 μm. The PM_{10} represented 94.4 % of TSP, while $PM_{2.5}$ was 68.9 % of TSP.

Airborne bacteria and endotoxins were measured with the MOUDI (Kujundzic et al., 2006). An environmentally controlled chamber was used to simulate conditions in a home during winter and summer seasons. Airborne bacteria were in the size range of 0.32 to 3.2 μm, while endotoxin ranged in size from 0.056 to 3.2 μm.

In cotton production, Miller et al. (2006) measured the size distribution of dust generated from field preparation during harvesting of cotton seed using a MOUDI. They reported that PM_{10} represented 96 % (disking) and 83 % (harvesting) of the total mass measured by the cascade impactor for disking and harvesting, respectively. In addition, $PM_{2.5}$ represented 51 % (disking) and 45 % (harvesting), respectively. Use of a tractor in agricultural field operations was studied by Wang et al. (2009). They reported that 92 % of the TSP collected by the impactor represented PM_{10} particles.

2.2.4 Laser Diffraction Method

2.2.4.1 Light Scattering Theory

Laser diffraction, in a strict sense, is not a true particle size measurement technique, rather it is a particulate system characterization technique (Xu, 2000). Particle size distribution arises from the "best fit" model for light scattering data with the assumption of having spherical particles (Tinke et al., 2008). Mühlenweg and Hirleman (1998) argued that there is not a unique size and shape related diffraction diameter that comes from a diffraction pattern of non-spherical

particle. Merkus (2008) stated that laser diffraction is a model-based particle size distribution calculation from an angular pattern of scattered intensities, and the distribution generated is based on the volume of a collection of spherical particles that has identical light scattering patterns as that of the dispersed sample. As the conditioned beam of light strikes the surface of a particle (Figure 2.3), four types of interactions exist between the particle and beam of light (Merkus, 2008):

(a) Fraunhofer diffraction –diffraction of light at the contour of the particle;
(b) reflection of light at the particle's surface, both inside and outside the particle;
(c) refraction of light at the interface of particle and dispersion medium; and
(d) absorption of light inside the particle.

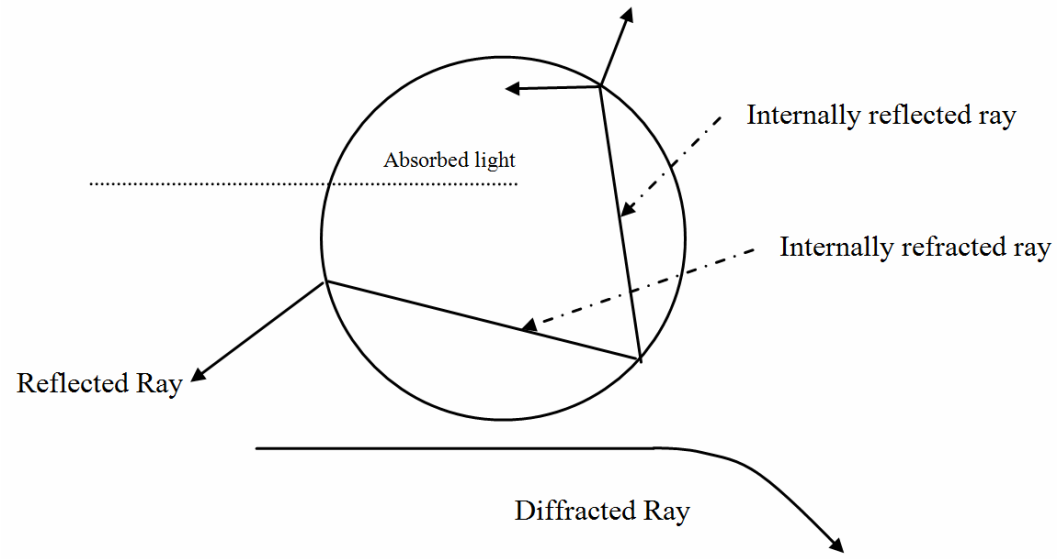

Figure 2.3 Interactions between particle and light beam (adapted from: Merkus, 2008)

The basic approximation for particle size that was developed as the first optical model was the Fraunhofer theory. Assumptions of the theory include (1) interaction exists only between the light and the particle contour; (2) particles are opaque (i.e., without promoting secondary scattering), circular, and two-dimensional; (3) angle of scattered light is small; (4) wavelength of light is much smaller than particle size; and (5) refractive index difference is large.

2.2.4.2 Laser Diffraction Applications

The laser diffraction technique is widely used in pharmaceutical and medical fields and has been standardized (ISO, 1999). Kippax (2005) cited the following advantages:

(a) range of applicability – characterization of a wide variety of products/components can be done, from aerosols (sprays, dry powders) to suspension and other wet samples;

(b) wide dynamic range – a single measurement can detect equally the well-dispersed and agglomerated particles;

(c) speed of measurement – single measurement done within 400 μs;

(d) measurement repeatability – allows a rapid acquisition of data within a single result that promotes multiple repetitive measurements to be averaged;

(e) ease of verification – no calibration needed and can be verified with readily available NIST-traceable standards.

Tinke et al. (2008) noted that in measuring particle size distribution, it is important to consider (a) the orientation of non-spherical particles, (b) the limited angular resolution of detectors, and (c) the limited angular scattering information and intensities for small particles. Results from laser diffraction instruments may vary and are known to be affected by (a) sphericity assumption, (b) type of curve fitting, and (c) limitations of applied algorithms in the deconvolution/conversion of scattered data.

Merkus (2008) stated that materials for analysis can undergo dispersion via a liquid or a gaseous media as long as the dispersion medium is transparent and that the refractive index of the media (dispersant) is different from that of particles. Dry dispersion is used to prevent the dissolution of particles into the medium. Air is the common medium for this type of dispersion. Steady streams of particles can be achieved using a vibrating tray and powder container, while zigzag channels are used for cohesive powders to minimize agglomeration of particles. Very cohesive powders or particles that are already in a mixture with a liquid (suspensions, emulsions, pastes) require that they undergo analysis using wet dispersion. This type of dispersion is advantageous because it allows for the analysis of the same sample aliquot and also promotes optimization of dispersion parameters, such as the dispersant amount, concentration of particles, time, and dispersion energy.

Numerous studies, particularly in the medical and pharmaceutical fields, have applied laser diffraction. Different starch granules suspended in water were analyzed by Manek et al. (2005) using the Beckman Coulter LS 13 320 with the universal liquid module. The same instrument was also used by Griffitt et al. (2008) in characterizing sizes of nanometallic particles in aquatic organisms. Rodríguez and Uriarte (2009) compared the instrument with the dry-sieving method and found an $R^2 = 0.76$ between the two methods.

Pilcer et al. (2008) investigated correlation between a laser diffraction analyzer (Mastersizer 2000 and Spraytec) and inertial impactors, such as the multi-stage liquid impinger (MsLI) and the new generation impactor (NGI), when applied to size distribution determination of aerosolized powder formulations. Results showed linear relationships with $R^2 > 0.9$.

Cao (2009) studied particulate emissions from a layer operation in southeastern U.S and reported that different seasons affected particle size distribution. The laser diffraction analyzer Beckman Coulter LS 13 320 measured particle size distributions of 19.2 ± 1.27 μm during the fall season, 17.1 ± 0.81 μm in winter, and 18.4 ± 1.44 μm during spring.

Comparative studies of various methodologies have been well documented using a range of materials such as sediments, soils, industrial powders, and reference materials (Rodríguez and Uriarte, 2009). Previous studies have compared dry-sieving methodology and laser diffraction (Rodríguez and Uriarte, 2009), sedimentation and laser diffraction (Di Stefano et al., 2010), cascade impaction and laser diffraction (Pilcer et al., 2008; Martin et al., 2006; Ziegler and Wachtel, 2005; Kwong et al., 2000), and laser diffraction and image analysis (Kelly et al., 2006). However, very few studies (Guo et al., 2009; Purdy et al., 2007) have used PM from cattle feedlots as media for comparison.

2.3 Emissions from Unpaved Roads and Wind Erosion

2.3.1 Unpaved Roads

Unpaved roads are another major source of dust from agricultural areas (Table 2.1). Compared to paved roads in which a finite reservoir of particles is available for resuspension (Kuhns et al., 2010), there exists an infinite ensemble of PM ready for resuspension in unpaved roads (Gillies et al., 2005). Large amounts of PM are generated through the action of the rolling

wheels of vehicles on roads composed of graded and compacted roadbeds. Pulverization occurs after, thus creating much smaller particles that are easily ejected (US EPA, 2006b).

Factors that affect the extent of dust generation from unpaved roads include the nature of the road surface (dirt or gravel roads) and traffic volume (Succarieh, 2000). Thenoux et al. (2007) mentioned that the amount of dust emitted is dictated by the amount of fine particles that comprise the surface material, physicochemical properties (percentage of fine particles, particle size and plasticity), and state of the road (compaction and homogeneity). Since emission from unpaved roads is contributed by the movement of vehicles, effects of this action are influenced most commonly by weather conditions and behavior of the operator driving the vehicle (Etyemezian et al., 2003).

2.3.1.1 Control Strategies for Unpaved Roads

Control of unpaved road dust emissions requires application of different materials that attract moisture, bind dust particles together, and/or seal the surface. Ferguson et al. (1999) enumerated control strategies, including application of chloride salts that act as moisture attractants and application of organic or synthetic compounds that promote aggregation. The latter method provides a road surface much like that of a pavement, but at a lower cost.

Application of water is the simplest method of suppressing dust particles in unpaved roads, although water must be applied more frequently during prolonged dry periods. Reed and Organiscak (2007) observed TSP control efficiencies of 74 % for 3-4 h following water application at 2.08 L/m^2 (0.46 $gallons/yd^2$) and 95 % for 30 min after water application at 0.59 L/m^2 (0.13 $gallons/yd^2$). Critical time interval between two trucks was also studied and the maximum dust concentration existed at 20 s. About a 41 % to 52 % reduction in airborne respirable dust was achieved when the critical time interval was exceeded.

Freeman and Bowders (2007) reported that geotextile application was effective in lowering dust emission for a period of at most 6 months. Dust emission rate from an untreated surface was around two to three times that from a surface with geotextile application. Also, silt content, which was initially 3 % for both treated and untreated surfaces, increased for both surfaces. The treated surface's silt content increased after 6 months to a range of 6 to 12 %, while silt content of the untreated surface increased to about 23 %.

Thenoux et al. (2007) stated that high costs are involved with frequent maintenance on unpaved roads; therefore it is necessary to maintain an effective road management method that

complies with minimum road standards. Whether to control the generation of dust or maintain an unpaved road is a critical management decision.

US EPA has published a control efficiency guide that was the basis for US EPA AP-42 calculations for emissions on unpaved roads (Table 2.3). The control efficiency guide was based on management practice, process change, control device, and reformulation of material for suppression (Countess Environmental, 2006).

Table 2.3 Control efficiency guide (Countess Environmental, 2006)

Control Measure	PM_{10} Control Efficiency	References/Comments
Limit maximum speed on unpaved roads to 25 mph	44 %	Assumes linear relationship between PM_{10} emissions and vehicle speed and an uncontrolled speed of 45 mph
Paved, unpaved roads and unpaved parking areas	99 %	Based on comparison of paved road and unpaved road PM_{10} emission factors
Implement watering twice a day for industrial unpaved roads	55 %	Midwest Research Institute (MRI), 2001
Apply dust suppressant annually to unpaved parking areas	84 %	California Air Resources Board (CARB), 2002

2.3.1.2 Previous Research on Unpaved Road Dust Emissions

Pinnick et al. (1985) reported a bimodal size distribution for the dust generated by various types of vehicles (5-ton shop truck, US Army armored carrier, and US Army tank) on unpaved roadways. Modal mass mean diameters of 4 μm and 45 μm were observed regardless of the type of vehicle or its speed, which ranged from 5 to 12 m/s. The dust loading based on type of soil was also analyzed, with silty soil having predominantly smaller particles and sandy soil having predominantly large particles.

Padgett et al. (2008) measured an hourly average of 6 $\mu g/m^3$ for $PM_{2.5}$ for off-highway vehicles traveling on unpaved roads. Light winds were observed during the sampling day (0.9

m/s to 1.8 m/s) while an average of 3.7 m/s was measured for wind gusts during sampling. TSP concentrations ranged from 50 to 300 $\mu g/m^3$, indicating that most of the dust emitted by off-highway vehicles were larger than $PM_{2.5}$.

Reed and Organiscak (2007) measured haul road dust emissions. A particle size distribution with the majority (85.5 %) as coarse particles was obtained, with 14.5 % being PM_{10} and 3.5 % were less than 3.5 μm in size. Concentrations decreased dramatically 15 m from the haul road and back to background level 30 m away (respirable dust were at 0.05 to 0.04 mg/m^3).

Thenoux et al. (2007) devised a method that facilitated measurement of dust generated from unpaved roads via movement of vehicles. Vehicle speed had the greatest influence on dust generation; size of truck (light vs. medium) and type of tires did not significantly influence dust emission. At approximately 40 km/h, there was a sudden increase in amounts of PM_{10} and $PM_{2.5}$ emitted. This speed can be considered as the speed below which dust emissions from unpaved roads can be minimized.

Padgett et al. (2008) monitored fugitive dust emissions of vehicles traveling on dry, unpaved roads. The dust plume was heterogeneous, with predominantly smaller particles in the upper portion of the plume and predominantly larger particles in the lower portion.

Kuhns et al. (2010) determined the ratio of emission factor (measured in g PM_{10} per km traveled) to vehicle momentum (product of mass and speed, kg-m/s). They found ratios of 0.004 to 0.006 (g PM_{10}/vkt)/(kg-m/s) for a field in Colorado that consisted of a Hueco loamy fine sand (79 % sand, 16 % silt, and 5 % clay) and a value of 0.38 (g PM_{10}/vkt)/(kg-m/s) for a field in Washington that consisted of Selah silt loam and Benwy silt loam (35 % sand, 48 % silt, and 17 % clay). The discrepancy in emission factors was attributed to the unique volcanic ash soil type in the field in Washington. Also, they found that wheeled vehicles (i.e., Heavy Expanded Mobility Tactical Trucks) emitted more PM_{10} than tracked vehicles (i.e., tanks). This difference can be caused by the relative presence of a number of tires for the wheeled vehicle as compared to a tank in which the weight is distributed only to two threads, thereby having more sections or portions of the vehicle for fine particle emission.

2.3.1.3 Unpaved Road Dust Emission Models

Empirical models for estimating emission factors from unpaved roads have been developed. Calculation of emission factors of vehicles traveling on haul roads neglects the effect of vehicle speed (US EPA, 2003). Vehicles traveling at industrial sites follow the equation:

$$EF(g\ PM_{10}/vkt) = 29s^{0.9}M^{0.45} \quad (2.3)$$

where s = silt content of the surface material

M = vehicle mass (metric tons)

vkt = vehicle kilometers traveled per day (vehicle-km/day)

US EPA AP-42 presented the following empirical equation (Countess Environmental, 2006):

$$E = 1.5\left(\frac{s}{12}\right)^{0.9}\left(\frac{W}{3}\right)^{0.45}(VMT)\left(\frac{\text{emission days}}{\text{year}}\right)\left(\frac{1\text{ ton}}{2000\text{ lbs}}\right) \quad (2.4)$$

where E = PM_{10} emission factor (tons/yr)

s = surface material silt content (%)

W = mean vehicle weight (short tons)

VMT = vehicle miles traveled per day (vehicle-miles/day)

2.3.2 Wind Erosion

Wind erosion generally removes the finest particles on the top surface of the parent material. It can cause loss of soil nutrients (Gomes et al., 2003) and water, which makes for a drier environment, degrades sedimentation crusts on the surface of stripped soils, and/or causes abrasion, weathering of rocks at their base where they are in contact with the soil (FAO, 1996). Wind erosion is dominant in arid, exposed areas with insufficient plant cover. Soil erodibility is dictated by topography and texture. Ferguson et al. (1999) stated that, in general, heavy clay soils are less susceptible to wind erosion than loamy soils and that rolling slopes are less vulnerable to wind erosion compared to flat areas or long, gentle slopes.

2.3.2.1 Mechanism of Wind Erosion

Initiation of particle mobilization by wind is governed by different forces acting on particles. Forces such as weight, friction, wind shear stress, and size-dependent inter-particle

cohesion forces determine the extent through which the particle will move. Wind momentum transfer to the erodible surface is brought about by shear stress, which is further dependent on roughness of the particle surface. Threshold wind stress necessary to particle motion initiation is determined by momentum transfer that occurs. The square root of wind shear stress divided by the air density is termed friction velocity, u^*. It is therefore necessary to obtain the roughness length and u^* in order to compute the amount of wind erosion (Gomes et al., 2003).

Shi et al. (2004) stated that forces acting on soil surface particles are classified into external and internal forces. External forces include frontal drag and lifting caused by wind action and impact forces caused by saltating particles as they fall back to the ground. Gravity, attractive force (electrostatic force between particles), water-film, and biological adhesive forces govern internal forces acting upon particles.

Simultaneous processes occurring during wind erosion are shown in Figure 2.4 and are described by Saxton et al. (1999). Particles >500 μm in diameter, too large to be carried away by wind, move along the soil surface via surface creep. Medium-sized particles, about 70-500 μm in diameter, are detached and partially transported with wind, but are then pulled back to the soil surface by gravity in a process called saltation. Continuous saltation tends to set other particles in motion. Both surface creep and saltation become constant at a distance downwind of a non-eroding surface, because these processes are dictated by wind energy. Particles < 100 μm (commonly <50 μm) are liberated and remain suspended as a result of saltation. Such particles can be transported great distances (Saxton et al., 1999). Although wind energy controls the processes, the volume of suspended particles is dictated by PM availability at the soil surface (Gillette, 1977).

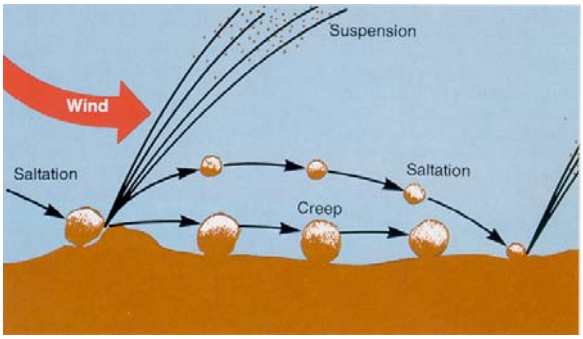

Figure 2.4 Soil erosion by wind (source: http://www.weru.ksu.edu/weps/wepshome.html)

Factors that affect the extent of wind erosion include aridity of climate, soil texture, soil structure, state of the soil surface, vegetation, and soil moisture (FAO, 1996). Climate dryness coupled with the relative strength of prevailing wind is one of the major factors that trigger wind erosion, because these stresses cause the soil to become barren, resulting in the ready ejection of fine particles from the parent surface material. Type of soil dictates the extent to which wind erosion can carry particles from one location to another. If the soil is sticky (clay type), particles resist ejection from the surface; if the soil is composed of coarse particles, on the other hand, particles may be too heavy to be removed by wind erosion. To initiate wind erosion, particles should be at most 80 μm in diameter. Presence of structure-improving materials (i.e., organic matter, iron, lime) makes the soil less fragile and less vulnerable to wind erosion. Presence of sodium or salt leads to a dust layer formation, which is vulnerable to erosion by wind. Presence of stubble and crop residues minimizes wind speed at ground level, inhibiting the action of wind on the soil surface. Soil water content is also important in retarding particle ejection by wind by increasing cohesion of sand and loam (FAO, 1996).

2.3.2.2 Control Strategies for Wind Erosion

Wind erosion is generally controlled by increasing soil cohesion, reducing wind speed at ground level by intercepting some of the wind, reducing amount of exposed bare soil, and reducing amount of time the soil is exposed. Control can be achieved by application of water and organic matter, which can effectively improve soil structure. Alteration of soil properties such as roughness is also effective in reducing wind speed at ground level. A practice considered to be costly is windbreak establishment. Vegetation protects downwind land for approximately ten times its height. Trees are considered to be the most effective windbreaks as they provide the widest area of protection (Ferguson et al., 1999). Aside from trees, small grains, corn, sorghum, sudangrass, sunflowers, tall wheatgrass, sugarcane, and rye strips could also be effective (Skidmore, 1986).

Carter (2006) indicated that since soil particles greater than about 0.5 mm cannot be picked up by wind, soil can be aggregated to a size greater than 0.5 mm. Adequate aggregation is needed if no ground covers exists especially for water repellent sands. Ground covers such as straw and other dry residues are effective if at least 50% of the surface is covered by non-movable residues. Since wind speeds cannot be controlled mechanically as it is naturally

occurring, its impact on the soil surface can be reduced by windbreaks. A 10-m windbreak of two row pines can prevent erosion of up to 100 to 150 m downwind.

2.3.2.3 Wind Erosion Models

Stetler and Saxton (1997) presented the analysis of meteorological data for the calculation of soil loss due to wind. Wind speed was the major factor influencing soil loss, although other factors such as wind direction, precipitation, and temperature also affected soil loss. Stetler and Saxton (1997) reported that variation of wind energy is great at 1-min interval wind speed data than those at 15-min or 60-min intervals. They recommended that 15-min averages of wind speed could provide reasonable estimates for wind energy. Fryrear (1995) presented an equation to calculate wind erosive energy, W^*_e, energy contained in a specific period wind that is readily vulnerable for transport as the threshold condition is exceeded:

$$W_e^* = u(u - u_t)^2 \tag{2.5}$$

where u = average wind speed for each 1-, 15-, and 60-min period (m/s)

u_t = event threshold wind speed (m/s)

W^*_e = erosive wind energy (m^3/s^3)

According to US EPA AP-42 (Countess Environmental, 2006), emissions due to wind erosion on a dry exposed surface can be computed using the following empirical equations:

$$E = 0.5\sum_{i=1}^{N} P_i \tag{2.6}$$

$$P = 58(u^* - u_t^*)^2 + 25(u^* - u_t^*) \tag{2.7}$$

where E = PM_{10} emission factor (g/m^2)

N = number of disturbances per year (total number of days excluding rainy days – a rainy day is a day with at least 0.254 mm of rain – per year)

P = erosion potential (%)

u^* = friction velocity (m/s)

u^*_t = threshold friction velocity (m/s)

Friction velocity is calculated from measured velocity assuming a logarithmic distribution at the surface boundary layer:

$$u(z) = \frac{u^*}{\kappa} \ln \frac{z}{z_o} \quad (2.8)$$

where u(z) = wind speed (m/s)

z = height (m)

z_o = surface roughness (m)

κ = von Karman's constant (0.4)

Friction velocity, u^*, obtained from equation 2.8 is assessed whether it exceeds u^*_t and if it indeed exceeds, then it is regarded as an erosion potential which is then computed using equation 2.7. The corresponding emission factor is computed using equation 2.6. The annual PM_{10} emission is estimated using the following equation (Countess Environmental, 2006):

$$\text{Annual } PM_{10} \text{ Emission} = (E)(\text{field size in } m^2) \quad (2.9)$$

The emission factor for $PM_{2.5}$ is assumed to be 15% of PM_{10} emission factor. Also, different values of control efficiency are given in the literature and controlled PM emissions are estimated by the following equation (Countess Environmental, 2006):

$$\text{Controlled E} = (\text{Uncontrolled E})(1 - \text{Control Efficiency}) \quad (2.10)$$

Several wind erosion models have been developed to quantify soil loss and PM emissions (Webb and McGowan, 2009). One of the modeling systems is the process-based Wind Erosion Prediction System (WEPS) model developed by USDA-ARS. WEPS has a stand-alone sub-model program, Single-event Wind Erosion Evaluation Program (SWEEP). SWEEP includes the erosion sub-model of WEPS and has a graphic interface that enables a single high wind event, wind erosion simulation (Feng and Sharratt, 2009). Input parameters include field, crop, soil, and weather parameters. SWEEP is used to simulate components of soil loss/deposition over a rectangular field as influenced by surface conditions, field orientation, wind direction, and hourly wind speeds (USDA ARS, 2008). Calculated within the model is the u^*_t, which when exceeded promotes soil loss. The model computes soil loss over a series of individual grid cells. The SWEEP model was developed mainly for agricultural lands and croplands; it has not been

tested for open feedlots. McCullough et al. (2001) mentioned that common natural soil profiles are completely different from that of the soil surface profile of feedlots. They added that vegetation is not sustained in feedlots; thereby inhibiting soil water extraction by plant roots. Mielke et al. (1974) stated that uniform moisture content can be found on cattle feedlot profiles.

2.3.2.4 Threshold Friction Velocity

An important factor in wind erosion is u^*_t because it controls both erosion frequency and intensity. This velocity is the capacity of an aeolian surface to resist wind erosion and is the minimum value required for wind erosion to occur. Several factors affect u^*_t: soil moisture, soil salt content, soil texture, surface crust, vegetation distribution, and roughness elements (Shao and Lu, 2000).

Empirical equations for u^*_t are available. For dry, well-sorted sand, Bagnold (1941) came up with the following equation:

$$u_t^* = A\left(\frac{\rho_p - \rho_a}{\rho_a} g d_p\right)^{0.5} \tag{2.11}$$

where A = empirical coefficient of turbulence approximately equal to 1.0 for particle friction Reynolds number > 3.5

ρ_p = particle density (kg/m^3)

ρ_a = air density (1.22 k/m^3)

g = acceleration due to gravity (9.80 m/s^2)

d_p = mean particle diameter (m)

Bagnold (1941) also provided an equation for calculating wind speed at different heights in the form of a Prandtl equation:

$$u = (5.75)(u^*)\left(\log\frac{z}{z_o}\right) \tag{2.12}$$

where u^* = threshold shear velocity (u^* = 0.326 m/s)

z = height for which calculated wind speed is required (m)

z_o = surface roughness based on field data (m)

u = wind speed at height z (m/s)

Shao and Lu (2000) recommended the equation from Greeley and Iversen (1985) based on wind tunnel measurements:

$$u_t^* = \sqrt{A_N\left(\rho_p g \mathrm{d_p} + \frac{\gamma}{\rho_a \mathrm{d_p}}\right)} \tag{2.13}$$

where $A_N = 0.0123$

$\gamma =$ constant ($3\text{x}10^{-4}$ kg/s^2)

In addition to aerodynamic drag and gravity forces considered by Bagnold (1941), cohesive forces and aerodynamic lift were incorporated in equation 2.13. Such was taken into account because equation 2.12 failed to predict existence of the minimum u^*_t for particles with diameters of about 75 μm and further increase of u^*_t with decreasing particle size, making equation 2.13 an accepted predictor for u^*_t for the entire particle size range. Increase of u^*_t with decreasing particle size is attributed to the stronger effect of cohesive forces compared to that of gravitational forces. For particles with d < 50 μm, cohesive force is at least 100 times the gravitational force.

Marticorena et al. (1997) presented the following equations relating u^*_t with soil d_p and ρ_p, depending on the value of Reynolds number (Re):

$$\mathrm{Re} = a\mathrm{d_p}^x + b \tag{2.14}$$

For $0.03 < \mathrm{Re} \leq 10$,

$$u_t^*(\mathrm{d_p}) = 0.129\frac{\left[\frac{\rho_p\, g\, \mathrm{d_p}}{\rho_a}\right]^{0.5}\left[1+\frac{0.006}{\rho_p\, g\, \mathrm{d_p}^{2.5}}\right]^{0.5}}{\left[1.928\left(a\,\mathrm{d_p}^x + b\right)^{0.092} - 1\right]^{0.5}} \tag{2.15}$$

For Re > 10,

$$u_t^*(\mathrm{d_p}) = 0.12\left[\frac{\rho_p\, g\, \mathrm{d_p}}{\rho_a}\right]^{0.5}\left[1+\frac{0.006}{\rho_p\, g\, \mathrm{d_p}^{2.5}}\right]^{0.5}\left(1 - 0.0858\exp\left\{-0.0617\left[\left(a\,\mathrm{d_p}^x + b\right) - 10\right]\right\}\right) \tag{2.16}$$

where $a = 1331$

$b = 0.38$

$x = 1.56$

Equations 2.14 – 2.16 are valid for a large set of experimental threshold velocities obtained using a wind tunnel, with particle densities ranging from 0.21 to 11.35 g/cm^3 and particle diameters ranging from 12 to 1290 μm.

Li et al. (2010) used a simple method to estimate u^*_t for wind erosion in a field in Moab, southeastern Utah. Though the method used the wind tunnel procedures done by Marticorena et al. (1997) and Belnap et al. (2007), this model focused on obtaining the soil surface resistance to disturbance instead of relying mostly on measurement of soil texture or surface roughness. It was also suggested that model inputs normally derived from wind tunnel experiments require assumptions that can be inappropriate for field use, especially for conditions in which soil and roughness elements are heterogeneous.

2.4 Summary

Large cattle feedlots are faced with environmental challenges, including emissions of particulate matter. Research is needed to establish health and environmental effects of particulate matter from cattle feedlots. Measurement, characterization, and modeling of particulate emissions also are important in developing a better understanding of the magnitude of emissions and their sources. Various methods, including laser diffraction, need to be evaluated in reference with more common measurement devices (e.g., cascade impactors) to determine their appropriateness in feedlots. Current standards do not address particulate emissions specifically from cattle feedlots. There exists a need to characterize and identify particulate emissions from cattle feedlots and from what types of sources they originate.

2.5 References

Alberta Cattle Feeders' Association (ACFA). 2002. Beneficial management practices – Environmental manual for feedlot producers in Alberta. Calgary, Alberta: ACFA. Available at http://www1.agric.gov.ab.ca/$department/deptdocs.nsf/all/epw5837/$FILE/bmp_feedlot.pdf. Accessed 15 May 2010.

ARD-42. 2010. Environmental fact sheet: Fugitive dust. New Hampshire Department of Environmental Services Air Resources Division. Available at http://des.nh.gov/organization/commissioner/pip/factsheets/ard/documents/ard-42.pdf. Accessed 10 July 2010.

Bagnold, R.A. 1941. The physics of blown sand and desert dunes. London: Methuen.

Belnap, J., S.L. Phillips, J.E. Herrick, and J.R. Johansen. 2007. Wind erodibility of soils at Fort Irwin, California (Mojave Desert), USA, before and after trampling disturbance: Implications for land management. *Earth Surface Processes Landforms* 32: 75-84.

Bonifacio, H., R. G. Maghirang, E. B. Razote, B. W. Auvermann, J. P. Harner, J. P. Murphy, L. Guo, J. W. Sweeten, and W. L.Hargrove. 2011. Particulate control efficiency of a water sprinkler system at a beef cattle feedlot in Kansas. *Transactions of the ASABE* (In press).

Bosquillon, C., P. Rouxhet, F. Ahimou, D. Simon, C. Culot, V. Préat, and R. Vanbever. 2004. Aerosolization properties, surface composition and physical state of spray-dried protein powders. *Journal of Controlled Release* 99: 357-367.

Bunton, B., P. O'Shaughnessy, S. Fitzsimmons, J. Gering, S. Hoff, M. Lyngbye, P.S. Thorne, J. Wasson and M. Werner. 2007. Monitoring and modeling of emissions from concentrated animal feeding operations: Overview of methods. *Environmental Health Perspectives* 115(2): 303-307.

Cao, Z. 2009. Determination of particle size distribution of particulate matter emitted from a layer operation in Southeastern U.S. MS Thesis. Raleigh, N.C.: North Carolina State University.

Carter, D. 2006. Wind erosion – prevention and management. Department of Agriculture and Food, Government of Western Australia. Available at http://www.agric.wa.gov.au/PC_92240.html?s=1001. Accessed 15 May 2010.

Countess Environmental. 2006. WRAP fugitive dust handbook. Prepared for Western Governor's Association, Denver, Colo. Available at http://www.wrapair.org/forums/dejf/fdh/content/FDHandbook_Rev_06.pdf. Accessed 21 March 2010.

Davis, J.G., T.L. Stanton, and T. Haren. 1997. Feedlot manure management. *Livestock Series No. 1.220*, Colorado State University Cooperative Extension. Available at http://www.cde.state.co.us/artemis/UCSU20/UCSU2062212202002INTERNET.pdf. Accessed July 10, 2010.

Di Stefano, C., V. Ferro, and S. Mirabile. 2010. Comparison between grain-size analyses using laser diffraction and sedimentation methods. *Biosystems Engineering* 106(2): 205-215.

Etyemezian, V., H. Kuhns, J. Gillies, M. Green, M. Pitchford, and J. Watson. 2003. Vehicle-based road dust emission measurement: I – Methods and calibration. *Atmospheric Environment* 37: 4559-4571.

Fang, G., Y. Wu, J. Rau, and S. Huang. 2005. Traffic aerosols (18 nm ≤ particle size ≤ 18 μm) source apportionment during the winter period. *Atmospheric Research* 80: 294-308.

Feng, G. and B. Sharratt. 2009. Evaluation of the SWEEP model during high winds on the Columbia Plateau. *Earth Surface Processes and Landforms* 34: 1461-1468.

Ferguson, J.H., H.W. Williams, and D.L.Pfost. 1999. Fugitive dust: Nonpoint sources. Columbia, Miss.: University of Missouri-Columbia. Available at http://extension.missouri.edu/explorepdf/agguides/agengin/g01885.pdf. Accessed 15 May 2010.

Food and Agriculture Organization (FAO). 1996. Land husbandry – Components and strategy. FAO Soils Bulletin – 70. Available at http://www.fao.org/docrep/t1765e/t1765e0t.htm. Accessed 15 May 2010.

Freeman, E.A. and J.J. Bowders. 2007. Geotextiles for dust control on unpaved roads. Geosynthetics, January16-19, 2007, Washington, DC. Available at http://www.geotech.missouri.edu/pdf/Freeman-Bowders-Dust-GT-Geosyn07-11.21.06DistrCopy.pdf. Accessed 15 May 2010.

Fryrear, D.W. 1995. Soil loss by wind erosion. *Soil Science Society of America Journal* 59: 668-672.

Gillette, D.A. 1977. Fine particulate emissions due to wind erosion. *Transactions of the ASABE* 20(5): 890-897.

Gillies, J.A., V. Etyemezian, H. Kuhns, D. Nicolich, and D. Gillette. 2005. Effect of vehicle characteristics on unpaved road dust emissions. *Atmospheric Environment* 39: 2341-2347.

Gomes, L., J.L. Arŕue, M.V. López, G. Sterk, D. Richard, R. Gracia, M. Sabre, A. Gaudichet, and J.P. Frangi. 2003. Wind erosion in a semiarid agricultural area of Spain: the WELSONS project. *Catena* 52: 235-256.

Greeley, R. and J.D. Iversen. 1985. Wind as a geological process on earth, mars, venus and titan. New York: Cambridge University Press.

Griffitt, R.J., J. Luo, J. Gao, J.C. Bonzongo, and D.S. Barber. 2008. Effects of particle composition and species on toxicity of metallic nanomaterials in aquatic organisms. *Environmental Toxicology and Chemistry* 27(9): 1972-1978.

Guo, L., R. G. Maghirang, E. B. Razote, J. Tallada, J. P. Harner, and W. Hargrove. 2009. Field comparison of PM_{10} samplers. *Applied Engineering in Agriculture* 25(5): 737-744.

Hamm, L.B. 2005. Engineering analysis of fugitive particulate matter emissions from cattle feedyards. MS thesis. College Station, Tex.: Texas A&M University.

Heyder, J., J. Gebhart, G. Rudolf, C.F. Schiller, and W. Stahlhofen. 1986. Deposition of particles in the human respiratory tract in the size range 0.005-15 μm. *Journal of Aerosol Science* 17(5): 811-825.

Hinds, W.C. 1999. Aerosol technology: properties, behavior, and measurement of airborne particles. 2nd ed. New York: John Wiley & Sons.

ISO, 1999. ISO13320-1 Particle size analysis – Laser diffraction methods, part 1: General principles. ISO Standards Authority. Available at http://www.iso.org. Accessed 15 May 2010.

Kelly, R.N., K.J. DiSante, E. Stranzl, J.A. Kazanjian, P. Bowen, T. Matsuyama, and N. Gabas. 2006. Graphical comparison of image analysis and laser diffraction particle size analysis data obtained from the measurements of nonspherical particle systems. *American Association of Pharmaceutical Scientists* 7(3): E1-E14.

Kippax, P. 2005. Appraisal of the laser diffraction particle-sizing technique. *Pharmaceutical Technology* 29(3): 88-96.

Kleeman, M.J., J.J. Schauer, and G.R. Cass. 1999. Size and composition distribution of fine particulate matter emitted from wood burning, meat charbroiling and cigarettes. *Environmental Science & Technology* 33(20): 3516-3523.

Kleeman, M.J., J.J. Schauer, and G.R. Cass. 2000. Size and composition distribution of fine particulate matter emitted from motor vehicles. *Environmental Science & Technology* 34(7): 1132-1142.

Kuhns, H., J. Gillies, V. Etyemezian, G. Nikolich, J. King, D. Zhu, S. Uppapalli, J. Engelbrecht, and S. Kohl. 2010. Effect of soil type and momentum on unpaved road particulate matter emissions from wheeled and tracked vehicles. *Aerosol Science and Technology* 44: 187-196.

Kujundzic, E., M. Hernandez, and S. Miller. 2006. Particle size distributions and concentrations of airborne endotoxin using novel collection methods in homes during winter and summer seasons. *Indoor Air* 16(3): 216-226.

Kwong, W.T.J., S.L. Ho, and A.L. Coates. 2000. Comparison of nebulized particle size distribution with Malvern laser diffraction analyzer versus Andersen cascade impactor and low-flow Marple personal cascade impactor. *Journal of Aerosol Medicine* 13(4): 303-314.

Li, J., G.S. Okin, J.E. Herrick, J. Belnap, S.M. Munson, and M.E. Miller. 2010. A simple method to estimate threshold friction velocity of wind erosion in the field. *Geophysical Research Letters* 37(L10402): 1-5.

Lin, C., S. Chen, and K. Huang. 2005. Characteristics of metals in nano/ultrafine/fine/coarse particles collected beside a heavily trafficked road. *Environmental Science & Technology* 39(21): 8113-8122.

Manek, R. V., O. O. Kunle, M. O. Emeje, P. Builders, G. V. Rama, and G.P. Lopez. 2005. Physical, thermal and sorption profile of starch obtained from Tacca leontopetaloides. *Starch/Stärke* 57(2): 55–61.

Marple, V.A., K.L. Rubow, and S.M. Behm. 1991. A microorifice uniform deposit impactor (MOUDI): Description, calibration and use. *Aerosol Science and Technology* 14(4): 434-446.

Marticorena, B., G. Bergametti, D. Gillette, and J. Belnap. 1997. Factors controlling threshold friction velocity in semiarid and arid areas of the United States. *Journal of Geophysical Research* 102(D19): 23,277-23,287.

Martin, G.P., H.B. MacRitchie, C. Marriott, and X.M. Zeng. 2006. Characterisation of a carrier-free dry powder aerosol formulation using inertial impaction and laser diffraction. *Pharmaceutical Research* 23(9): 2210-2219.

Martuzevicius, D., S. Grinshpun, T. Reponen, R. Górny, R. Shukla, J. Lockey, S. Hu, R. McDonald, P. Biswas, L. Kliucininkas, and G. LeMasters. 2004. Spatial and temporal variations of $PM_{2.5}$ concentration and composition throughout an urban area with high freeway density – the Greater Cincinnati study. *Atmospheric Environment* 38: 1091-1105.

McCollough, M.C., D.B. Parker, C.A. Robinson, and B.W. Auvermann. 2001. Hydraulic conductivity, bulk density, moisture content, and electrical conductivity of a new sandy loam feedlot surface. *Applied Engineering in Agriculture* 17(4): 539-544.

McGinn, S.M., T.K. Flesch, D. Chen, B. Crenna, O.T. Denmead, T. Naylor, and D. Rowell. 2010. Coarse particulate matter emissions from cattle feedlots in Australia. *Journal of Environmental Quality* 39(3): 791-798.

Merkus, H.G. 2008. Particle size measurements: Fundamentals, practice, quality. Particle Technology Series Volume 17. The Netherlands: Springer.

Mielke, L.N., N.P. Swanson, and T.M. McCalla. 1974. Soil profile conditions of cattle feedlots. *Journal of Environmental Quality* 3(1): 14-17.

Miller, D., B. Holmen, A. Hiscox, W. Yang, J. Wang, T. Sammis, and R. Bottoms. 2006. Dust emissions from cotton farming operations. ASABE Paper No. 064024. St. Joseph, Mich.: ASABE.

MSP Corporation. 2006. Model 100/110 MOUDI™ user guide. Shoreview, Minn.: MSP Corp.

Mühlenweg, H. and E.D. Hirleman. 1998. Laser diffraction spectroscopy: Influence of particle shape and a shape adaptation technique. *Particle & Particle Systems Characterization* 15: 163-169.

Mulholland, B. and M.A. Fullen. 1991. Cattle trampling and soil compaction on loamy sands. *Soil Use and Management* 7(4): 189-193.

Padgett, P.E., D. Meadows, E. Eubanks, and W.E. Ryan. 2008. Monitoring fugitive dust emissions from off-highway vehicles traveling on unpaved roads and trails using passive samplers. *Environmental Monitoring and Assessment* 144(1-3): 93-103.

Pilcer, G., F. Vanderbist, and K. Amighi. 2008. Correlations between cascade impactor analysis and laser diffraction techniques for the determination of the particle size of aerosolized powder formulations. *International Journal of Pharmaceutics* 358: 75-81.

Pinnick, R.G., G. Fernandez, B.D. Hinds, C.W. Bruce, R.W. Schaefer, and J.D. Pendleton. 1985. Dust generated by vehicular traffic on unpaved roadways: Sizes and infrared extinction characteristics. *Aerosol Science and Technology* 4(1): 99-121.

Purdy, C.W., R.N. Clark, and D.C. Straus. 2007. Analysis of aerosolized particulates of feedyards located in the Southern High Plains of Texas. *Aerosol Science and Technology* 41(5): 497–509.

Rahman, S., S. Mukhtar, and R. Wiederholt. 2008. Managing odor nuisance and dust from cattle feedlots. NM-1391. Fargo, N.D.: North Dakota State University. Available at http://www.ag.ndsu.edu/pubs/h2oqual/watnut/nm1391.html. Accessed 10 July 2010.

Razote, E.B., R.G. Maghirang, B.Z. Predicala, J.P. Murphy, B.W. Auvermann, J.P. Harner III, and W.L. Hargrove. 2006. Laboratory Evaluation of the dust-emission potential of cattle feedlot surfaces. *Transactions of the ASABE* 49(4): 1117-1124.

Razote, E.B., R.G. Maghirang, J.P. Murphy, B.W. Auvermann, J.P. Harner III, D.L. Oard, D.B. Parker, W.L. Hargrove, and J.M. Sweeten. 2007. Air quality measurements from a water-sprinkled beef cattle feedlot in Kansas. ASABE Paper No. 074108. St. Joseph, Mich.: ASABE.

Reed, W.R. and J.A. Organiscak. 2007. Haul dust control: Fugitive dust characteristics from surface mine haul roads and methods of control. Coal Age: 34-37. Available at http://www.cdc.gov/niosh/mining/pubs/pdfs/hrdcf.pdf. Accessed 21 March 2010.

Rodríguez, J.G. and A. Uriarte. 2009. Laser diffraction and dry-sieving grain size analyses undertaken on fine- and medium-grained sandy marine sediments: A note. *Journal of Coastal Research* 25(1): 257-264.

Romanillos, A. and B.W. Auvermann. 1999. Effect of stocking density on fugitive PM_{10} emissions from a cattle feedyard. ASABE Paper No. 994192. St. Joseph, Mich.: ASABE.

Saxton, K., D. Chandler, and W. Schillinger. 1999. Wind erosion and air quality research in the northwest U.S. Columbia plateau: Organization and progress. In E.E. Stott, R.H. Mohtar, and G.C. Steinhardt (eds). *Sustaining the Global Farm – Selected papers from the 10th International Soil Conservation Organization Meeting*, 24-29 May, West Lafayette, Ind.

Scholefield D. and D.M. Hall. 1985. A method to measure the susceptibility of pasture soils to poaching by cattle. *Soil Use and Management* 1(4): 134-138.

Shao, Y. and H. Lu. 2000. A simple expression for wind erosion threshold friction velocity. *Journal of Geophysical Research* 105(D17): 22,437-22,443.

Shi, P., P. Yan, Y. Yuan, and M.A. Nearing. 2004. Wind erosion research in China: past, present, and future. *Progress in Physical Geography* 28(3): 366-386.

Skidmore, E.L. 1986. Wind erosion control. *Climatic Change* 9: 209-218.

Stetler, L.D. and K.E. Saxton. 1997. Analysis of wind data used for predicting soil erosion. In *Proc. Wind Erosion: An International Symposium/Workshop*, 3-5 June 1997. Manhattan, Kan.: USDA-ARS.

Succarieh, M. 2000. Final report: Control of dust emissions from unpaved roads. Alaska Cooperative Transportation and Public Facilities Research Program. Available at http://www.dot.state.ak.us/stwddes/research/assets/pdf/fhwa_ak_rd_92_05.pdf. Accessed 15 May 2010.

Sweeten, J.M., C.B. Parnell, R.S. Etheredge, and D. Osborne. 1988. Dust emissions in cattle feedlots. *Veterinary Clinics of North America. Food Animal Practice* 4(3): 557-578.

Sweeten, J.M., C.B. Parnell, B.W. Shaw, and B.W. Auvermann. 1998. Particle size distribution of cattle feedlot dust emission. *Transactions of the ASAE* 41(5): 1477-1481.

Thenoux, G., J.P. Bellolio, and F. Halles. 2007. Development of a methodology for measurement of vehicle dust generation on unpaved roads. *Transportation Research Record: Journal of the Transportation Research Board* 1989(1): 299-304.

Tinke, A.P., A. Carnicer, R. Govoreanu, G. Scheltjens, L. Lauwerysen, N. Mertens, K. Vanhoutte, and M.E. Brewster. 2008. Particle shape and orientation in laser diffraction and static image analysis size distribution analysis of micrometer sized rectangular particles. *Powder Technology* 186(2): 154-167.

TSI. 2009. Health-based particle-size-selective sampling. Application Note ITI-050. Available at

http://www.tsi.com/uploadedFiles/Product_Information/Literature/Application_Notes/ITI-050.pdf. Accessed 15 May 2010.

U.S. Department of Agriculture (USDA). 2000. 2000 Agricultural statistics annual. National Agricultural Statistics Service. Available at http://www.nass.usda.gov/Publications/Ag_Statistics/2005/00_ch7.pdf. Accessed 10 July 2010.

U.S. Department of Agriculture (USDA). 2005. 2005 Agricultural statistics annual. National Agricultural Statistics Service. Available at http://www.nass.usda.gov/Publications/Ag_Statistics/2005/05_ch7.pdf. Accessed 10 July 2010.

U.S. Department of Agriculture (USDA). 2009. 2009 Agricultural statistics annual. National Agricultural Statistics Service. Available at http://www.nass.usda.gov/Publications/Ag_Statistics/2009/chp07.pdf. Accessed 10 July 2010.

U.S. Department of Agriculture – Agricultural Research Service (USDA-ARS). 2008. SWEEP user manual draft. Manhattan, Kan.: USDA ARS.

U.S. Environmental Protection Agency (US EPA). 1997. Emission inventory improvement program. Available at http://www.epa.gov/ttn/chief/eiip/techreport/volume09/feedlots.pdf. Accessed 15 May 2010.

U.S. Environmental Protection Agency (US EPA). 2003. AP-42, 5th ed., Vol. 1, Miscellaneous Sources. Research Triangle Park, N.C.: US EPA. Available at http://www.epa.gov/ttn/chief/ap42/ch13/final/c13s0202.pdf. Accessed 21 March 2010.

U.S. Environmental Protection Agency (US EPA). 2004. Preparation of fine particulate emission inventories: Student manual APTI Course 419B. Research Triangle Park, N.C.: US EPA. Available at http://www.epa.gov/apti/course419b/studentmanual/sm_chapter_6.pdf. Accessed 15 May 2010.

U.S. Environmental Protection Agency (US EPA). 2006a. PM Standards. Available at http://www.epa.gov/pm/standards.html. Accessed 15 May 2010.

U.S. Environmental Protection Agency (US EPA). 2006b. Unpaved roads. Available at http://www.epa.gov/ttn/chief/ap42/ch13/final/c13s0202.pdf. Accessed 21 March 2010.

U.S. Environmental Protection Agency (US EPA). 2010. Module 3: Characteristics of particle size distribution. US EPA, Air Pollution Training Institute Virtual Training Course. Available at http://www.epa.gov/eogapti1/bces/module3/distribu/distribu.htm. Accessed 10 July 2010.

Vincent, J.H. 2007. Aerosol sampling: Science, standards, instrumentation and applications. England: John Wiley & Sons Ltd.

Watson, J.G., J.C. Chow and T.G. Pace. 2000. Fugitive dust emissions. In: W.T. Davis (ed), *Air Pollution Engineering Manual.* 2nd ed. New York: John Wiley & Sons, Inc., pp. 117-135.

Wang, J., A. Hiscox, D. Miller, T. Sammis, W. Yang, and B. Holmen. 2009. A note on the measurement of dust emissions from moving sources in agricultural field operations. New Mexico State University. Research Report 767. Available at http://aces.nmsu.edu/pubs/research/weather_climate/RR-767.pdf. Accessed 15 May 2010.

Webb N.P. and H.A. McGowan. 2009. Approaches to modeling land erodibility by wind. *Progress in Physical Geography* 33(5): 587-613.

Wilson, S.C., J. Morrow-Tesch, D.C. Straus, J.D. Cooley, W.C. Wong, F.M. Mitlöhner, and J.J. McGlone. 2002. Airborne microbial flora in a cattle feedlot. *Applied and Environmental Microbiology* 68(7): 3238-3242.

Xu, R. 2000. Particle characterization: light scattering methods. Particle Technology Series. The Netherlands: Kluwer Academic Publishers.

Ziegler, J. and H. Wachtel. 2005. Comparison of cascade impaction and laser diffraction for particle size distribution measurements. *Journal of Aerosol Medicine* 18(3): 311-324.

CHAPTER 3 - Laser Diffraction Analysis of Cattle Feedlot Dust

3.1 Introduction

Open beef cattle feedlots emit various air pollutants, including particulate matter (PM). Recent research has characterized PM emissions from cattle feedlots. Sweeten et al. (1988) reported a mean mass median diameter (MMD) of 10.9 ± 1.4 μm for total suspended particulates (TSP) in a cattle feedlot in Texas using a Coulter counter (model TAII). In a related study in three cattle feedlots in Texas, Sweeten et al. (1998) reported MMDs of 9.5 ± 1.5 μm for TSP samplers and 6.9 ± 0.8 μm for PM_{10} samplers. Using a Coulter Counter Multisizer 3, Hamm (2005) observed mean MMD of 16.0 μm, geometric standard deviation (GSD) of 2.1, and PM_{10}/TSP ratio of 0.28 for a cattle feedlot in Texas. Guo et al. (2011) measured particle size distribution downwind of a feedlot in Kansas using micro-orifice uniform deposit impactor and reported geometric mean diameters ranging from 7 to 18 μm. McGinn et al. (2010) measured PM_{10} concentrations in two cattle feedlots in Australia using beta attenuation mass monitors; feedlot PM_{10} 24-h concentrations were close to or exceeded European Union (EU) and Australian standards twice during the 10-day sampling period but did not exceed the US EPA 24-h NAAQS for PM_{10}.

Laser diffraction is one of the most widely used instruments in determining particle size distribution in the medical field because of its relative ease of operation, high speed, and wide range of size determination (Xu, 2000). The performance of the laser diffraction technique has been compared with that of other techniques. Kwong et al. (2000) used nebulized aerosols to compare a Malvern Mastersizer X laser diffraction analyzer and the Marple Personal Cascade Impactor. Their results showed the Malvern Mastersizer had significantly ($p < 0.05$) higher MMD and smaller GSD than the Marple Personal Cascade Impactor. Ziegler and Wachtel (2005) compared a Sympatec HELOS laser diffraction analyzer with an Andersen Mark II cascade impactor and reported high correlation ($R^2 = 0.99$) in cumulative fractions of particles between the two instruments.

Martin et al. (2006) used powder aerosols in comparing a Malvern 2600 laser diffraction analyzer and Andersen impactor. The two instruments did not significantly differ in particle size distribution, especially for the fine particle size range. Pilcer et al. (2008) compared the laser

diffraction-based Malvern Spraytec, multi-stage liquid impinger (MsLI), and cascade impactor using aerosolized powder formulations. High correlations were observed with R^2 values ranging from 0.90 to 0.98 between the instruments.

In agricultural operations, Cao (2009) compared a laser diffraction particle size analyzer (LS 13 320), laser scattering particle size analyzer (LA-300), Coulter Counter Multisizer 3 (CCM 3), and laser diffraction particle size analyzer (LS 320) in measuring the particle size distribution in a layer operation. There was no significant difference between the values obtained using the LS 13 320 and LS 320. The greatest mean MMD value was from the LA-300 (22.6 ± 2.7 μm), while the smallest mean MMD was from the CCM 3 (14.0 ± 0.7 μm). Mean GSDs were 2.67 ± 0.11 μm (for LS 13 320), 1.99 ± 0.15 μm (for LA-300), 1.84 ± 0.04 μm (for CCM 3) and 2.65 ± 0.22 μm (for LS 230).

Cattle feedlot emissions were rarely used as media for comparing the performance of different instruments in determining particle size distribution. Purdy et al. (2007) quantified PM emissions from cattle feedlots using Reference Ambient Air Sampler (RAAS) PM_{10} and $PM_{2.5}$ samplers and particle size distribution instruments and compared them to the Elzone 112 electrozone analyzer and scanning electron microscope. Similarities in reported PM_{10} and $PM_{2.5}$ mass concentrations and size distribution data were observed for the RAAS PM_{10} and $PM_{2.5}$ samplers and electrozone analyzer. Also, comparison of the electrozone analyzer with the scanning electron microsope revealed similar size distribution. With limited data on performance comparisons of laser diffraction analyzers with other instruments (i.e., cascade impactor), it is best to apply laser diffraction in emissions in cattle feedlots, because laser diffraction uses a wide size range that enables researchers to pinpoint specific sizes at specific concentrations.

With the current state of regulating emissions from the agricultural industry, there exists a debate as to whether or not US EPA has done its part in protecting people living and working in rural areas (Crutchfield, 2010). More stringent regulations could be on the horizon. It will be better for operators and managers of the cattle feedlot industry to learn more about the state and magnitude of dust emissions.

As for dust regulations, particle size characterization plays an integral part in determining risks involved. Epidemiologic researchers have noted that $PM_{2.5}$ promotes greater risk to human health, resulting in vascular inflammation and atherosclerosis (Pope et al., 2002), incidence of

asthma (Gilmour et al., 2006), and other respiratory infections (Dockery et al., 1993; Gordian et al., 1996; Schwartz and Dockery 1992). There is a need to better quantify and characterize PM emissions to provide science-based data for developing air quality standards and/or management practices for mitigating emissions.

The objectives of this research were to:

1) Determine the applicability of laser diffraction (LD) method in measuring particle size distribution in feedlots.
2) Compare PM_{10} and $PM_{2.5}$ concentration measurements using the LD method and gravimetric samplers.
3) Determine effects of meteorological factors and sampling period on particle size distribution.

3.2 Materials and Methods

3.2.1 Feedlot Description

This research was conducted on a commercial cattle feedlot in Kansas (Feedlot 1) from July 2007 to July 2009. The feedlot had approximately 30,000 head with 50 ha pen area. It had a water sprinkler system (Fig. 3.1) for controlling dust that was normally operated from April to October and during prolonged dry periods. Pens were cleaned two to three times per year and manure was removed at least once per year.

Figure 3.1 Feedlot 1 equipped with a water sprinkler system

Cattle were fed three times a day. In general, it took about 2.5 h per truck to feed a section of the feedlot and there were three feed trucks used for the feedlot.

During the course of the 3-year measurement period (2007-2009), average annual precipitation was 540 mm. Daily temperatures ranged from -16 to 31 °C with a daily mean of 12 °C. Average daily wind speed was about 4.6 m/s ranging from 0.55 to 12.9 m/s. On average, 64% of the time the wind came from the south, 8% from the north, 14% from the east, and 14% from the west.

3.2.2 Particulate Sampling and Measurement

Low-volume (LV) samplers were used to collect PM at north and south edges of Feedlot 1 (Fig. 3.2). Samplers were equipped with size-selective inlets for TSP, PM_{10}, and $PM_{2.5}$. The north and south sampling locations were approximately 3 m and 30 m, respectively, from the closest pens. These sampling locations were selected based on feedlot layout, power availability, and access.

Before field sampling, each sampler was flow-audited and tested for leaks. Each sampler had a cartridge equipped with polytetrafluoroethylene (PTFE) filter (Whatman, Inc., Clifton, NJ) that was placed in a conditioning chamber (at 25 °C and 40% RH) for 24 h prior to weighing before and after sampling. During sampling, samplers were operated for 12 h at a flow rate of 5 Lpm.

Mass of dust was obtained by the difference of the masses of the conditioned filter before sampling and used filter after sampling and conditioning. Concentrations were obtained by dividing the mass of dust collected by the total volume of air sampled.

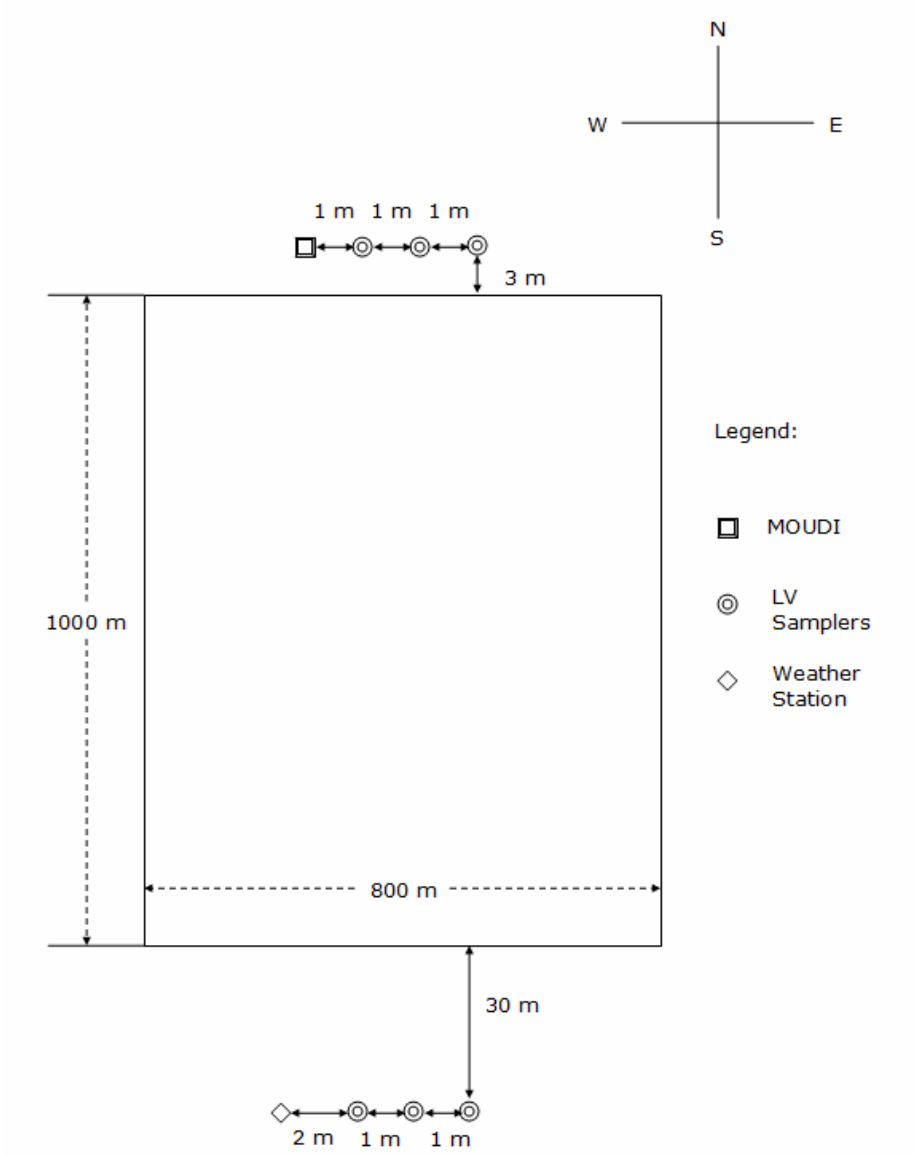

Figure 3.2 Schematic diagram of the feedlot showing relative locations of samplers and weather station (not drawn to scale).

3.2.3 Particle Size Distribution

Particle size distribution at the north sampling location (typically the downwind location) was measured using a Micro-Orifice Uniform Deposit Impactor or MOUDI (Model M100/110R, Thermo Fisher Scientific, Inc., Franklin, MA) that was collocated with the LV samplers. In addition, particles collected on filters of TSP samplers were analyzed with a laser diffraction analyzer (Model LS 13 320, Beckman Coulter, Inc., Fullerton, CA).

The MOUDI was operated with six stages with cut point diameters of 18, 9.9, 6.2, 3.1, 1.8, 1.0, and 0.9 μm. The bottom filter of the MOUDI was Teflon, while the upper 5 stages had aluminum foil substrates. The Teflon filter was conditioned for 24 h before weighing and after sampling while the aluminum foil substrates were greased and dried in an oven prior to weighing before sampling. The grease was necessary to prevent particle bounce. The MOUDI was operated for 24 h at a flow rate of 30 Lpm. Filter cartridges with PTFE filters were used to collect particles that were operated simultaneously with the MOUDI (24 h) at a flowrate of 20 Lpm. The geometric mean diameter (GMD) and the geometric standard deviation (GSD) were calculated using (Hinds, 1999):

$$\mathrm{GMD} = \exp\left[\frac{\sum\left(m_j \ln d_j\right)}{\sum m_j}\right] \tag{3.1}$$

$$\mathrm{GSD} = \exp\left[\frac{\sum\left\{m_j\left[\left(\frac{d_j}{\mathrm{GMD}}\right)\right]^2\right\}}{\sum m_j}\right]^{0.5} \tag{3.2}$$

where m_j = mass fraction of particles in the j^{th} stage of the MOUDI

d_j = geometric mean diameter of particles in the j^{th} stage of the MOUDI (μm).

Measurements by the MOUDI were corrected for particle losses/bounce according to manufacturer's specifications.

The laser diffraction analyzer had an operating size range of 0.4 to 2000 μm. The instrument had a universal liquid module that can be used for different dispersing medium (dispersant). Use of this instrument first involved conditioning a monochromatic beam (laser) that is allowed to pass through an ensemble of particles along the sample module (Fig. 3.3). Patterns of scattered light are then measured by a series of detector elements positioned at various angles. Using a model-based matrix, which contains the calculated signals at every detector per unit volume of spherical particles, signals detected were converted to particle size distribution.

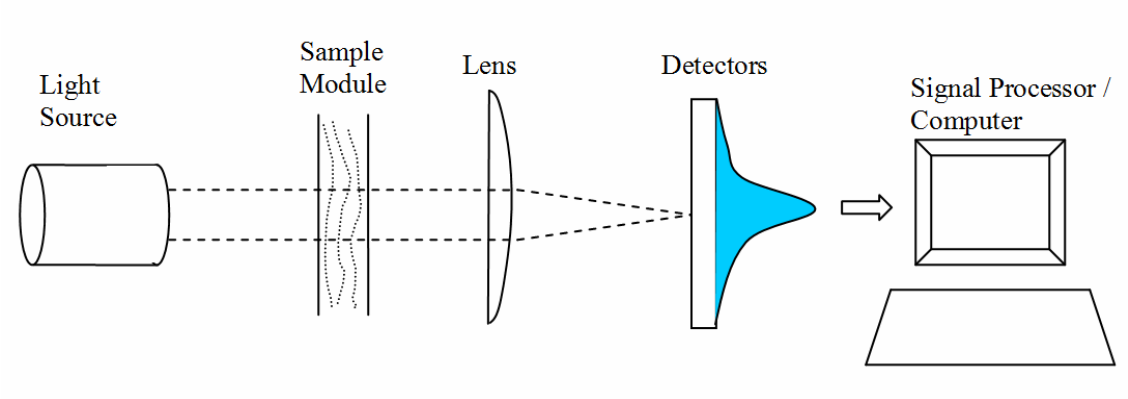

Figure 3.3 Beckman Coulter LS 13 320 Operation
(adapted from: http://www.beckmancoulter.com)

Based on preliminary work, the instrument requires at least 1 mg of particles to achieve the desired obscuration range of 8 to 12 % (Beckman Coulter, 2003). Too many particles will promote multiple scattering, that is, there is a high probability of scattering the light again and again from one particle to another before reaching the detectors. On the other hand, too low of a concentration could lead to low signal-to-noise ratio and poor repeatability.

Filters used for LD analyses were those from TSP samplers. PM from each filter was first extracted by washing the filter with isopropyl alcohol, which was used as the dispersant to minimize aggregation of dust particles. The resulting dust-isopropyl alcohol mixture was then transferred to a 50 mL plastic centrifuge tube and was centrifuged for 5 min at 4000 rpm using the Durafuge (Model Precision Durafuge 300, Thermo-Fisher Scientific, Inc., Waltham, Mass.). Excess isopropyl alcohol was decanted leaving about 15 mL of dust suspension, which was then agitated using a vortex mixer (Model Sybron Thermolyne Maxi Mix, Thermolyne Corp., Dubuque, Iowa) prior to analysis in the LD analyzer.

Drops of the subsample dust suspension were added into the LD analyzer wet module until until the recommended 8 to 12% obscuration was attained. A 90-sec sonication was done before analysis to minimize formation of clumps of dust subsamples. Duplication of the 60-sec analysis time for each subsample was done by the instrument (Pearson et al., 2007; Boac et al., 2009).

Size distribution statistics based on equivalent sphere diameter and volume distribution were obtained with the bundled software for the instrument. Output data included GMD and

GSD of equivalent sphere particles. The equivalent aerodynamic diameter (d_a) was calculated using the relationship (Hinds, 1999):

$$d_a = d_p\sqrt{\frac{\rho_p}{\rho_o}} \tag{3.3}$$

where ρ_o = unit density (1.0 g/cm^3)

ρ_p = particle density (g/cm^3)

Mean particle density was 1.8 ± 0.1 g/cm^3, based on measurements with a multipycnometer (Model MVP-1, Quantachrome Corp., Syosset, N.Y.).

From the LD data, the following empirical expression (Hinds, 1999) was used to calculate the fraction of particles of diameter d_a that are included in the $PM_{2.5}$ fraction, $PF_{2.5}$:

$$PF_{2.5} = \left[1+\exp\left(3.233d_a - 9.495\right)\right]^{-3.368} \tag{3.4}$$

Also, the fraction of particles of diameter d_a in the PM_{10} fraction, PF_{10}, was obtained using (Hinds, 1999):

$$\begin{aligned} PF_{10} &= 1.0 && \text{for } d_a < 1.5\ \mu m \\ PF_{10} &= 0.9585 - 0.00408d_a^{\,2} && \text{for } 1.5 < d_a < 15\ \mu m \\ PF_{10} &= 0 && \text{for } d_a > 15\ \mu m \end{aligned} \tag{3.5}$$

On the basis of the equivalent aerodynamic diameter, cumulative volume percentages corresponding to $PF_{2.5}$ and PF_{10} fractions were used to determine $PM_{2.5}$ and PM_{10} concentrations, respectively.

3.2.4 Weather Conditions and Pen Surface Moisture Content

The feedlot was equipped with a weather station (Campbell Scientific, Inc., Logan, UT) to measure and record at 20-min intervals atmospheric pressure (Model CS100), air temperature and relative humidity (Model HMP45C), precipitation (Model TE525), and wind speed and direction (Model 05103-5).

For each sampling period, manure samples were collected from three randomly selected pens for moisture content (MC) determination. For each pen, loose manure (approximately 2-3

cm) was collected at various points from the center of the pen to the feed apron using a trowel and then placed in a sealed plastic bag. The sample MC was determined in accordance with ASTM D 2216-98 oven-drying method (ASTM, 2002).

3.2.5 Statistical Analysis

Data on concentrations and particle size distributions were screened based on wind direction. Since samplers were located at north and south edges of the feedlot, an angle of 45º within the centerline of north and south directions was chosen to be acceptable data points. For the MOUDI, when concentrations were small, negative PM mass readings were observed. Those measurements were not considered in the analysis. Data sets were also tested for outliers in which data points that had vertical distances exceeding four times the standard error were eliminated (Cornbleet and Gochman, 1979; Lee et al., 2005). Two outliers (out of 16 total data points) for comparison of the MOUDI and LD analyzer were not considered.

In comparing mean values (e.g., MOUDI vs. LD analyzer), assumptions of normality and homogeneity of variances were first tested. If assumptions were satisfied, standard statistical tests (e.g., analysis of variance, paired t-test) were applied. If assumptions were not satisfied, nonparametric statistical methods were used together with standard tests. In general, both tests showed similar results; as such, results of standard tests are presented here (Montgomery, 1984; Weaver, 2002).

Paired t-tests (Microsoft Excel, Microsoft Corp., Redmond, WA) were used to compare the MOUDI and LD method in measuring particle size distribution and the LD and LV samplers for PM concentration measurement. Effects of meteorological factors on size distribution were analyzed using the Mixed procedure in SAS (SAS 9.1.3, SAS Institute, Inc., Cary, NC). Effects of pen surface MC on size distribution, PM concentrations, and PM fractions were also examined using the same procedure. In all cases, a 5% level of significance was used.

3.3 Results and Discussion

Of the chosen data points used for analysis, 78% were associated with south wind directions (south was the upwind site while north was the downwind site) and 22% were associated with north wind directions (north was the upwind site while south was the downwind site). During these periods, daily temperatures ranged from -3.5 to 33.7 °C with an average of

17.6 °C; daily precipitations ranged from 0.00 to 0.31 mm with an average of 0.0084 mm; and daily wind speeds ranged from 1.47 to 12.9 m/s with an average of 4.51 m/s.

3.3.1 Laser Diffraction vs. Cascade Impactor

For comparison of MOUDI and LD, 14 data points were acceptable. For those 14 points, GMDs from MOUDI ranged from 7.2 to 18.2 μm, with an overall mean of 13.0 μm, and those from LD analyzer ranged from 8.3 to 28.0 μm, with an overall mean of 13.7 μm (Table 3.1). Relatively coarse particles were emitted from the feedlot as indicated by the GMD range. The GMD values in this study were within the range of published values. GMDs in this study were higher than those measured by Sweeten et al. (1988) of 8.5 ± 2.1 μm and also those reported by Sweeten et al. (1998) of 9.5 ± 1.5 μm. Difference in methodology, type of samplers, and feedlot characteristics (e.g., soil type [Miller and Woodbury, 2003]) could help explain this difference. GMDs in this study were close to that measured by Sweeten et al. (1998) (14.2 ± 0.8 μm).

Paired t-tests did not show any significant ($P > 0.5$) difference in GMD between MOUDI and LD analyzer. Figure 3.4 shows strong correlation between measurements with the LD method and MOUDI. The R^2 value is an indication that there exists a good linear fit between measurements of the MOUDI and LD method. Also, the regression coefficient was close to unity, implying strong agreement between MOUDI and LD values.

Table 3.1 Comparison of laser diffraction and cascade impactor in geometric mean diameter and geometric standard deviation

Method	n	Geometric Mean Diameter (GMD) (μm) ± SEM	Geometric Standard Deviation (GSD) ± SEM
Laser Diffraction (LD)	14	13.7 ± 1.3	2.9 ± 0.1
MOUDI	14	13.0 ± 0.9	2.3 ± 0.1

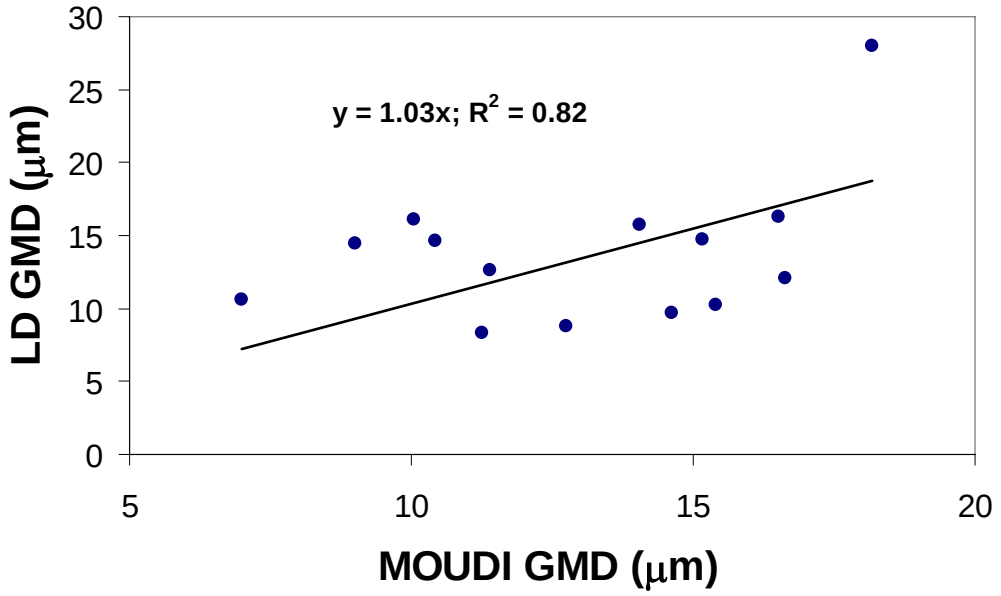

Figure 3.4 Comparison of the MOUDI and LD in geometric mean diameters (GMDs)

Note that the MOUDI is a gravimetric method, while the LD method is an indirect method. For the LD method, there were particle losses during filter washing as indicated by mean percent recovery for extraction of 93.7 ± 1.1 %, ranging from 78 % to 99 %. Percent recovery was calculated by dividing the washed particulate mass (obtained by mass difference of filter with dust and filter after washing off the dust) by the total mass collected during sampling. Other potential sources of error include aggregation/deaggregation of particles during the sonication process for the LD method, particle losses/bounce on the MOUDI, and sampling errors associated with MOUDI and TSP samplers.

Paired t-test showed a significant difference ($P<0.05$) between the MOUDI and LD in mean GSD. GSD values for the LD method ranged from 2.3 to 3.6, with an overall mean of 2.9. Those for the MOUDI, on the other hand, ranged from 2.1 to 2.9, with an overall mean of 2.3 (Fig. 3.5). The broader range of GSD values for the LD can be attributed to its wider operating size range and the sonication process. During sonication, some aggregates might have been broken down into much smaller particles. On the other hand, although the MOUDI has a sharp cutpoint, aggregation cannot be prevented, especially for moist air with particles being sampled from the source. Collision between particles could also have stimulated the aggregation process between smaller particles, resulting in narrower size range. Note that errors in measurements

using cascade impactors are mainly attributed to particle bounce (Dzubay et al., 1975), in which particles bounce from the top stage to bottom stages, increasing the mass of smaller particles. Based on measured GMD and GSD values from the two instruments, particle bounce was likely minimized for the MOUDI as indicated by a much lower GSD.

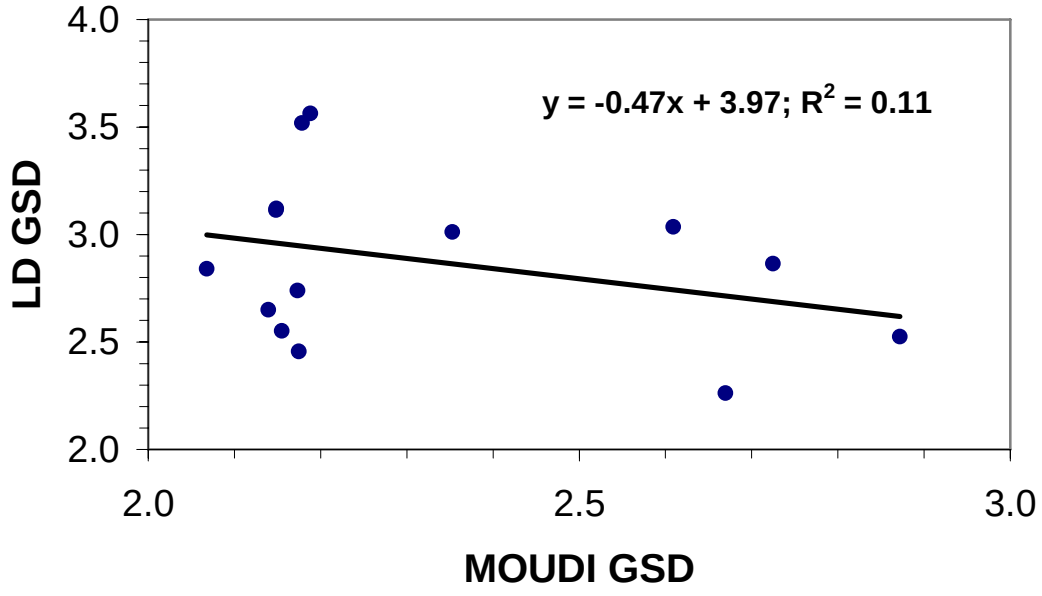

Figure 3.5 Comparison of MOUDI and LD in geometric standard deviations (GSDs)

3.3.2 Cumulative Fraction vs. Particle Fraction Method

From the LD data, fractions of PM_{10} (PF_{10}) and $PM_{2.5}$ ($PF_{2.5}$) and corresponding concentrations can be obtained using equations 3.4 and 3.5 (particle fraction method) or determining the cumulative fraction of particles ≤ 2.5 µm and ≤ 10 µm (cumulative fraction method). Table 3.2 summarizes fractions and concentrations from the two methods for the upwind and downwind sampling locations. Paired t-tests did not show any significant difference ($P > 0.05$) between the two methods in $PM_{2.5}$ and PM_{10} fractions and concentrations, indicating that either method can be used to determine PF_{10} and $PF_{2.5}$ fractions and concentrations.

Table 3.2 Comparison of cumulative fraction and particle fraction methods in determining PM fractions and concentrations.

Type of Method		Downwind (n = 39)		Upwind (n = 18)	
		Fraction ± SEM	Concentration ($\mu g/m^3$) ± SEM	Fraction ± SEM	Concentration ($\mu g/m^3$) ± SEM
Cumulative Fraction Method	PM_{10}	0.33 ± 0.01	129 ± 31	0.35 ± 0.02	99 ± 19
	$PM_{2.5}$	0.07 ± 0.00	29 ± 7	0.07 ± 0.00	20 ± 4
Particle Fraction Method	PM_{10}	0.31 ± 0.01	123 ± 29	0.33 ± 0.02	92 ± 17
	$PM_{2.5}$	0.07 ± 0.00	27 ± 6	0.07 ± 0.00	18 ± 3

3.3.3 Laser Diffraction vs. Low-Volume Sampler

Tables 3.3 and 3.4 summarize the $PM_{2.5}$ and PM_{10} concentrations from the LD method and LV samplers for the downwind and upwind sampling locations, respectively. For each method, as expected, downwind concentrations were greater than upwind concentrations. Paired t-tests did not show any significant ($P > 0.05$) difference between the LD and LV samplers in both downwind and upwind PM_{10} and $PM_{2.5}$ concentrations. For upwind concentrations, only 18 events were obtained to compare the LD method and LV samplers, because the LD method required at least 1 mg of sample to achieve the required obscuration level.

Table 3.3 Downwind 24-h mass concentrations ($\mu g/m^3$) - laser diffraction vs. low-volume samplers

		n	Min.	Max.	Mean	SEM
Laser Diffraction (LD)	PM_{10}	39	3	679	122	20
	$PM_{2.5}$	39	1	133	26	4
Low-Volume	PM_{10}	39	14	380	131	15
	$PM_{2.5}$	39	7	136	35	5

Table 3.4 Upwind 24-h mass concentrations (μg/m^3) - laser diffraction vs. low-volume samplers

		n	Min.	Max.	Mean	SEM
Laser Diffraction	PM_{10}	18	1	223	92	17
	$PM_{2.5}$	18	0.4	43	19	3
Low-Volume	PM_{10}	18	29	212	94	13
	$PM_{2.5}$	18	6	119	28	6

The slight discrepancies with the values can be attributed also to losses during filter washing before LD analysis. As for LD measurements being slightly less than those of LV samplers, agglomeration might have been encountered, which could have shifted particle size distribution to a larger size range, thereby decreasing computed $PM_{2.5}$ and PM_{10} concentration values.

3.3.4 Factors Affecting Size Distribution

Analysis of LD GMD data with the PROC Mixed procedure in SAS showed that the two main factors affecting GMD were wind speed and time of sampling. Other factors such as temperature, precipitation, and relative humidity did not significantly affect GMD. Figure 3.6 shows that mean GMD values from the LD method increased slightly with increasing mean wind speed. This result is expected, because as wind speed increases, coarse PM are generated through wind-induced resuspension (Jones et al., 2010), rendering a greater mass of large suspended particles. With low wind speed, on the other hand, there would be less resuspension of particles. Also, most of the large particles would settle out after only a short distance causing a shift towards smaller particle sizes, decreasing mean GMD (Lundgren et al., 1984).

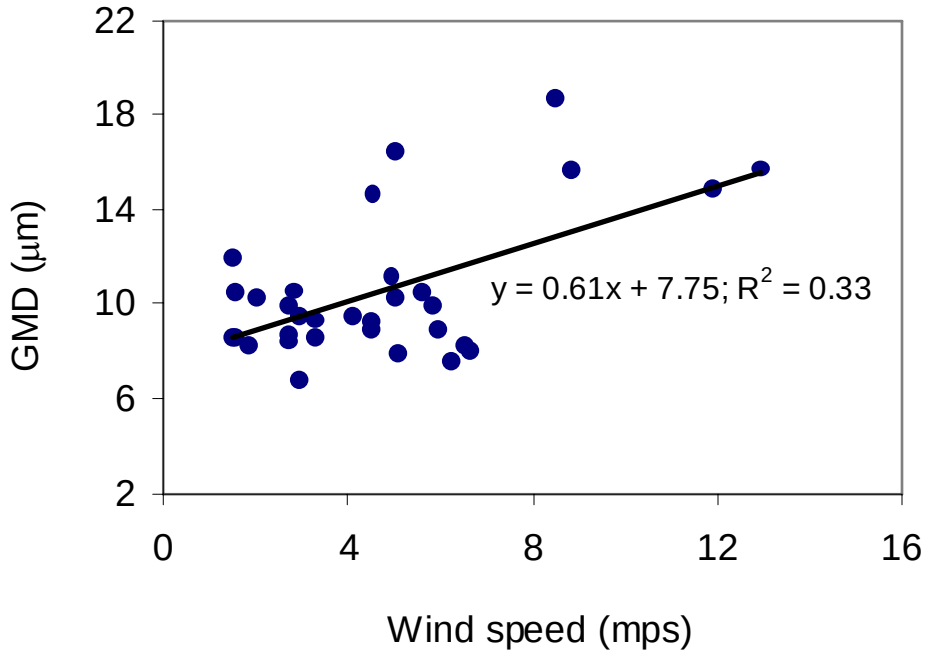

Figure 3.6 Effect of wind speed on geometric mean diameter (GMD) obtained from LD method

Analysis using F-test showed that mean GMD values were significantly higher during the daytime sampling period (6 AM to 6 PM) than during the nighttime sampling period (6 PM to 6 AM). Summarized in Table 3.5 are mean GMD values for daytime and nighttime sampling periods downwind of the feedlot. Only 4 samples were considered as day sampling events, because of filtering of LD data based on obscuration level and wind directions.

Table 3.5 Effect of sampling period (day vs night) on geometric mean diameter (from LD method)

Time of Sampling (Warm Months Considered)	n	Geometric Mean Diameter (μm)	Wind Speed (m/s)
6 AM – 6 PM	4	18.2 ± 2.7	5.9 ± 0.9
6 PM – 6 AM	16	14.4 ± 1.0	4.1 ± 0.7

Although increased cattle activity (i.e., antagonistic interactions, walking and running behavior [Gonyou and Stricklin, 1984]) during the night causes peaks in dust concentration (Bonifacio, 2009), the average wind speed was smaller during the evening than during the day (Table 3.5). The same phenomenon was also observed by Auvermann et al. (2000), who indicated that wind speed decreased during the evening and the dust plume floated above the feedlot. Note that measurements considered were during warmer months in which water on the pen surface evaporates during the late afternoon due to the day's temperature and cattle activity increases because of cooler temperatures during the evening (Amosson et al., 2006). With a difference of greater than 1 m/s in wind speed, such phenomenon could have affected measured PM concentrations during the day and night sampling. Padgett et al. (2008) reported that large particles occurred in the lower portion of the plume and deposition occurred closer to the source and that smaller particles existed at the upper portion of the plume and traveled at least 100 m away from the source. Since the samplers were about 3 m away from the closest pen (north site), GMD was expected large in this study.

3.3.5 Warm vs. Cold Months

Measurements with the LD method during warm months (April to October) and cold months (November to March) were compared. Classification of warm and cold months was based on operation of the sprinkler system. During warm months (April to October), GMD ranged from 9.2 μm to 37.5 μm, while during cold months, particle GMD ranged from 10.2 μm to 21.8 μm. Figure 3.7 shows the mean volume percent of different sizes of particles based on the type of month. Mean values for GMD and GSD are tabulated in Table 3.6. Analysis using an F-test showed no significant difference ($P > 0.05$) between measured values during warm and cold months.

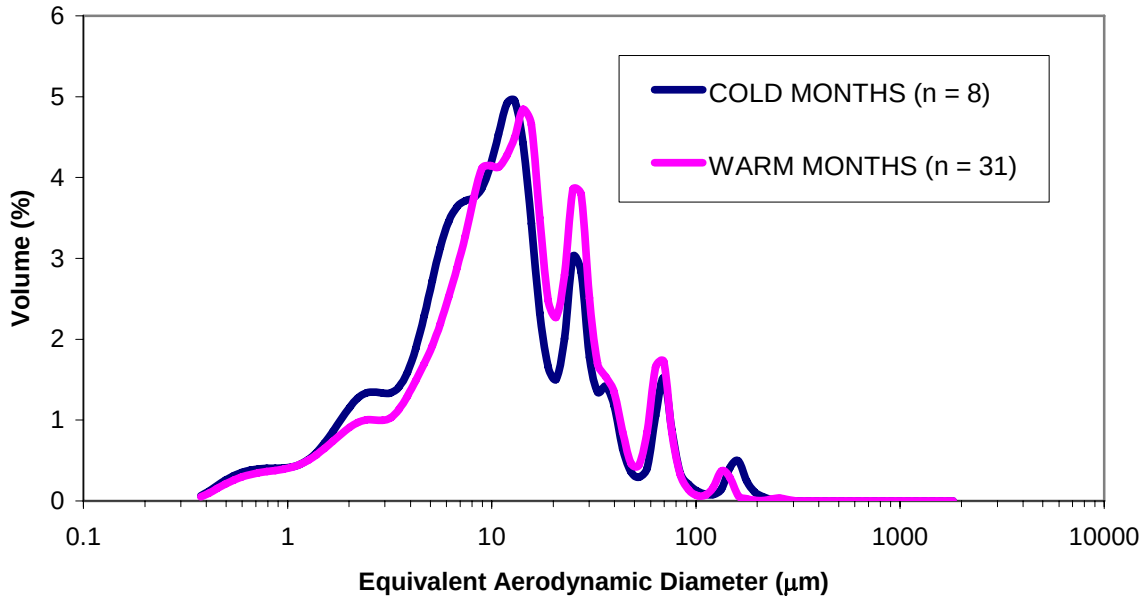

Figure 3.7 Mean volume percent at different aerodynamic diameters

Table 3.6 Comparison of mean geometric mean diameter and mean geometric standard deviation between the warm and cold months

Month Type	n	GMD (μm)	GSD
Warm Months (April to October)	31	16.3 ± 1.0	2.8 ± 0.1
Cold Months (November to March)	8	13.7 ± 1.2	2.9 ± 0.1

3.3.6 Effect of Pen Surface Moisture Content

There was difficulty in correlating the actual amount of water applied using the sprinklers to the pen surface before, during, or even after sampling since there was no continuous monitor of parameters with which particle size distribution was being measured. Only a limited amount of data was correlated for the events having water application as compared to events without water application. The effect of an event with water application was standardized by choosing days in which water was applied to the pen and making sure that previous to and after there was no water applied. Events without water application included those without water application before, during, and after sampling. Figure 3.8 shows a slight shift into larger particles as water was applied to the pens. This implies that emission of larger particles was minimized and was

impacted by application of water, lowering the mean GMD. Statistical analysis, however, did not show any significant ($P > 0.05$) effect of water application on GMD and GSD (Table 3.7).

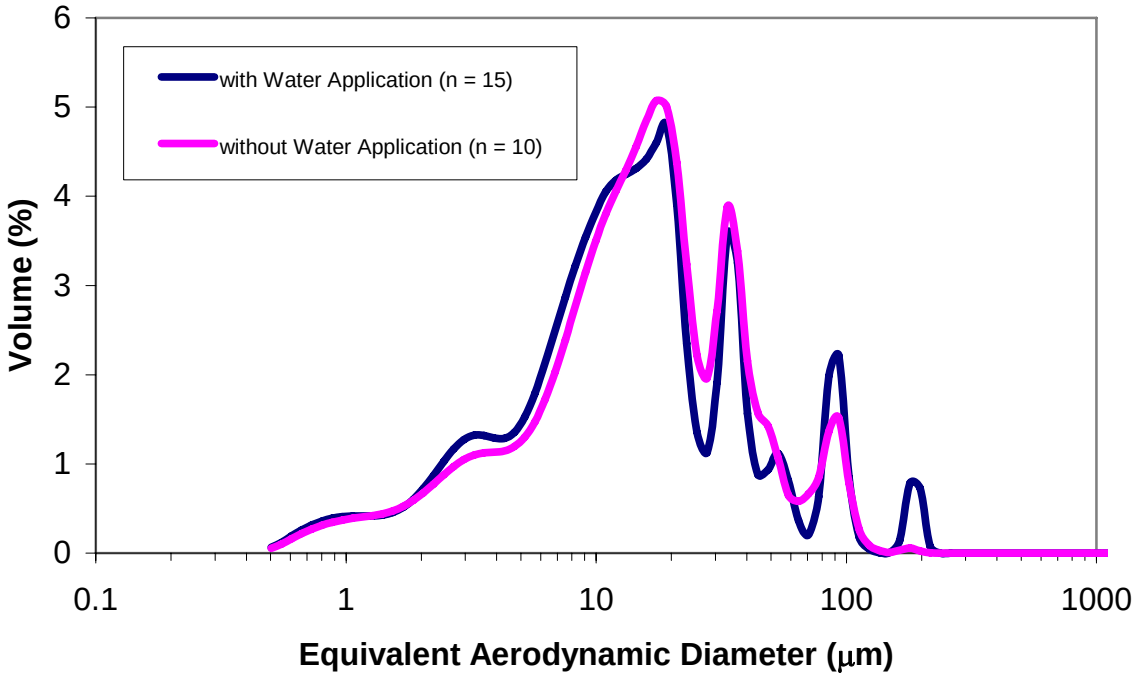

Figure 3.8 Particle size distribution comparison between events with water application and events without water application

Table 3.7 Effects of water application on geometric mean diameter and geometric standard deviation.

Condition	n	GMD (μm)	GSD
With Water Application	15	13.7 ± 1.0	3.0 ± 0.1
Without Water Application	10	14.3 ± 1.3	2.8 ± 0.1

$PM_{2.5}$ and PM_{10} concentrations were correlated with pen surface MC. Figure 3.9 shows concentrations of both PM_{10} and $PM_{2.5}$ decreased as pen surface MC increased. Concentrations generally tapered off starting at 20 % MC; this MC level could be considered the threshold MC for dust control. The 20 % threshold MC for the feedlot surface was within what Funk et al. (2008) has reported for organic soils and was close to the 25-30% threshold MC reported by Sweeten et al. (1988) for cattle feedlot in Texas. Too much water in the pen surface increases

odor problems and fly presence, while too little water promotes dust generation (Davis et al., 1997; Amosson et al., 2006).

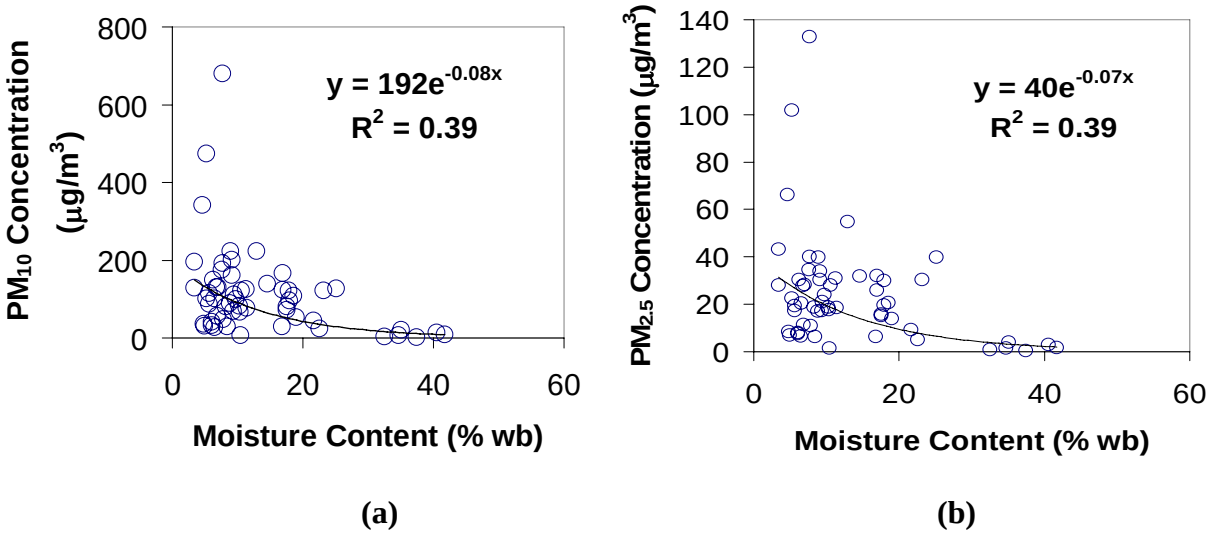

(a) **(b)**

Figure 3.9 Effects of pen surface moisture content on PM concentrations measured using the LD method: (a) PM_{10} and (b) $PM_{2.5}$.

PM fractions serve as basis of predicting long-term emissions from a source (Countess Environmental, 2006). The level of pen surface MC was also correlated with parameters that reflect size distribution, namely, PF_{10} and $PF_{2.5}$ fractions and $PM_{2.5}/PM_{10}$ ratio. Figure 3.10 shows PF_{10} and $PF_{2.5}$ fractions decreased as pen surface MC increased.

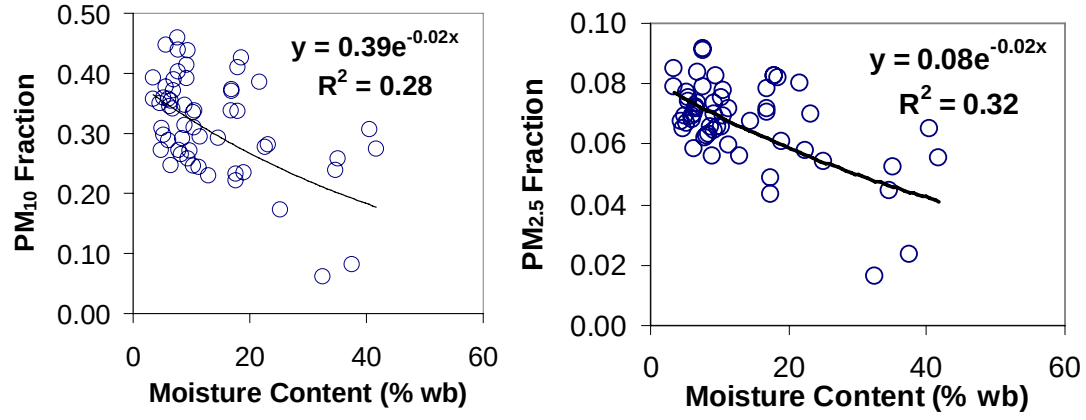

(a) **(b)**

Figure 3.10 Pen surface moisture content dependence of PM fractions measured using the LD method: (a) PM_{10} fraction and (b) $PM_{2.5}$ fraction.

A weak correlation ($R^2 = 0.05$) was obtained when $PM_{2.5}/PM_{10}$ ratio was plotted against pen surface MC (Fig. 3.11). This was expected because the data showed decrease in both the PF_{10} and $PF_{2.5}$ fractions with increasing pen surface MC.

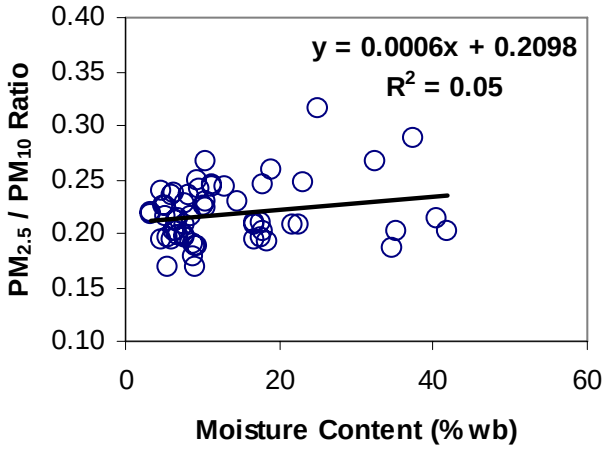

Figure 3.11 Effect of pen surface moisture content on $PM_{2.5}/PM_{10}$ ratio measured using the LD method

The mean GMD obtained from the LD method was also plotted against pen surface MC (Fig. 3.12). The GMD decreased slightly as pen surface MC increased; R^2 value, however, was close to zero.

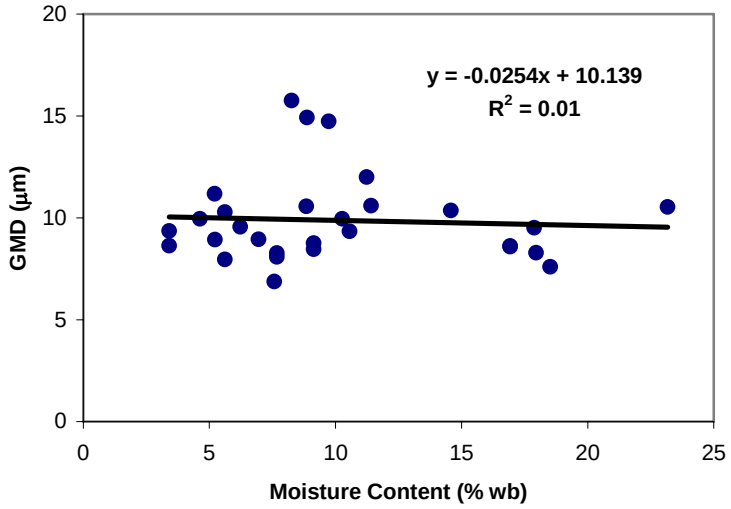

Figure 3.12 Effect of pen surface moisture content on mean geometric mean diameter measured using the LD method

3.4 Summary and Conclusions

This study measured particle size distribution and concentrations of PM_{10} and $PM_{2.5}$ at a commercial cattle feedlot in Kansas (Feedlot 1). The feedlot had a capacity of 30,000 head and total pen area of 50 ha and was equipped with a sprinkler system for dust control. Collocated low-volume samplers for TSP, PM_{10}, and $PM_{2.5}$ were used to measure concentrations of TSP, PM_{10}, and $PM_{2.5}$ at upwind and downwind edges of the feedlot. Dust samples that were collected by TSP samplers were analyzed with a laser diffraction analyzer to determine particle size distribution. Particle size distribution at the downwind edge of the feedlot was also measured with a micro-orifice uniform deposit impactor (MOUDI). The laser diffraction method and MOUDI did not differ significantly in mean geometric mean diameter (13.7 vs. 13.0 µm), but differed significantly in geometric standard deviation. From the laser diffraction data and TSP data, PM_{10} and $PM_{2.5}$ concentrations were also calculated and were not significantly different from those measured by low-volume PM_{10} and $PM_{2.5}$ samplers (122 vs. 131 µg/m^3 for PM_{10}; 26 vs. 35 µg/m^3 for $PM_{2.5}$). Both PF_{10} and $PF_{2.5}$ fractions decreased as pen surface moisture content increased, while the $PM_{2.5}/PM_{10}$ ratio did not change much with pen surface moisture content.

3.5 References

Amosson, S.H., B. Guerrero, and L.K. Almas. 2006. Economic analysis of solid-set sprinklers to control dust in feedlots. *Journal of Agricultural & Applied Economics* 38.2 (August 2006): 456.

ASTM. 2002. D2216-98: Standard test method for laboratory determination of water (moisture) content of soil and rock by mass. In *Annual Book of American Society for Testing Materials Standards*. Philadelphia, Penn.: ASTM.

Auvermann, B.W., D.B. Parker, and J.M. Sweeten. 2000. Manure harvesting frequency – The key to feedyard dust control in a summer drought. Amarillo, Tex.: Texas Agricultural Extension Service.

Beckman Coulter, Inc., 2003. LS 13 320 Laser diffraction particle size analyzer instrument manual. Miami, Fla.: Beckman Coulter, Inc.

Bonifacio, H. F. 2009. Particulate matter emissions from commercial beef cattle feedlots in Kansas. MS Thesis. Manhattan, Kan.: Kansas State University.

Boac, J.M., R.G. Maghirang, M.E. Casada, J.D. Wilson, and Y.S.Yung. 2009. Size distribution and rate of dust generated during grain elevator handling. *Applied Engineering in Agriculture* 25(4): 533-541.

Cao, Z. 2009. Determination of particle size distribution of particulate matter emitted from a layer operation in Southeastern U.S. MS Thesis. Raleigh, N.C.: North Carolina State University.

Cornbleet, P.J., and N. Gochman. 1979. Incorrect least-squares regression coefficients in method-comparison analysis. *Clinical Chemistry* 25(3): 432-438.

Countess Environmental. 2006. WRAP fugitive dust handbook. Prepared for Western Governor's Association, Denver, Colo. Available at http://www.wrapair.org/forums/dejf/fdh/content/FDHandbook_Rev_06.pdf. Accessed 21 March 2010.

Crutchfield, J.A. 2010. Comment: More than dust in the wind: Regulation of rural coarse particulate matter. *UMKC Law Review* 78(3): 785-808.

Davis, J.G., T.L. Stanton, and T. Haren. 1997. Feedlot manure management. Colorado State University Cooperative Extension. Available at http://www.cde.state.co.us/artemis/UCSU20/UCSU2062212202002INTERNET.pdf. Accessed July 10, 2010.

Dockery, D.W., C.A. Pope, X. Xu, J.D. Spengler, J.H. Ware, B.G. Ferris, and F.E. Speizer. 1993. An association between air-pollution and mortality in 6 United-States cities. *New England Journal of Medicine* 329(24): 1753-1759.

Dzubay, T.G., L.E. Hines, and R.K. Stevens. 1975. Particle bounce errors in cascade impactors. *Atmospheric Environment* 10(3): 229-234.

Funk, R., H. Reuter, C. Hoffmann, W. Engel, and D. Öttl. 2008. Effect of moisture on fine dust emission from tillage operations on agricultural soils. *Earth Surface Processes and Landforms* 33: 1851-1863.

Guo, L., R. G. Maghirang, E. B. Razote, S. L. Trabue, and L. McConnell. 2011. Concentration of particulate matter in large cattle feedlots in Kansas. *Journal of Air & Waste Management* (In review).

Gilmour, I. M., M. S. Jaakkola, S. J. London, A. E. Nel, and C. A. Rogers. 2006. How exposure to environmental tobacco smoke, outdoor air pollutants, and increased pollen burdens influences the incidence of asthma. *Environmental Health Perspectives* 114(4): 627-633.

Gonyou, H.W. and W.R. Stricklin. 1984. Diurnal behavioral patterns of feedlot bulls during winter and spring in northern latitudes. *Journal of Animal Science* 58: 1075-1083.

Gordian, M.E., H. Ozkaynak, J.P. Xue, S.S. Morris, and J.D. Spengler. 1996. Particulate air pollution and respiratory disease in Anchorage, Alaska. *Environmental Health Perspectives* 104(3): 290-297.

Hamm, L.B. 2005. Engineering analysis of fugitive particulate matter emissions from cattle feedyards. MS thesis. College Station, Tex.: Texas A&M University.

Hinds, W.C. 1999. Aerosol technology: properties, behavior, and measurement of airborne particles. 2nd ed. New York: John Wiley & Sons.

Jones, A.M., R.M. Harrison, and J. Baker. 2010. The windspeed dependence of the concentrations of airborne particulate matter and NO_x. *Atmospheric Environment* 44(13): 1682-1690.

Kwong, W.T.J., S.L. Ho, and A.L. Coates. 2000. Comparison of nebulized particle size distribution with Malvern laser diffraction analyzer versus Andersen cascade impactor and low-flow Marple personal cascade impactor. *Journal of Aerosol Medicine* 13(4): 303-314.

Lee, J.H., P.K. Hopke, T.M. Holsen, and A.V. Polissar. 2005. Evaluation of continuous and filter-based methods for measuring $PM_{2.5}$ mass concentration. *Aerosol Science and Technology* 39(4): 290-303.

Lundgren, D.A., B.J. Hausknecht, and R.M. Burton. 1984. Large particle size distribution in five U.S. cities and the effect on a new ambient particulate matter standard (PM_{10}). *Aerosol Science and Technology* 3(4): 467-473.

Martin, G.P., H.B. MacRitchie, C. Marriott, and X.M. Zeng. 2006. Characterisation of a carrier-free dry powder aerosol formulation using inertial impaction and laser diffraction. *Pharmaceutical Research* 23(9): 2210-2219.

McGinn, S.M., T.K. Flesch, D. Chen, B. Crenna, O.T. Denmead, T. Naylor, and D. Rowell. 2010. Coarse particulate matter emissions from cattle feedlots in Australia. *Journal of Environmental Quality* 39(3): 791-798.

Miller D.N. and B.L. Woodbury. 2003. Simple protocols to determine dust potentials from cattle feedlot soils and surface samples. *Journal of Environmental Quality* 32(5): 1634-1640.

Montgomery, D. C. 1984. Design and analysis of experiments. New York: John Wiley & Sons.

Padgett, P.E., D. Meadows, E. Eaubanks, and W.E. Ryan. 2008. Monitoring fugitive dust emissions from off-highway vehicles travelling on unpaved roads and trails using passive samplers. *Environmental Monitoring and Assessment Journal* 144: 93-103.

Pearson, T., J. D. Wilson, J. Gwirtz, E. Maghirang, F. Dowell, P. McClusky, and S. Bean. 2007. Relationship between single wheat kernel particle-size distribution and Perten SKCS 4100 hardness index. *Cereal Chemistry* 84(6): 567-575.

Pilcer, G., F. Vanderbist, and K. Amighi. 2008. Correlations between cascade impactor analysis and laser diffraction techniques for the determination of the particle size of aerosolized powder formulations. *International Journal of Pharmaceutics* 358: 75-81.

Pope, C.A., R.T. Burnett, M.J. Thun, E.E. Calle, D. Krewski, K. Ito, and G.D. Thurston. 2002. Lung cancer, cardiopulmonary mortality, and long-term exposure to fine particulate air pollution. *Journal of American Medical Association* 287(9): 1132-1141.

Purdy, C.W., R.N. Clark, and D.C. Straus. 2007. Analysis of aerosolized particulates of feedyards located in the Southern High Plains of Texas. *Aerosol Science and Technology* 41(5): 497–509.

Schwartz, J. and D.W. Dockery. 1992. Particulate air pollution and daily mortality in Steubenville, Ohio. *American Journal of Epidemiology* 135(1): 12-19.

Sweeten, J.M. 1998. Cattle feedlot manure and wastewater management practices. In J.L. Hatfield and B.A. Stewart (ed.), Animal waste utilization: Effective use of manure as a soil resource, pp.125-155. Chelsea, Mich.: Ann Arbor Press.

Sweeten, J.M., C.B. Parnell, R.S. Etheredge, and D. Osborne. 1988. Dust emissions in cattle feedlots. *Veterinary Clinics of North America, Food Animal Practice* 4(3): 557-578.

Sweeten, J.M., C.B. Parnell, B.W. Shaw, and B.W. Auvermann. 1998. Particle size distribution of cattle feedlot dust emission. *Transactions of the ASAE* 41(5): 1477-1481.

Weaver, B. 2002. Chapter 3: Nonparametric tests. Available at http://www.angelfire.com/wv/bwhomedir/notes/nonpar.pdf. Accessed 14 October 2010.

Xu, R. 2000. Particle characterization: light scattering methods. Particle Technology Series. The Netherlands: Kluwer Academic Publishers.

Ziegler, J. and H. Wachtel. 2005. Comparison of cascade impaction and laser diffraction for particle size distribution measurements. *Journal of Aerosol Medicine* 18(3): 311-324.

CHAPTER 4 - Estimating Particulate Emissions from Unpaved Roads and Wind Erosion in Cattle Feedlots

4.1 Introduction

Particulate matter (PM) emissions from cattle feedlots result from pen surface disturbance by cattle hoof action. Vehicle traffic on unpaved roads and alleyways also produces significant PM emissions. Particulate emissions from unpaved roads could create problems, including impairment in visibility and hindrance to plant transpiration/photosynthesis.

Considerable research has been conducted to determine particulate emissions from unpaved roads; however, little is known about the contribution of vehicle traffic on unpaved roads to total emissions for cattle feedlots. As much as 10 million tons of PM is emitted each year due to disturbance of unpaved roads in the U.S. (Ferguson et al., 1999; Williams et al., 2008). Gillies et al. (2005) reported PM_{10} emission factors (grams PM_{10} emitted per vehicle kilometer traveled) for unpaved roads ranging from 0.8 g/km-h (for light passenger vehicles ~ 1200 kg) to 48 g/km-h (for heavy military vehicles ~18000 kg). Wanjura et al. (2004) reported an emission factor of 16 kg/1000 hd-day from unpaved roads using inverse dispersion modeling and assuming that emissions from unpaved roads represented the difference between nighttime and daytime emission rates. Such emission factors represented about 80% of total emissions from the cattle feedlot. Using similar method and assumption, Hamm (2005) reported 53% contribution from unpaved roads to total emissions from a cattle feedlot. An emission factor of 0.72 kg/hd-yr from unpaved roads was reported by the San Joaquin Valley Air Pollution Control District (SJV APCD) based on California Air Resources Board's (CARB) PM_{10} emissions methodology (Countess Environmental, 2006).

With large, exposed pen areas in cattle feedlots, wind erosion can also be a major source of PM emissions. Much research has been conducted on open, agricultural lands; however, little information is available on the contribution of wind erosion to total cattle feedlot emissions.

This study was conducted to (1) estimate PM_{10} emission rates in cattle feedlots due to vehicle movement on unpaved roads and wind erosion and (2) determine contributions of unpaved roads and wind erosion to total PM_{10} emissions in the feedlots.

4.2 Materials and Methods

4.2.1 Site Description

Two commercial cattle feedlots in Kansas (i.e., Feedlot 1 and Feedlot 2) were considered. Feedlot 1 had approximately 30,000 head of cattle, total pen area of about 50 ha, and total feedlot area of about 80 ha. It had a water sprinkling system (maximum application rate of 5.0 mm/day), which was operated from April to October and during prolonged dry periods. Manure harvesting was done at least once a year and pens were cleaned two to three times each year. Feedlot 2 also had 30,000 head, total pen area of about 59 ha, and total feedlot area of about 81 ha. Similar to Feedlot 1, manure harvesting and pen cleaning were done at Feedlot 2. Water trucks were used during dry periods to control dust from roads and pens.

Meteorological data were recorded at 20-min intervals using a weather station (Campbell Scientific, Inc., Logan, UT) that was located at the south sampling location at Feedlot 1. Feedlot 2 is about 2 km from Feedlot 1 therefore the same weather data were used in analysis. The weather station was equipped with sensors to monitor atmospheric pressure (Model CS100), air temperature and relative humidity (Model HMP45C), precipitation (Model TE525), and wind speed and direction (Model 05103-5). Rainfall events throughout the two year span of 2008-2009 were accounted for during the warm months (April to October). There were 52 "wet days" in 2008 and 56 "wet days" in 2009. A day was considered wet when there was at least 0.254 mm of precipitation (Bonifacio, 2009; Countess Environmental, 2006).

4.2.2 Field Measurement of Surface Characteristics

Samples of loose surface material by the roadside and inside the pens were collected in accordance with US EPA procedure for sampling surface/bulk dust loading (US EPA, 1993). At least 500 g for each sample was collected from the topmost layer with a whisk broom and pan and then transferred to a sealed plastic bag. Sampling was done randomly throughout the feedlot with at least two samples taken from various areas (i.e., unpaved road near the PM samplers, unpaved road near the feeding apron, and center and near the edges of the pen).

Samples were analyzed for texture at the KSU Soil Testing Laboratory. Samples were first dried overnight in an oven at 500°C. Dried samples were then ground using a 2-mm sieve. Fifty grams of sieved sample was subjected to texture analysis, which was done using the hydrometer method (Gee and Bauder, 1979) to determine sand, silt, and clay contents. Organic

matter content was determined using the Walkley-Black procedure (Walkley and Black, 1934). The two feedlots were compared in sand, silt, clay, and organic matter contents of surface materials.

4.2.3 Estimation of Emissions from Unpaved Roads

The PM_{10} emission factor brought about by vehicle travel on unpaved roads in the feedlots was determined using (Countess Environmental, 2006):

$$E = 1.5\left(\frac{s}{12}\right)^{0.9}\left(\frac{W}{3}\right)^{0.45}(VMT)\left(\frac{\text{emission days}}{\text{year}}\right)\left(\frac{1\,\text{ton}}{2000\,\text{lbs}}\right) \quad (4.1)$$

where $E = PM_{10}$ emission factor (tons/yr)

s = silt content (%)

W = vehicle weight (short tons)

VMT = vehicle-miles traveled (vehicle-miles/day)

Each feedlot had three feed trucks, each weighing 19,000 kg without feed and 30,000 kg with feed. Each feed truck had 6 feed loads per day and feeding for the feedlot occurred three times a day with each feed truck taking 2.5 h to finish each feeding. To estimate VMT, truck routes were randomly selected and distances traveled by each truck were estimated based on the shortest distance a truck could travel from the feed mill to the feed bunkers/troughs. Feed trucks were estimated to travel 9.85 mi per feeding and 14.6 mi per feeding for Feedlot 1 and Feedlot 2, respectively. Maintenance trucks weighing 3,600 kg surveyed each feedlot three times a day were assumed to pass by the entirety of each feedlot once every time of survey. Maintenance trucks were estimated to travel 4.88 mi per survey and 4.93 mi per survey for Feedlot 1 and Feedlot 2, respectively.

Mean vehicle weight, W, was determined from the sum of the product of the weight of each vehicle with its relative frequency of travel:

$$W = (\%\ \text{travel})*(\text{wt. of feed truck}) + (\%\ \text{travel})*(\text{wt. of maintenance truck}) \quad (4.2)$$

The weight of feed truck used for calculation was the mean weight of the feed truck with and without feed.

Estimated VMTs of feed trucks and maintenance trucks were 44.2 mi/day for Feedlot 1 and 58.6 mi/day for Feedlot 2. Emission days considered for the calculation of unpaved roads emissions was during warm months only (April to October) to be consistent with months used for wind erosion computations. Also, it was assumed that during the months of November to March, the road surface was damp due to snow thereby emissions are minimized.

4.2.4 Wind Erosion Emissions Calculation

PM_{10} emissions due to wind erosion were calculated using two methods: (1) US EPA AP-42 method and (2) Single-event Wind Erosion Evaluation Program (SWEEP) program.

4.2.4.1 EPA AP-42 Open Area Wind Erosion

With no field measurement of threshold friction velocity (u^*_t) at the feedlots, this research assumed the EPA-recommended value of 0.54 m/s (Countess Environmental, 2006). The corresponding friction velocity (u^*) was then calculated using equation 4.3 and erosion potential was calculated using equation 4.4.

$$u(z) = \frac{u^*}{\kappa} \ln \frac{z}{z_o} \tag{4.3}$$

$$P = 58\left(u^* - u^*_t\right)^2 + 25\left(u^* - u^*_t\right) \tag{4.4}$$

where P = erosion potential (%)

u^* = friction velocity (m/s)

u^*_t = threshold friction velocity (m/s).

u(z) = wind speed (m/s)

z = height (m)

κ = von Karman's constant (0.4)

z_o = surface roughness (m)

Surface roughness (z_o) is a measure of irregularities of the surface landscape (Turner and Schulze, 2007). Based on US EPA (2010) land classification tables, z_o was assumed equal to 0.05 m. US EPA AP-42 required the use of wind speeds at z = 10 m which was obtained by

using equation 4.3 and computing the corresponding 10 m height wind speeds from the known wind speeds at z = 2.5 m (actual height of anemometer).

Erosion potential (P_i) was computed for events exceeding the assumed threshold friction velocity of 0.54 m/s, while the corresponding emission factor (E) was computed using:

$$E = 0.5 \sum_{i=1}^{N} P_i \tag{4.5}$$

where E = PM_{10} emission factor (g/m^2)

N = number of disturbances per year

N represents total number of days excluding rainy days; a rainy day is a day with at least 0.254 mm of rain.

4.2.4.2 SWEEP Model for Wind Erosion

SWEEP is a process-based simulator for wind erosion for a single day event. It is a stand-alone program that is the same as the erosion sub-model of Wind Erosion Prediction System (WEPS). It computes erosion based on soil surface roughness, crust and rock cover, flat and standing biomass, aggregate size distribution, soil surface wetness, and loose erodible material on the crust (Hagen, 1996a).

Simulation is done for a rectangular area on a sub-hourly basis and soil loss/deposition is propagated on the basis of different parameter inputs, including wind speed, wind direction, soil surface characteristics, and soil condition. The program computes u^* and u^*_t. Soil characteristics are updated as soil movement occurs over a certain period of time. The program computes soil losses due to saltation, creep, and suspension, and PM_{10} loss, a component of suspension loss. Output information for the soil loss is converted into .emit files, while u^*_t and u^* are shown in the pop-up interface (Appendix C).

SWEEP is based on the following conservation of mass by suspension is (Hagen, 1996b):

$$\frac{\partial\left(\overline{C_{ss} H_{ss}}\right)}{\partial t} = -\frac{\partial (q_{ss})_x}{\partial x} - \frac{\partial (q_{ss})_y}{\partial y} + Gss_{en} + Gss_{an} - G_{ss} + Gss_{tp} \tag{4.6}$$

where C_{ss} = mean concentration of suspension particles (mg/m^3)

t = time (s)

q_{ss} = suspension discharge (kg/ms)

H_{ss} = height of suspension region over simulation region field (m)

x, y = horizontal distances in perpendicular directions parallel to simulation region boundaries (m)

Gss_{en} = net vertical flux of suspension from emission of loose soil (kg/m^2s)

Gss_{an} = net vertical flux of suspension from abrasion of clods and crust (kg/m^2s)

G_{ss} = net vertical flux of suspension from breakdown of saltation and creep (kg/m^2s)

Gss_{tp} = net vertical flux of suspension from trapping of suspension (kg/m^2s)

PM_{10} emission is based on conservation of mass for PM_{10} (Hagen, 1996b):

$$\frac{\partial\left(\overline{C10H10}\right)}{\partial t} = -\frac{\partial(q10)_x}{\partial x} - \frac{\partial(q10)_y}{\partial y} + G10_{en} + G10_{an} + G10_{ss} \qquad (4.7)$$

where C10 = mean concentration of PM_{10} particles (mg/m^3)

H10 = height of PM_{10} region over simulation region (m)

q10 = PM_{10} discharge (kg/ms)

$G10_{en}$ = net vertical flux of PM_{10} from emission of loose soil (kg/m^2s)

$G10_{an}$ = net vertical flux of PM_{10} from abrasion of clods and crust (kg/m^2s)

$G10_{ss}$ = net vertical flux of PM_{10} from breakdown of saltation and creep (kg/m^2s)

SWEEP requires input of soil properties and wind speed within the area of simulation. For this research, soil properties were obtained by finding the "best" soil parameters that approximate the threshold wind speed, u_t, calculated from results using the Tapered Element Oscillating Microbalance (TEOM™) PM_{10} monitoring. Details of TEOM measurements are presented in Bonifacio (2009). The u_t value was calculated by using TEOM data that did not include times with expected surface disturbances brought about by cattle activity (late afternoon and early evening) and vehicular activity (morning in which feeding starts at 6 AM until evening up to 8 PM) within the feedlot. Data that had minimal emissions (concentrations < 20-50 $\mu g/m^3$) at high wind speed (> 9 m/s) were also excluded, since they were believed to be affected by high pen surface moisture contents. Selected TEOM data were assumed to be under dry conditions, in which it was more appropriate to estimate u_t for both feedlots. Then, the flux (i.e., product of wind speed and net concentration) was plotted against wind speed and a curve was fitted using TableCurve 2D program (Systat Software, Inc., San Jose, CA). The following saltation flux

equation was used to determine the threshold velocity (Loosemore and Hunt, 2000; Gillette, 1974):

$$\text{Flux} = A u^2 (u - u_t) \quad (4.8)$$

where A = coefficient of proportionality.

Since the SWEEP program was used for feedlots, field and surface profile inputs into the SWEEP simulator were chosen in order to fit the feedlot description. A pen area of 2,500 m^2 (50 m x 50 m) was chosen as a representative area to minimize effects of feed troughs and fences. Barriers were not considered because fences and cattle provided little obstruction to wind. Crop parameters were set at zero. The surface moisture content was assumed constant and unchanged during individual event simulation (Feng and Sharratt, 2009). Surface moisture was assumed to be zero for SWEEP runs for dates with no measured pen surface moisture contents. Data were filtered from the effect of rain, snow, and high moisture content, so the whole simulation was run during dry periods.

The SWEEP model was used to calculate total, saltation/creep, suspension, and PM_{10} losses based on aggregate sizes for saltation, suspension, and PM_{10} generation processes (USDA ARS, 2008). For this research, only PM_{10} losses were considered and compared with those from US EPA AP-42 method for open area wind erosion.

4.3 Results and Discussion

4.3.1 Surface Material Texture Analysis

Table 4.1 summarizes the mean values of sand, silt, clay, and organic matter contents for pen surface and road surface materials. For each feedlot, the pen surface contained more clay and organic matter than unpaved roads. The road surface material in Feedlot 2 had higher silt content and smaller sand content than that at Feedlot 1. Statistical analysis showed that sand and silt contents from unpaved roads were significantly different ($P < 0.05$) between the two feedlots, while there was no significant difference ($P > 0.05$) in unpaved road clay and organic matter contents. The two feedlots did not differ significantly ($P>0.05$) in pen surface material contents.

Ashbaugh et al. (2003) examined soil dust and investigated different sources, including agricultural fields, public unpaved roads, and unpaved agricultural roads adjacent to fields. In their study, road dust was sandier than agricultural soils, even for agricultural roads adjacent to the field. This was due to frequent vehicle travel along unpaved roads and roads adjacent to the

field, which causes removal of fine particles, making roads exposed for a longer period of time with an enriched amount of sand as the surface material. The same is true for the observed higher percentage of sand for Feedlot 1 and Feedlot 2, where frequent movement of feed and maintenance trucks caused exposure of the sandier portion of the surface material.

Table 4.1 Mean percent surface material components for the two feedlots

Source		n	Sand	Silt	Clay	Organic Matter
Feedlot 1	Roads	4	81.5 ± 1.3	11.0 ± 1.0	7.5 ± 1.0	2.7 ± 0.8
	Pen Surface	2	70.5 ± 1.7	15.5 ± 2.8	14 ± 2.0	6.6 ± 0.1
Feedlot 2	Roads	4	68.8 ± 7.3	22.0 ± 6.2	9.2 ± 1.4	1.8 ± 0.5
	Pen Surface	2	72.0 ± 2.0	8.0 ± 2.3	20.0 ± 7.4	6.6 ± 2.4

Based on the soil texture chart (USDA SCS, 1987), the surface material for both feedlots can be classified as loamy sand (~70-80 % sand, ~10-20% silt and ~10-20% clay). On the other hand, based on the web soil survey on the USDA National Resources Conservation Service (USDA NRCS, 2010), Feedlot 1 is composed mainly of Pratt loamy fine sand (5-12 % slopes), which is about 89 % of the entire feedlot. Feedlot 2 is composed of 44% Pratt loamy fine sand (1-5 % slopes), 31 % Carwile fine sandy loam (0-1 % slopes) and 22 % Attica fine sandy loam (1-3 % slopes).

4.3.2 Emissions from Unpaved Roads

Uncontrolled fugitive emissions from unpaved roads were estimated. Emissions from unpaved roads can be controlled by watering or treatment with chemicals or other dust suppressants. Feedlot 1 used water sprinklers, while Feedlot 2 used water trucks to control PM emissions from pens and unpaved roads. Uncontrolled emission rates were used because for Feedlot 1, the water sprinkler system suppresses the dust coming only from pens and for Feedlot 2, water was applied on unpaved roads only on certain days. Also, the wetness of unpaved roads for both feedlots was not monitored so a worst case scenario of being dry was assumed.

Calculated PM_{10} emissions from unpaved roads were 13 and 17 tons/yr for Feedlot 1 and Feedlot 2, respectively. $PM_{2.5}$ emission rates for unpaved roads were assumed to be 10% of

above values (Countess Environmental, 2006). Feedlot 2 had greater PM emissions than Feedlot 1, because of greater mean VMT and silt contents. This is consistent with results by Kuhns et al. (2010), who reported greater PM_{10} emission from a field with silt content of 48 % than a field with silt content of 16 %. Kuhns et al. (2010) stated that the surface texture affects the amount of particles that are vulnerable for emission due to disturbance by vehicle movement, where surface materials are continuously compressed, lifted, and transported to the air. PM_{10} emission rates were 0.39 kg/hd-yr for Feedlot 1 and 0.51 kg/hd-yr for Feedlot 2; both values are smaller than the 0.72 kg/hd-yr for cattle feedlots in San Joaquin Valley (Countess Environmental, 2006). Emission rates in this study were based on April to October period, whereas the 0.72 kg/hd-yr was presumably based on the whole year. In addition, differences in climatic conditions, silt contents, feedlot layout, and feeding patterns can account for differences in calculated emission rates.

4.3.3 Emissions Due to Wind Erosion

4.3.3.1 US EPA AP-42 Method

Table 4.2 summarizes calculated PM_{10} and $PM_{2.5}$ emissions based on EPA AP-42 wind erosion equations. $PM_{2.5}$ emission rates for wind erosion were assumed to be 15% of PM_{10} emission rates (Countess Environmental, 2006). Emission rates were greater at Feedlot 2 than at Feedlot 1, largely because Feedlot 2 had a larger area than Feedlot 1 (59 vs 50 ha). The area is the only parameter that dictates the difference between values for Feedlot 1 and Feedlot 2, since all weather data came from the weather station at Feedlot 1.

Table 4.2 Annual emission rates (metric tons/year) from the two feedlots using US EPA AP-42 wind erosion on a dry exposed surface

Year	Feedlot 1		Feedlot 2	
	PM_{10}	$PM_{2.5}$	PM_{10}	$PM_{2.5}$
2008	37.0	5.6	44.2	6.6
2009	10.7	1.6	12.7	1.9
Mean	24.0	3.6	28.4	4.3

Emission rates were significantly greater in 2008 than in 2009, primarily because there were 29 wind erosion events in 2008 and 13 wind erosion events in 2009 (Table 4.3). The mean wind speed was higher in 2008 than in 2009, indicating that the pen surface was more susceptible to wind erosion in 2008 than in 2009. The mean friction velocity was also high in 2008, which denotes that the threshold friction velocity was exceeded, thereby initiating greater movement of aggregates or particles on the pen surface than in 2009. Also, the number of wet days was greater in 2009 (47) than in 2008 (45).

Table 4.3 Comparison of wind erosion parameters determined using US EPA AP-42 between 2008 and 2009

Year	n	Wind speed (m/s)			Friction velocity (m/s)		
		Min	Max	Mean	Min	Max	Mean
2008	29	7.2	12	8.9 ± 0.2	0.54	0.91	0.67 ± 0.02
2009	13	7.2	11	8.3 ± 0.4	0.54	0.83	0.62 ± 0.03

Figure 4.1 shows monthly PM_{10} emissions for both feedlots. As mentioned, Feedlot 2 had slightly higher emissions than Feedlot 1 because of greater total pen area. There were more emissions in 2008 (only July and August had minimal if no emission), while for 2009, only during the month of April was there an observed peak for wind erosion emissions. Other months in 2009 had minimal emissions.

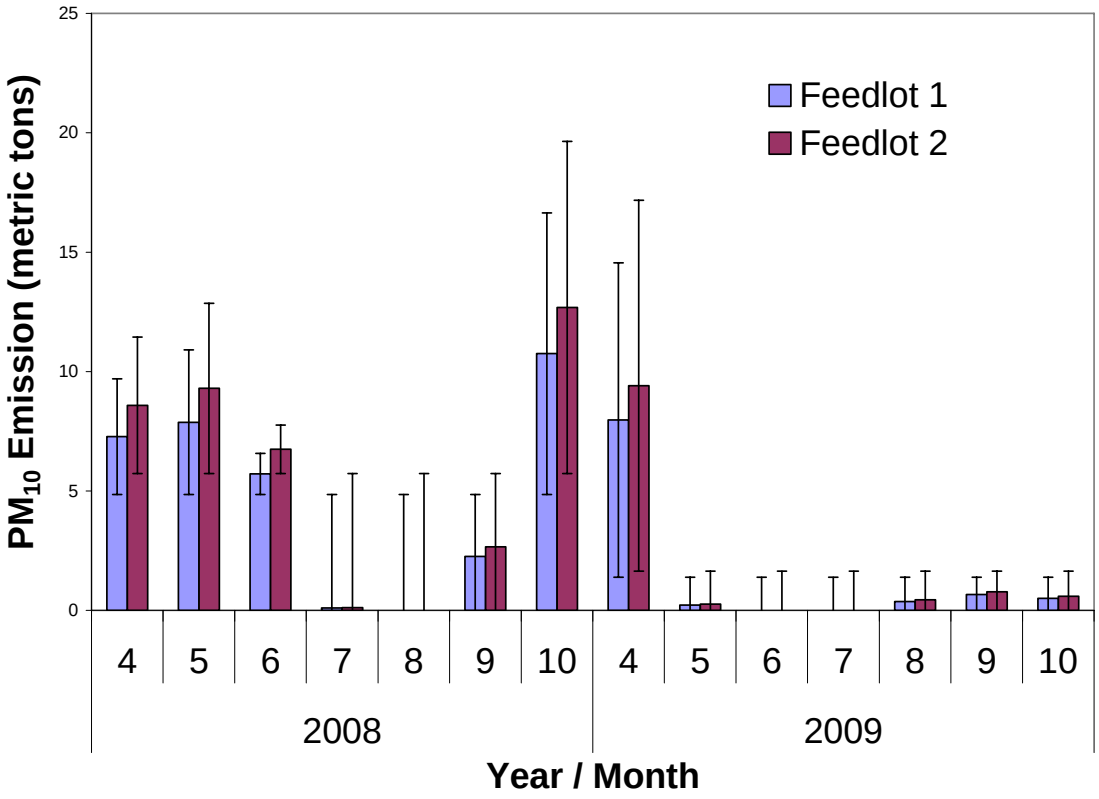

Figure 4.1 Monthly PM_{10} emissions (metric tons) using the US EPA AP-42 model. Error bars represent standard deviation of the PM_{10} measurements from the mean PM_{10} emissions.

4.3.3.2 SWEEP model

Figures 4.2 and 4.3 show the net PM_{10} fluxes from the TEOM data plotted against wind speed. Curve fitting showed threshold wind velocities of 4.0 m/s for Feedlot 1 and 3.9 m/s for Feedlot 2. Based on these threshold velocities, soil characteristic inputs for the SWEEP program were identified.

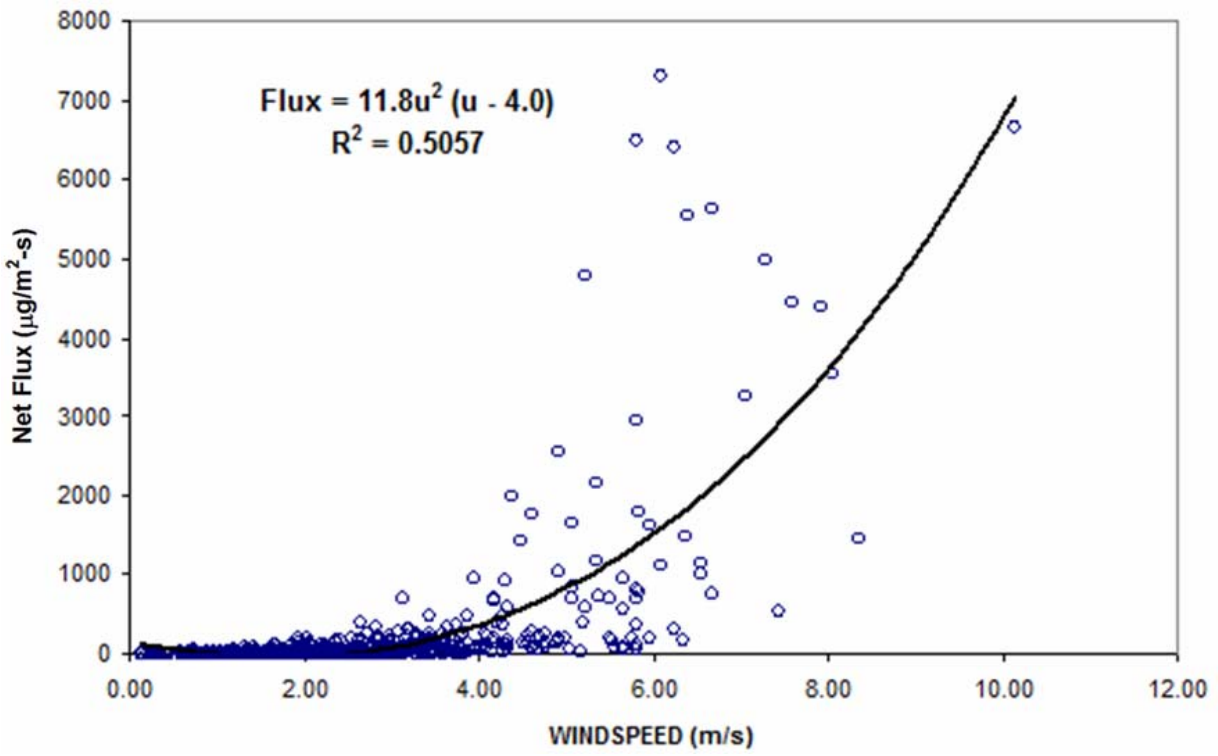

Figure 4.2 Feedlot 1 net PM_{10} flux vs. wind speed using TEOM data

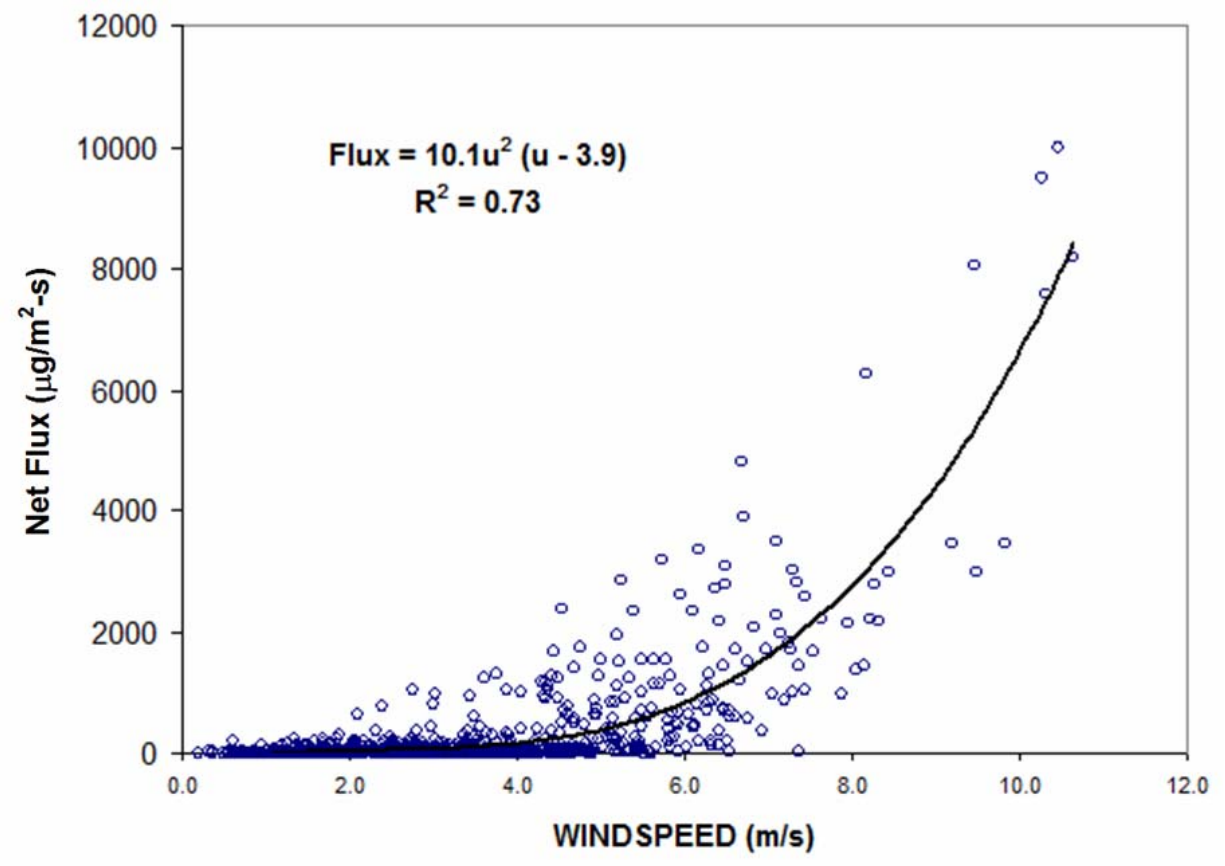

Figure 4.3 Feedlot 2 net PM_{10} flux vs. wind speed using TEOM data

Figure 4.4 summarizes the calculated monthly PM_{10} emissions for both feedlots. Feedlot 2 had higher emissions than Feedlot 1 due to its greater total pen surface area. Higher emissions in 2008 generally occurred during the months of April to June and October, while in 2009, emissions were higher in April only. This could have been due to the difference in the number of wet days between the two years considered as discussed previously. Also, higher emissions were expected during spring and fall periods since greater wind speeds existed during both periods (Fig. 4.5). Emissions were smaller during the summer even with high wind speeds possibly due to rainfall events.

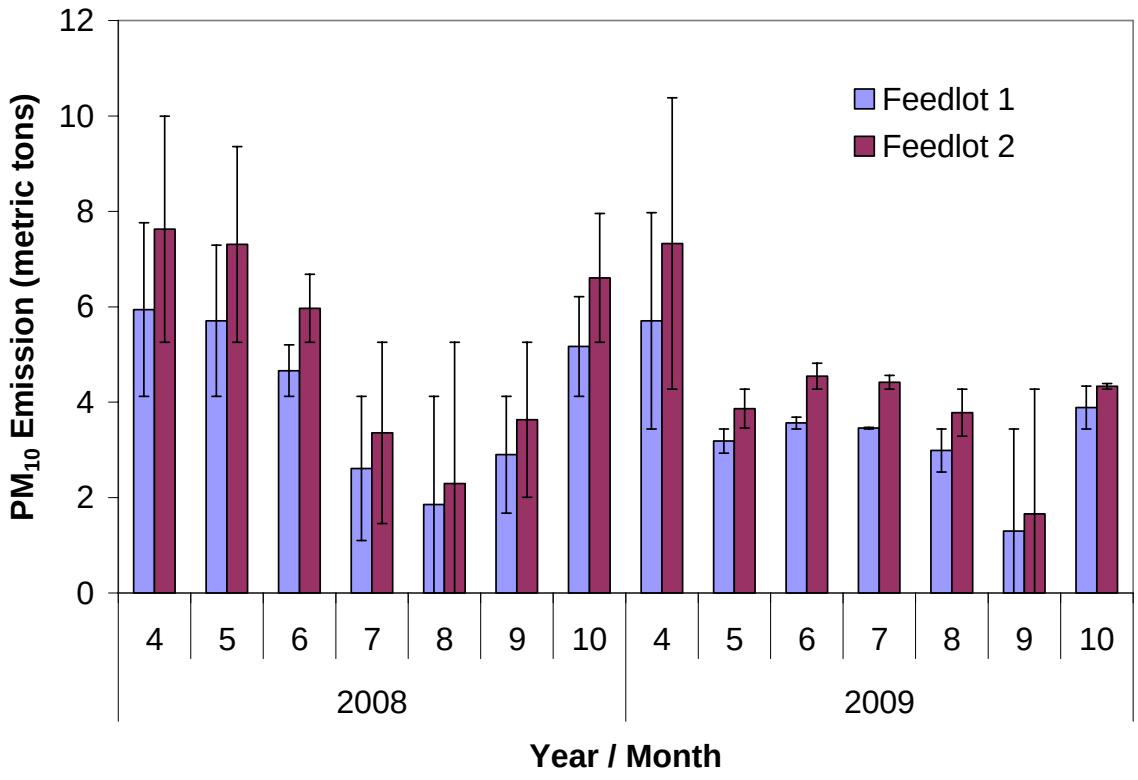

Figure 4.4 Monthly PM_{10} emissions (metric tons) using the SWEEP model. Error bars represent standard deviation of PM_{10} measurements from the mean PM_{10} emissions.

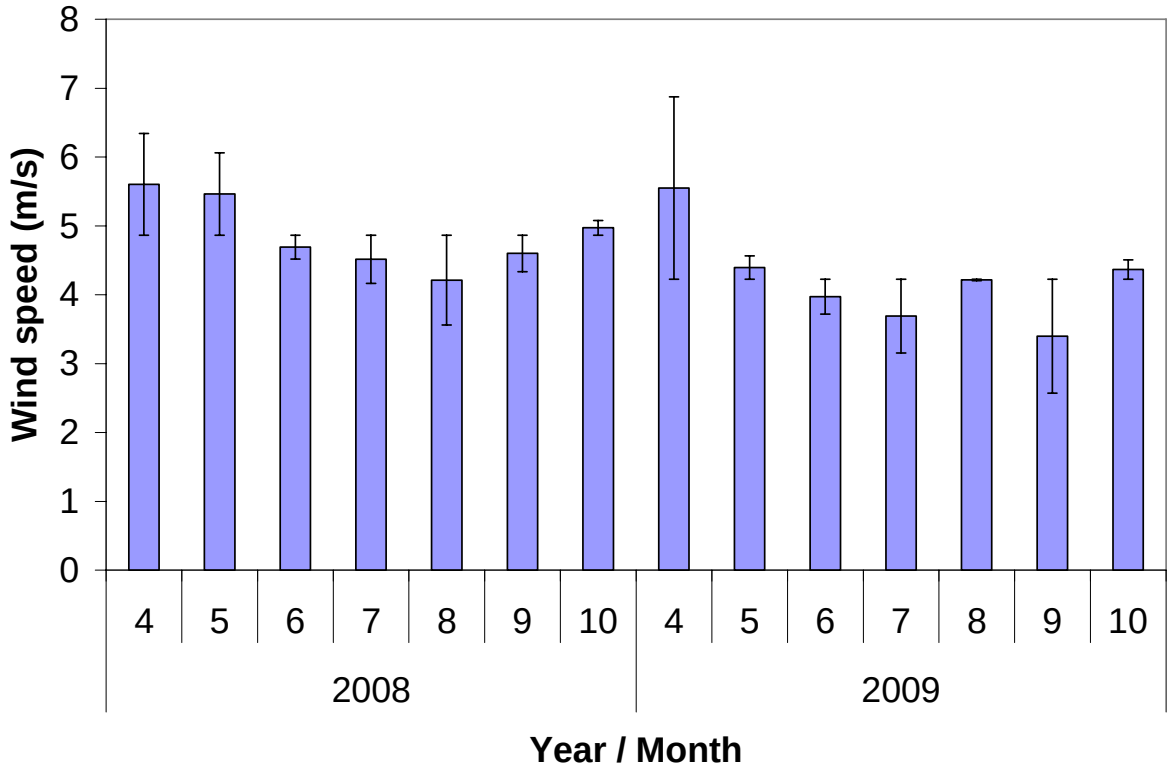

Figure 4.5 Monthly mean wind speed from 2008 – 2009. Error bars represent standard deviation of wind speeds from the mean monthly wind speed.

Total PM_{10} emission rates for the April to October period are summarized in Table 4.4. PM_{10} emission rates due to wind erosion using the SWEEP model for the two feedlots did not show any significant difference ($P > 0.05$). Estimated total PM_{10} emission rate due to wind erosion in 2009 was slightly smaller than but not significantly different from that in 2008. This can be explained by weather conditions during the two year span (Table 4.5).

Table 4.4 Estimated PM_{10} emission rates using the SWEEP model

Year	PM_{10} Emissions (metric tons/yr)	
	Feedlot 1	Feedlot 2
2008	32.5	41.3
2009	25.6	32.0
Mean	29.1	36.7

Table 4.5 Summary of the meteorological conditions

Year	Mean Temp (ºC)	Mean Wind Speed (m/s)	Total Precipitation (mm)
2008	11.9 ± 3.9	4.9 ± 0.2	455
2009	11.6 ± 3.7	4.2 ± 0.3	429
Mean	11.8	4.6	442

Only one weather data set was used for both feedlots since they were close to each other, so comparison was on a yearly basis only. Mean wind speed was higher in 2008 than in 2009 by about 0.7 m/s. As such, estimated emission rate was expected to be higher in 2008. Another parameter that could also have contributed to the lower wind erosion emission rate in 2009, although minimally, was temperature. It was lower than in 2008 and "longer" winter days were encountered and more winter days were discarded in calculating emissions brought about by wind erosion. The number of days considered for 2008 (April 1 to November 20) was 10 days more than that for 2009 (April 1 to November 10).

Table 4.6 summarizes wind speeds and friction velocities obtained from the SWEEP simulation. The mean wind speed and mean friction velocity for both years were almost identical in value. Note that since only one weather data set was used for running the SWEEP simulations (also taking into account the findings previously that Feedlot 1 and Feedlot 2 had almost similar soil characteristics), it was expected that values would greatly be affected by the total pen surface area.

Table 4.6 Comparison of wind erosion parameters for the SWEEP model between 2008 and 2009

Year	n	Wind speed (m/s)			Friction velocity (m/s)		
		Min	Max	Mean	Min	Max	Mean
2008	189	5.5	13	7.1 ± 0.1	0.41	0.97	0.49 ± 0.01
2009	165	5.5	11	6.9 ± 0.1	0.41	0.81	0.48 ± 0.01

4.3.3.3 Comparison of the EPA AP-42 and SWEEP Model for Wind Erosion

Values obtained using US EPA AP-42 and SWEEP models were significantly different from each other ($P<0.05$). As noted earlier, threshold friction velocity was assumed equal to 0.54 m/s for the US EPA AP-42 method. The threshold wind speed (at 10 m) corresponding to that threshold friction velocity was about 7.1 m/s. For the SWEEP model, on the other, estimated threshold wind speeds were around 4 m/s for both feedlots and calculated threshold friction velocity was 0.41. With greater threshold wind speed and threshold friction velocity, US EPA AP-42 method was expected to result in smaller emissions than the SWEEP model (Tables 4.2 and 4.4), since higher threshold speed means greater tolerance for the soil before being swept away from wind erosion, that is, soil is less susceptible from wind erosion at low wind speeds (De Oro and Buschiazzo, 2009).

4.3.4 Contributions to Total Emissions

Bonifacio et al. (2011), using inverse modeling with AERMOD, determined an average PM_{10} emission factor of 23 kg/1000 hd-day for Feedlot 1 for April - October 2008. Assuming this value as the total PM_{10} emission factor for Feedlot 1, emissions from unpaved roads represented about 5 % of total emissions and those due to wind erosion represented about 13-13.5 % of total emissions. Contribution from unpaved roads in this study was considerably smaller than those reported by Wanjura et al (2004) at 80% and Hamm (2005) at 53%. The difference could be accounted for by differences in methodology and feedlot conditions and locations. This study used empirical equations for unpaved roads. Values in Wanjura et al. (2004) and Hamm (2005), on the other hand, were based on inverse dispersion modeling combined with the assumption that the emission factor for unpaved roads can be represented by the difference between nighttime and daytime emission factors.

Results indicate that, on an annual basis, less than 20% of total emissions can be attributed to emissions from unpaved roads and wind erosion and that the major component of emissions is likely due to pen surface disturbance by cattle activity. Note, however, that in cases with high wind speeds and dry surface conditions (e.g., month of April), estimated emissions due to wind erosion were considerable and could be the major component of total feedlot emissions.

Table 4.7 Comparison of emission factors (kg/1000hd-day) for the two-year span

Year	Estimated Total Emissions[a]	Unpaved Roads (US EPA AP-42)		Wind Erosion (US EPA AP-42)		Wind Erosion (SWEEP)	
	Feedlot 1	Feedlot 1	Feedlot 2	Feedlot 1	Feedlot 2	Feedlot 1	Feedlot 2
2008	23	1.1	1.4	3.1	3.7	3.0	3.8
2009	-	1.1	1.4	0.9	1.0	2.3	2.9
Mean		1.1	1.4	2.0	2.4	2.7	3.4

[a]From inverse dispersion modeling for April to October 2008 (Bonifacio et al., 2011).

There were several limitations in this study that relate to emission estimation methods. Emission estimates were based on empirical models with their inherent limitations and assumptions. For example, US EPA AP-42 method was developed for industrial wind erosion and SWEEP was developed for agricultural areas. Further research is needed to establish the applicability of those models for cattle feedlots.

4.4 Summary and Conclusion

Emission rates of particulate matter associated with wind erosion from pen surfaces and vehicle traffic on unpaved roads were estimated for two cattle feedlots in Kansas using published empirical models. With greater silt content on unpaved roads and greater total pen area, Feedlot 2 had higher estimated PM_{10} emission rates than Feedlot 1. PM_{10} emission rates from unpaved roads and wind erosion were less than 20% of annual feedlot emissions, suggesting that pen surface disturbance due to cattle activity could be the major source of dust generation in feedlots. Further research is needed to establish the applicability of those empirical models in cattle feedlots.

4.5 References

Ashbaugh, L.L., O.F. Carvacho, M.S. Brown, J.C. Chow, J.G. Watson, and K.C. Magliano. 2003. Soil sample collection and analysis for the fugitive dust characterization study. *Atmospheric Environment* 37(9-10): 1163-1173.

Bonifacio, H. F. 2009. Particulate matter emissions from commercial beef cattle feedlots in Kansas. MS Thesis. Manhattan, Kan.: Kansas State University.

Bonifacio, H. F., R. G. Maghirang, E. B. Razote, B. W. Auvermann, J. P. Murphy, and J. P. Harner. 2011. PM_{10} emission rates from beef cattle feedlots in Kansas. *Journal of Environmental Quality* (In review).

Countess Environmental. 2006. WRAP fugitive dust handbook. Westlake Village, Calif.: Countess Environmental. Available at http://www.wrapair.org/forums/dejf/fdh/content/FDHandbook_Rev_06.pdf. Accessed 21 March 2010.

De Oro, L. A. and D. E. Buschiazzo. 2009. Threshold wind velocity as an index of soil susceptibility to wind erosion under variable climatic conditions. *Land Degradation and Development* 20: 14-21.

Feng, G. and B. Sharratt. 2009. Evaluation of the SWEEP model during high winds on the Columbia Plateau. *Earth Surface Processes and Landforms* 34: 1461-1468.

Ferguson, J.F., H.W. Downs, and D.L. Pfost. 1999. Fugitive dust: Nonpoint sources. Columbia, Miss.: University of Missouri - Columbia. Available at http://extension.missouri.edu/explore/agguides/agengin/g01885.htm. Accessed 21 March 2010.

Gee G.W. and J.W. Bauder. 1979. Particle size analysis by hydrometer: a simplified method for routine textural analysis and a sensitivity test of measured parameters. *Soil Science Society of America Journal* 43: 1004-1007.

Gillette, D.A. 1974. On the production of soil wind erosion aerosols having the potential for long range transport. *Journal de Recherches Atmospheriques* 8: 735-744.

Gillies, J.A., V. Etyemezian, H. Kuhns, D. Nicolich, and D. Gillette. 2005. Effect of vehicle characteristics on unpaved road dust emissions. *Atmospheric Environment* 39: 2341-2347.

Hagen, L. 1996a. An overview of the wind erosion prediction system. Manhattan, Kan.: USDA-ARS Wind Erosion Research Unit. Available at http://www.weru.ksu.edu/weps/docs/wepsoverview.pdf. Accessed 10 July 2010.

Hagen, L. 1996b. WEPS technical documentation: Erosion submodel. Manhattan, Kan.: USDA-ARS Wind Erosion Research Unit. Available at http://www.weru.ksu.edu/weps/docs/weps_tech.pdf. Accessed 10 July 2010.

Hamm, L.B. 2005. Engineering analysis of fugitive particulate matter emissions from cattle feedyards. MS thesis. College Station, Tex.: Texas A&M University.

Kuhns, H., J. Gillies, V. Etyemezian, G. Nikolich, J. King, D. Zhu, S. Uppapalli, J. Engelbrecht, and S. Kohl. 2010. Effect of soil type and momentum on unpaved road particulate

matter emissions from wheeled and tracked vehicles. *Aerosol Science and Technology* 44: 187-196.

Loosemore G.A. and J.R. Hunt. 2000. Dust resuspension without saltation. *Journal of Geophysical Research* 105(D16): 20663-20672.

Turner, D.B. and R.H. Schulze. 2007. Practical guide to atmospheric dispersion model. Dallas, Tex.: Trinity Consultants, Inc. and Air & Waste Management Association.

U.S. Department of Agriculture – Agricultural Research Service (USDA-ARS). 2008. SWEEP user manual draft. Manhattan, Kan.: USDA-ARS Wind Erosion Research Unit.

U.S. Department of Agriculture – National Resources Conservation Service (USDA NRCS). 2010. Web soil survey. Available at http://websoilsurvey.nrcs.usda.gov/app/WebSoilSurvey.aspx. Accessed 10 July 2010.

U.S. Department of Agriculture - Soil Conservation Service (USDA SCS). 1987. Soil mechanics level I, module 3 – USDA textural soil classification study guide. Available at http://www.wsi.nrcs.usda.gov/products/w2q/H&H/docs/training_series_modules/soil-USDA-textural-class.pdf. Accessed 21 March 2010.

U.S. Environmental Protection Agency (US EPA). 1993. Emissions factors and AP-42, compilation of air pollutant emission factors. Appendix C.1. Procedures for sampling surface/bulk dust loading. Available at http://www.epa.gov/ttn/chief/ap42/appendix/app-c1.pdf. Accessed 21 March 2010.

Walkley A. and I.A. Black. 1934. An examination of the Degtjareff method for determining organic carbon in soils: Effect of variations in digestion conditions and of inorganic soil constituents. *Soil Science* 63: 251-263.

Wanjura, J.D., C.B. Parnell, B.W. Shaw, and R.E. Lacey. 2004. A protocol for determining a fugitive dust emission factor from a ground level area source. ASAE/CSAE Paper No. 044018. St. Joseph, Mich.: ASAE.

Williams, D.S., M.K. Shukla, and J. Ross. 2008. Particulate matter emission by a vehicle running on unpaved road. *Atmospheric Environment* 42: 3899-3905.

CHAPTER 5 - Conclusions and Recommendations

5.1 Conclusions

This research was conducted to (1) determine the applicability of laser diffraction method combined with TSP sampling in measuring particle size distribution and concentration of various size fractions; and (2) determine contributions of unpaved roads and wind erosion to total particulate emissions in cattle feedlots. Results showed the following:

- The laser diffraction method can be used to measure size distribution and concentration of PM in cattle feedlots. It was highly correlated with the Micro-orifice Uniform Deposit Impactor (MOUDI) in determining the geometric mean diameter of particles. Measured geometric mean diameters ranged from 9.2 to 37.5 μm, indicating that particles generated from feedlots are generally large in size. The laser diffraction method also agreed well with low-volume samplers in determining fractions of PM_{10} and $PM_{2.5}$.
- Empirical models showed that for the feedlots in this study, estimated PM_{10} emissions from unpaved roads due to vehicle traffic and from pen surfaces due to wind erosion contributed about 5% and 13%, respectively, to total PM_{10} emissions.

5.2 Recommendations for Further Study

A. For laser diffraction method, determine the following
   1. Optical properties (e.g., refractive index) of feedlot dust.
   2. Effects of different dispersants.
   3. Effects of particle size

B. For estimating emissions from unpaved roads and wind erosion
   1. Measure directly or indirectly emissions from unpaved roads in cattle feedlots and compare with estimates from empirical models.
   2. Evaluate the applicability of wind erosion models in cattle feedlots.
   3. Monitor feeding schedules (time/duration) and vehicle traffic to assess actual vehicle miles traveled within the feedlot.

4. Determine effects of meteorological variables (e.g., RH) on emissions from wind erosion and unpaved roads.
5. Monitor pen surface moisture content and road surface moisture content.
6. Track cattle activity to determine times when cattle are active, which could influence sourcing of dust, especially during night and early morning periods.

Appendix A - Supporting Data for Chapter 2

Table A.1 Cattle on feed 1000+ capacity feedlots (USDA NASS, [2009, 2005, 2000])

State	2000	2005	2009
AZ	272	335	358
AR	11	10	2
CA	415	535	490
CO	1,200	1,100	1,020
ID	315	300	230
IL	230	210	180
IN	120	125	120
IA	1,100	920	1,300
KS	2,350	2,460	2,370
KY	15	10	10
MD	17	12	12
MI	200	190	165
MN	285	290	280
MO	100	70	60
MT	70	60	45
NE	2,440	2,470	2,500
NV	21	10	6
NM	116	126	165
NY	30	23	29
NC	5	4	2
ND	70	60	70
OH	190	200	195
OK	435	355	350
OR	50	80	75
PA	75	75	75
SD	350	400	390
TN	10	5	4
TX	2,910	2,720	2,800
UT	35	35	25
VA	27	30	29
WA	235	195	160
WV	7	7	9
WI	160	225	240
WY	90	80	70
Other States*	28	21	14.7
US Total	13,983	13,748	13,850.7

*AL, AK, CT, DE, FL, GA, HI, LA, MA, ME, MS, NH, NJ, RI, SC and VT.

Source: http://www.nass.usda.gov/Publications/Ag_Statistics/2009/chp07.pdf

Appendix B - Supporting Data for Chapter 3

Table B.1 Sample data from laser diffraction analysis

Channel Number	Channel Diameter (Lower) um	da (lower)	Average Vol (%) vi	$di = [(d_n * d_{n+1})]^{0.5}$	vi*di	vi*[ln(di)]	$vi*((\ln(di/dg))^2)$
1	0.38	0.50	0.05	0.39	0.02	-0.05	0.61
2	0.41	0.55	0.10	0.43	0.04	-0.09	1.08
3	0.45	0.61	0.16	0.47	0.08	-0.12	1.64
4	0.50	0.67	0.22	0.52	0.12	-0.15	2.09
5	0.54	0.73	0.27	0.57	0.15	-0.15	2.40
6	0.60	0.80	0.31	0.63	0.19	-0.15	2.57
7	0.66	0.88	0.34	0.69	0.23	-0.13	2.63
8	0.72	0.97	0.36	0.76	0.27	-0.10	2.61
9	0.79	1.06	0.37	0.83	0.31	-0.07	2.52
10	0.87	1.17	0.38	0.91	0.35	-0.04	2.40
11	0.95	1.28	0.39	1.00	0.39	0.00	2.29
12	1.05	1.40	0.42	1.10	0.46	0.04	2.23
13	1.15	1.54	0.45	1.20	0.54	0.08	2.23
14	1.26	1.69	0.50	1.32	0.67	0.14	2.29
15	1.38	1.86	0.58	1.45	0.84	0.21	2.40
16	1.52	2.04	0.67	1.59	1.06	0.31	2.52
17	1.67	2.24	0.77	1.75	1.34	0.43	2.63
18	1.83	2.46	0.87	1.92	1.68	0.57	2.70
19	2.01	2.70	0.97	2.11	2.04	0.72	2.69
20	2.21	2.96	1.04	2.31	2.41	0.87	2.58
21	2.42	3.25	1.08	2.54	2.75	1.01	2.37
22	2.66	3.57	1.09	2.79	3.03	1.11	2.08
23	2.92	3.92	1.08	3.06	3.30	1.21	1.80
24	3.21	4.30	1.11	3.36	3.72	1.34	1.59
25	3.52	4.72	1.20	3.69	4.42	1.57	1.47
26	3.86	5.18	1.37	4.05	5.53	1.91	1.40
27	4.24	5.69	1.59	4.44	7.05	2.37	1.34
28	4.66	6.25	1.84	4.88	8.97	2.91	1.25
29	5.11	6.86	2.12	5.35	11.34	3.55	1.14
30	5.61	7.53	2.43	5.88	14.26	4.30	0.99
31	6.16	8.26	2.75	6.45	17.76	5.13	0.82
32	6.76	9.07	3.07	7.08	21.72	6.00	0.63
33	7.42	9.96	3.38	7.78	26.31	6.94	0.44
34	8.15	10.93	3.75	8.54	31.97	8.03	0.27
35	8.94	12.00	4.05	9.37	37.96	9.07	0.12
36	9.82	13.17	4.14	10.29	42.63	9.66	0.03
37	10.78	14.46	4.23	11.29	47.74	10.25	0.00
38	11.83	15.87	4.43	12.40	54.88	11.15	0.05

39	12.99	17.43	4.61	13.61	62.74	12.04	0.19
40	14.26	19.13	4.74	14.94	70.83	12.82	0.41
41	15.65	21.00	4.35	16.40	71.40	12.18	0.65
42	17.18	23.05	3.21	18.00	57.85	9.29	0.74
43	18.86	25.30	2.28	19.76	45.00	6.79	0.75
44	20.71	27.78	2.08	21.69	45.17	6.41	0.93
45	22.73	30.49	2.60	23.81	61.90	8.24	1.50
46	24.95	33.48	3.65	26.14	95.44	11.91	2.66
47	27.39	36.75	3.56	28.70	102.13	11.95	3.19
48	30.07	40.34	2.33	31.50	73.40	8.04	2.52
49	33.01	44.28	1.62	34.58	55.96	5.73	2.08
50	36.24	48.61	1.51	37.97	57.16	5.48	2.26
51	39.78	53.37	1.31	41.68	54.40	4.87	2.27
52	43.67	58.59	0.80	45.75	36.78	3.07	1.61
53	47.94	64.31	0.44	50.22	22.18	1.73	1.00
54	52.62	70.60	0.41	55.13	22.48	1.63	1.04
55	57.77	77.50	0.75	60.52	45.25	3.07	2.14
56	63.41	85.08	1.51	66.44	100.18	6.33	4.81
57	69.61	93.40	1.67	72.94	121.99	7.17	5.91
58	76.42	102.53	0.85	80.07	68.24	3.74	3.32
59	83.89	112.55	0.33	87.90	29.08	1.48	1.41
60	92.09	123.55	0.16	96.49	14.98	0.71	0.72
61	101.10	135.64	0.08	105.92	8.68	0.38	0.42
62	110.98	148.90	0.07	116.28	8.60	0.35	0.41
63	121.83	163.45	0.15	127.65	18.73	0.71	0.87
64	133.74	179.43	0.32	140.12	44.55	1.57	2.04
65	146.81	196.97	0.32	153.82	48.97	1.60	2.19
66	161.17	216.23	0.17	168.86	28.60	0.87	1.25
67	176.92	237.36	0.08	185.37	15.21	0.43	0.65
68	194.22	260.57	0.03	203.49	6.55	0.17	0.27
69	213.21	286.05	0.01	223.39	3.29	0.08	0.13
70	234.05	314.01	0.02	245.23	5.13	0.12	0.20
71	256.94	344.72	0.03	269.21	7.42	0.15	0.28
72	282.06	378.42	0.01	295.52	3.23	0.06	0.12
73	309.63	415.41	0.00	324.41	0.30	0.01	0.01
74	339.90	456.02	0.00	356.13	0.01	0.00	0.00
75	373.13	500.61	0.00	390.94	0.00	0.00	0.00
76	409.61	549.55	0.00	429.17	0.00	0.00	0.00
77	449.66	603.28	0.00	471.13	0.00	0.00	0.00
78	493.62	662.26	0.00	517.19	0.00	0.00	0.00
79	541.88	727.01	0.00	567.75	0.00	0.00	0.00
80	594.85	798.08	0.00	623.25	0.00	0.00	0.00
81	653.01	876.10	0.00	684.19	0.00	0.00	0.00
82	716.85	961.76	0.00	751.07	0.00	0.00	0.00
83	786.93	1055.78	0.00	824.50	0.00	0.00	0.00
84	863.87	1159.00	0.00	905.11	0.00	0.00	0.00
85	948.32	1272.30	0.00	993.58	0.00	0.00	0.00
86	1041.00	1396.65	0.00	1090.71	0.00	0.00	0.00

87	1142.80	1533.23	0.00	1197.35	0.00	0.00	0.00
88	1254.50	1683.09	0.00	1314.42	0.00	0.00	0.00
89	1377.20	1847.71	0.00	1442.93	0.00	0.00	0.00
90	1511.80	2028.29	0.00	1583.98	0.00	0.00	0.00
91	1659.60	2226.59	0.00	1738.86	0.00	0.00	0.00
92	1821.90	2444.34	0.00	1908.87	0.00	0.00	0.00
SUM			100			241.03	113.85

$GMD = \text{EXP}(241.03/100) = 11.13\ \mu\text{m}$ (equivalent sphere diameter)

$GMD = 11.13 * \left(\sqrt{1.8}\right) = 14.94\ \mu\text{m}$ (equivalent aerodynamic diameter)

$GSD = \text{EXP}((113.85/100)^{0.5}) = 2.91$

Table B.2 Geometric mean diameter (GMD) and geometric standard deviation (GSD) values for comparing LD and MOUDI

MOUDI		Laser Diffraction (LD)	
GMD (μm)	GSD	GMD (μm)	GSD
10.00	2.72	16.07	2.86
12.74	2.17	8.80	2.46
16.64	2.17	12.04	2.74
18.18	2.67	27.98	2.26
9.00	2.61	14.46	3.04
6.99	2.87	10.65	2.52
11.39	2.35	12.64	3.01
15.17	2.19	14.74	3.56
10.42	2.07	14.66	2.84
11.25	2.14	8.28	2.65
16.51	2.18	16.25	3.52
14.05	2.15	15.77	3.12
14.63	2.15	9.72	2.55
15.41	2.15	10.28	3.11

Table B.3 Geometric mean diameter (GMD) and geometric standard deviation (GSD) values for Feedlot 1 (downwind) during warm months (April to October)

Event	Temp (°C)	GMD (μm) *	GSD
1	21.9	12.5	2.5
2	27.5	15.0	2.7
3	16.0	11.6	2.5
4	24.0	25.2	3.0
5	12.3	13.9	2.5
6	14.1	12.8	2.8
7	18.4	21.4	3.1
8	20.6	9.2	2.4
9	20.3	11.8	2.5
10	14.9	12.8	2.5
11	22.9	16.2	2.7
12	20.2	21.1	3.7
13	21.9	37.5	2.3
14	26.8	19.4	3.0
15	25.7	14.3	2.5
16	27.7	17.0	3.0
17	25.5	22.2	2.7
18	21.4	15.6	2.5
19	20.1	16.1	2.6
20	23.0	15.1	2.5
21	20.6	14.2	2.7
22	25.3	19.8	3.6
23	24.2	12.0	2.5
24	17.7	19.7	2.8
25	17.8	16.7	3.3
26	21.5	13.0	2.6
27	19.0	13.3	2.7
28	23.5	14.2	2.9
29	29.7	14.8	2.8
30	33.7	13.8	3.1
31	26.3	12.6	3.2

*based on aerodynamic diameter

Table B.4 Geometric mean diameter (GMD) and geometric standard deviation (GSD) values for Feedlot 1 (downwind) during cold months (November to March)

Event	Temp (°C)	GMD (μm) *	GSD
1	13.6	10.8	2.4
2	12.3	12.0	3.0
3	11.4	10.2	2.4
4	11.7	11.3	2.6
5	4.3	11.3	2.5
6	2.8	11.1	2.7
7	-2.2	21.8	3.5
8	16.7	21.2	3.1

*based on aerodynamic diameter

Appendix C - Supporting Information for Chapter 4

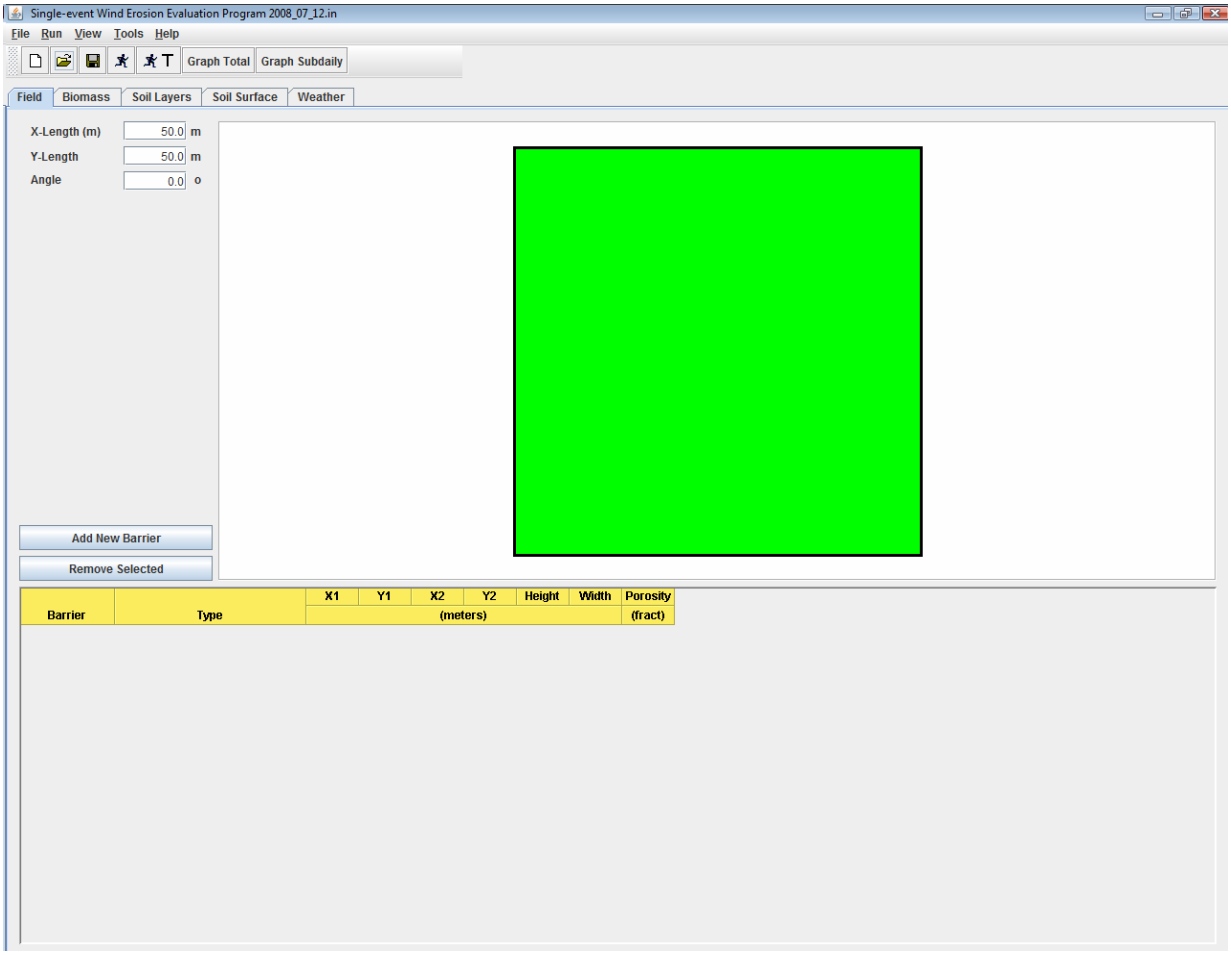

Figure C.1 SWEEP "Field Tab" Interface

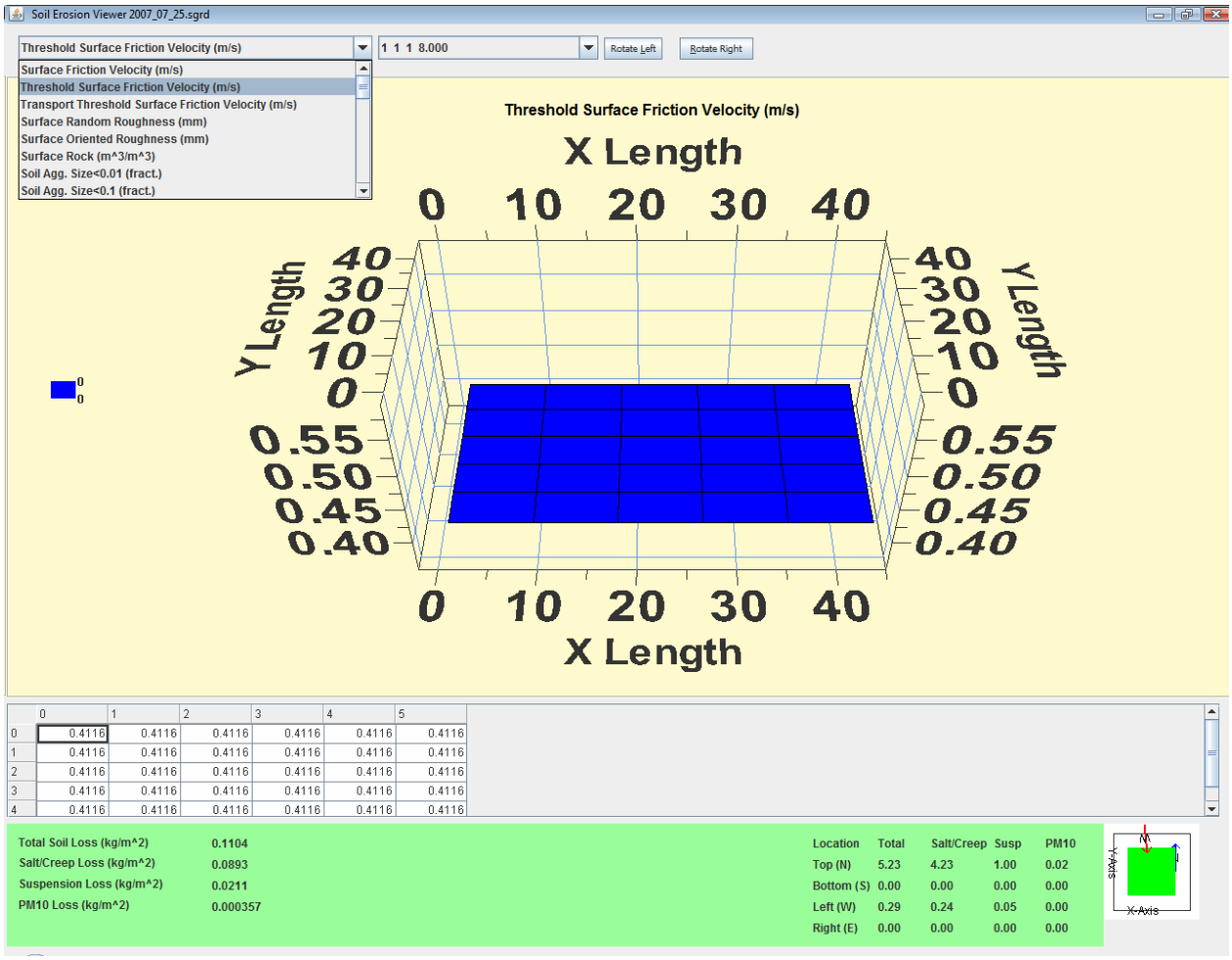

Figure C.2 Daily output information showing the scroll down option to choose between calculated friction velocities and threshold friction velocity.

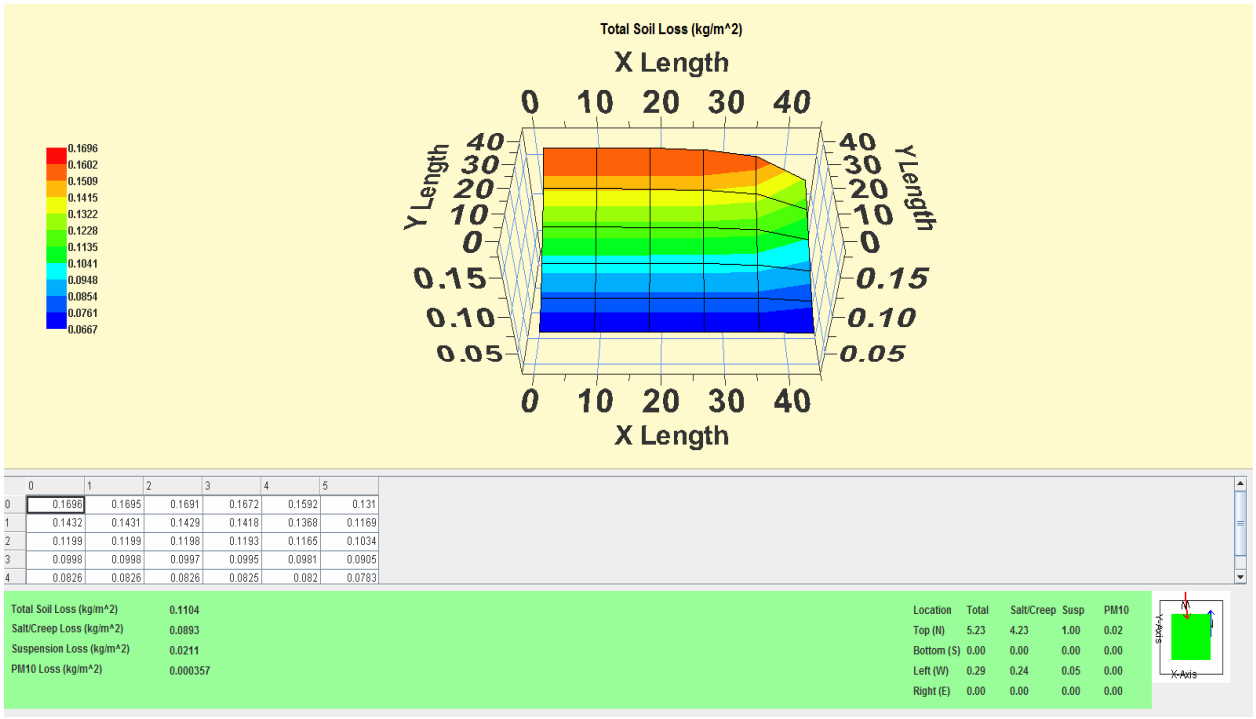

	0	1	2	3	4	5
0	0.1696	0.1695	0.1691	0.1672	0.1592	0.131
1	0.1432	0.1431	0.1429	0.1418	0.1368	0.1169
2	0.1199	0.1199	0.1198	0.1193	0.1165	0.1034
3	0.0998	0.0998	0.0997	0.0995	0.0981	0.0905
4	0.0826	0.0826	0.0826	0.0825	0.082	0.0783

Figure C.3 Sample output from SWEEP showing soil loss parameters